

Summer 1997

# Endothelial Nitric Oxide Synthase and Growth Factor Regulation of Flow-Mediated Vascular Remodeling

David Anthony Tulis  
*Old Dominion University*

Follow this and additional works at: [https://digitalcommons.odu.edu/biomedicalsciences\\_etds](https://digitalcommons.odu.edu/biomedicalsciences_etds)

Part of the [Animal Structures Commons](#), [Biophysics Commons](#), [Cardiovascular System Commons](#), [Physiology Commons](#), and the [Surgery Commons](#)

---

## Recommended Citation

Tulis, David A.. "Endothelial Nitric Oxide Synthase and Growth Factor Regulation of Flow-Mediated Vascular Remodeling" (1997). Doctor of Philosophy (PhD), dissertation, , Old Dominion University, DOI: 10.25777/3mza-eb82 [https://digitalcommons.odu.edu/biomedicalsciences\\_etds/87](https://digitalcommons.odu.edu/biomedicalsciences_etds/87)

This Dissertation is brought to you for free and open access by the College of Sciences at ODU Digital Commons. It has been accepted for inclusion in Theses and Dissertations in Biomedical Sciences by an authorized administrator of ODU Digital Commons. For more information, please contact [digitalcommons@odu.edu](mailto:digitalcommons@odu.edu).

**ENDOTHELIAL NITRIC OXIDE SYNTHASE AND GROWTH FACTOR  
REGULATION OF FLOW-MEDIATED VASCULAR REMODELING**

by

**DAVID ANTHONY TULIS**

**B.S., May 1987, University of North Carolina at Chapel Hill**

**M.S., May 1990, North Carolina State University**

**A Dissertation submitted to the Faculty of  
Old Dominion University and Eastern Virginia Medical School  
in Partial Fulfillment of the  
Requirement for the Degree of**

**DOCTOR OF PHILOSOPHY**

**CARDIOVASCULAR SCIENCE**

**OLD DOMINION UNIVERSITY**

**and**

**EASTERN VIRGINIA MEDICAL SCHOOL**

**August 1997**

Approved by:

\_\_\_\_\_  
**Russell L. Prewitt, Ph.D. (Director)**

\_\_\_\_\_  
**Stephen J. Beebe, Ph.D. (Member)**

\_\_\_\_\_  
**Mark S. Elliott, Ph.D. (Member)**

\_\_\_\_\_  
**Thomas J. Lauterio, Ph.D. (Member)**

\_\_\_\_\_  
**Paul H. Ratz, Ph.D. (Member)**

## **ABSTRACT**

### **ENDOTHELIAL NITRIC OXIDE SYNTHASE AND GROWTH FACTOR REGULATION OF FLOW-MEDIATED VASCULAR REMODELING**

**David Anthony Tulis**  
**Old Dominion University and Eastern Virginia Medical School**  
**1997**  
**Director: Dr. Russell L. Prewitt**

This study was designed to characterize structural remodeling of male Wistar rat mesenteric arteries exposed to elevated blood flow *in vivo* for 1, 3, or 7 days. A series of arterial ligations induced blood flow increases in ileal and second-order branch arteries compared to same animal control vessels. Neither mean carotid nor local mesenteric arterial pressures changed significantly pre- to post-ligation. The primary flow-mediated force in both vessels was shear stress with possible involvement of acute stretch-induced wall stress in the ileal artery. Significant luminal expansion and medial wall hypertrophy occurred in the ileal and second-order arteries in a time-dependent fashion. Increases in extracellular connective tissue occurred concomitantly with arterial remodeling. Wall thickness to lumen diameter ratios did not change in any vessel at any time when compared to controls, suggesting normalization of flow-induced wall stress through vascular remodeling.

Immunostaining for proliferating cell nuclear antigen and nuclear profile analyses indicate that both medial SMC and intimal EC hyperplasia contribute to flow-induced remodeling of the vessel wall. Immunostaining for eNOS suggests its upregulation in response to elevated flow at all time points. Results from *in situ* hybridization reveal

significantly elevated PDGF-A mRNA expression in the media after 24 hours and in the endothelium after 3 and 7 days. Medial wall and endothelial expression of bFGF and TGF- $\beta$ 1 were negligible in both control and high flow vessels at all time points. Basal levels of PDGF-B transcripts were detected in control and high flow vessels, with no significant differences between the two groups. The findings from this study suggest flow-stimulated arterial remodeling *in vivo* involves SMC and EC hyperplasia and increases in extracellular connective tissue. This vessel wall restructuring may involve the actions of NO and PDGF-A as regulators of flow-stimulated growth; however, bFGF, TGF- $\beta$ 1, and PDGF-B do not seem to be involved.

**I would like to dedicate this work to my parents, Dr. and Mrs. Jerry J. Tulis. Their unwavering love and support helped me persevere through the most difficult times and ultimately reach my goal. Thanks, Mom and Dad. I love you both very much.**

## **ACKNOWLEDGMENTS**

First and foremost I would like to thank God, without whom none of this would have been achieved.

I would like to thank my academic mentor and Chairman of my Research Committee, Russell L. Prewitt, Ph.D., for providing me the opportunity to pursue my interests in cardiovascular research. I would like to acknowledge Joseph Unthank, Ph.D., Indiana University School of Medicine, for your guidance and input helped make this research project possible.

My sincere thanks to the members of my Research Committee: Stephen J. Beebe, Ph.D., Mark S. Elliott, Ph.D., Thomas J. Lauterio, Ph.D., and Paul H. Ratz, Ph.D. Your time, help, and guidance are all very much appreciated.

I would like to thank Paul Kolm, Ph.D., for providing valuable assistance, and Gerald J. Pepe, Ph.D., the Chairman of the Department of Physiology.

I would also like to thank Suzanne and Víctor for picking me up when I was down, for always being there when I needed them, and for making me laugh.

I would like to thank my family: Sherrie, Kevin, Nicholas, Elizabeth, Tim, Marilu, Melissa, Katy, and Strohs. Thanks for always being there and putting this all in perspective.

I would like to acknowledge the parish community at Sacred Heart Catholic Church for helping me learn what is really important.

Finally, I thank my parents, for providing the love, guidance, and support needed to travel life's journeys.

## TABLE OF CONTENTS

	PAGE
ABSTRACT . . . . .	ii
DEDICATION . . . . .	iv
ACKNOWLEDGMENTS. . . . .	v
COPYRIGHT. . . . .	vi
TABLE OF CONTENTS . . . . .	vii
LIST OF FIGURES . . . . .	x
LIST OF ABBREVIATIONS. . . . .	xii
 Chapter	
I. INTRODUCTION . . . . .	1
II. BACKGROUND AND LITERATURE REVIEW . . . . .	3
Arterial Anatomy and Physiology . . . . .	3
Arterial Remodeling . . . . .	4
Biophysical Forces in the Vasculature . . . . .	5
Studies on Flow-mediated Vascular Alterations . . . . .	8
Mechanisms of Flow-mediated Vascular Alterations . . . . .	16
Endothelial Nitric Oxide Synthase . . . . .	19
Platelet-derived Growth Factor . . . . .	25
Fibroblast Growth Factor . . . . .	32
Transforming Growth Factor . . . . .	35
III. HYPOTHESIS . . . . .	38
IV. RESEARCH DESIGN, MATERIALS, AND METHODS . . . . .	39
Rat Mesenteric Flow Model . . . . .	39
Hemodynamic Parameter Measurements . . . . .	45
Tissue and Slide Preparation . . . . .	46
Morphological Analysis . . . . .	48

	PAGE
Immunocytochemistry Protocols . . . . .	49
Proliferating Cell Nuclear Antigen . . . . .	49
Endothelial Nitric Oxide Synthase . . . . .	50
Extracellular Connective Tissue Staining . . . . .	51
cDNA Subcloning . . . . .	52
PDGF-A . . . . .	53
PDGF-B . . . . .	53
bFGF . . . . .	54
TGF- $\beta$ 1 . . . . .	54
<sup>35</sup> S-CTP Riboprobe Synthesis . . . . .	54
<i>In Situ</i> Hybridization . . . . .	55
Emulsion, Developing, and Counterstaining . . . . .	57
Statistical Analysis. . . . .	58
V.    RAT MESENTERIC FLOW MODEL INDUCES SIGNIFICANT INCREASES IN SHEAR STRESS WITH POSSIBLE CONTRIBUTION FROM WALL STRESS . . . . .	60
Introduction . . . . .	60
Results. . . . .	61
Discussion . . . . .	63
VI.   FLOW INDUCES ARTERIAL LUMINAL ENLARGEMENT AND MEDIAL WALL HYPERTROPHY THROUGH ENDOTHELIAL AND SMOOTH MUSCLE NUCLEAR REPLICATION AND CELLULAR HYPERPLASIA . . . . .	67
Introduction . . . . .	67
Results. . . . .	68
Rat Mesenteric Flow Model . . . . .	68
Morphological Analysis . . . . .	68
ICC Results for PCNA/SMC Nuclear Profile Analysis . . . . .	73
EC Nuclear Profile Analysis . . . . .	79
Discussion . . . . .	82
VII.  INCREASES IN EXTRACELLULAR CONNECTIVE TISSUE CONTRIBUTE TO FLOW-INDUCED VESSEL WALL HYPERTROPHY . . . . .	89
Introduction . . . . .	89
Results. . . . .	90
Discussion . . . . .	90

	PAGE
VIII. ENDOTHELIAL-DERIVED NITRIC OXIDE MAY MEDIATE FLOW-INDUCED VASCULAR REMODELING . . . . .	95
Introduction . . . . .	95
Results. . . . .	95
Discussion . . . . .	96
IX. EARLY MEDIAL AND SUBSEQUENT ENDOTHELIAL PLATELET-DERIVED GROWTH FACTOR-A CHAIN MAY BE INVOLVED IN FLOW-MEDIATED VASCULAR REMODELING <i>IN VIVO</i> . . . . .	101
Introduction . . . . .	101
Results. . . . .	102
Discussion . . . . .	102
X. PLATELET-DERIVED GROWTH FACTOR-B CHAIN IS NOT INVOLVED IN FLOW-INDUCED VASCULAR REMODELING. . . . .	109
Introduction . . . . .	109
Results. . . . .	110
Discussion . . . . .	110
XI. NEITHER bFGF NOR TGF- $\beta$ 1 CONTRIBUTE TO VESSEL WALL REMODELING FROM INCREASED BLOOD FLOW. . . . .	116
Introduction . . . . .	116
Results. . . . .	117
Discussion . . . . .	121
XII. CONCLUSIONS AND INFERENCES . . . . .	126
LITERATURE CITED . . . . .	127
VITA . . . . .	145

## LIST OF FIGURES

FIGURE	PAGE
4-1 Rat Mesenteric Flow Model . . . . .	41
6-1 Flow-Induced Alterations in Lumen Diameter . . . . .	70
6-2 Flow-Induced Alterations in Medial Wall Area . . . . .	71
6-3 Percent Change in Lumen Diameter and Medial Wall Area . . . . .	72
6-4 Medial Wall Thickness to Lumen Diameter Ratio . . . . .	74
6-5 Medial Wall Area to Lumen Area Ratio . . . . .	75
6-6 Medial Wall SMC PCNA Ratio . . . . .	76
6-7 Absolute Medial Wall SMC Nuclear Counts . . . . .	77
6-8 Normalized Medial Wall SMC Nuclear Counts . . . . .	78
6-9 Absolute Intimal EC Nuclear Counts . . . . .	80
6-10 Normalized Intimal EC Nuclear Counts . . . . .	81
7-1 Percent Extracellular Connective Tissue in Medial Wall . . . . .	91
7-2 Photomicrographs of Trichrome-Stained Extracellular Connective Tissue . . . . .	92
8-1 Endothelial NOS Protein Levels . . . . .	97
8-2 Photomicrographs of ICC Slides for eNOS . . . . .	98
9-1 Medial SMC PDGF-A mRNA Expression . . . . .	103
9-2 Endothelial PDGF-A mRNA Expression . . . . .	104
9-3 Autoradiographs for PDGF-A mRNA Expression . . . . .	105

	<b>PAGE</b>
10-1 Medial SMC PDGF-B mRNA Expression . . . . .	111
10-2 Endothelial PDGF-B mRNA Expression . . . . .	112
10-3 Autoradiographs for PDGF-B mRNA Expression . . . . .	113
11-1 Medial SMC bFGF mRNA Expression . . . . .	118
11-2 Endothelial bFGF mRNA Expression . . . . .	119
11-3 Autoradiographs for bFGF mRNA Expression . . . . .	120
11-4 Medial SMC TGF- $\beta$ 1 mRNA Expression . . . . .	122
11-5 Endothelial TGF- $\beta$ 1 mRNA Expression . . . . .	123
11-6 Autoradiographs for TGF- $\beta$ 1 mRNA Expression . . . . .	124

**LIST OF ABBREVIATIONS**

<b>AII</b>	<b>Angiotensin II</b>
<b>ANOVA</b>	<b>Analysis of Variance</b>
<b>ANF</b>	<b>Atrial Natriuretic Factor</b>
<b>BAEC</b>	<b>Bovine Aortic Endothelial Cell</b>
<b>bFGF</b>	<b>Basic Fibroblast Growth Factor</b>
<b>bNOS</b>	<b>Brain Nitric Oxide Synthase</b>
<b>cDNA</b>	<b>Complimentary Deoxyribonucleic Acid</b>
<b>cGMP</b>	<b>Guanosine 3',5'-Cyclic Monophosphate</b>
<b>CHO</b>	<b>Chinese Hamster Ovary</b>
<b>cNOS</b>	<b>Constitutive Nitric Oxide Synthase or Ca<sup>2+</sup>-calmodulin-dependent Nitric Oxide Synthase</b>
<b>CNS</b>	<b>Central Nervous System</b>
<b>CPM</b>	<b>Counts Per Minute</b>
<b>CTP</b>	<b>Cytosine Triphosphate</b>
<b>DAB</b>	<b>Diaminobenzidine Tetrahydrochloride</b>
<b>DEPC</b>	<b>Diethyl Pyrocarbonate</b>
<b>DNA</b>	<b>Deoxyribonucleic Acid</b>
<b>EC</b>	<b>Endothelial Cell</b>
<b>ECM</b>	<b>Extracellular Matrix</b>
<b>EDRF</b>	<b>Endothelium-Derived Relaxing Factor</b>
<b>EDTA</b>	<b>Ethylenediaminetetraacetic Acid</b>

<b>EGF</b>	<b>Epidermal Growth Factor</b>
<b>eNOS</b>	<b>Endothelial Nitric Oxide Synthase</b>
<b>FAD</b>	<b>Flavin Adenine Dinucleotide</b>
<b>FGF</b>	<b>Fibroblast Growth Factor</b>
<b>FMN</b>	<b>Flavin Mononucleotide</b>
<b>GTN</b>	<b>Glyceryl Trinitrate</b>
<b>HUVEC</b>	<b>Human Umbilical Vein Endothelial Cell</b>
<b>ICC</b>	<b>Immunocytochemistry</b>
<b>IGF-1</b>	<b>Insulin-like Growth Factor 1</b>
<b>iNOS</b>	<b>Inducible Nitric Oxide Synthase</b>
<b>ISDN</b>	<b>Isosorbide Dinitrate</b>
<b>ISH</b>	<b>In Situ Hybridization</b>
<b>L-NAME</b>	<b>N<sup>ω</sup>-Nitro-L-Arginine Methyl Ester</b>
<b>L-NMMA</b>	<b>N<sup>ω</sup>-Monomethyl-L-Arginine</b>
<b>LPS</b>	<b>Lipopolysaccharide</b>
<b>macNOS</b>	<b>Macrophage Nitric Oxide Synthase</b>
<b>MAP</b>	<b>Mean Arterial Pressure</b>
<b>mRNA</b>	<b>Messenger Ribonucleic Acid</b>
<b>NADPH</b>	<b>Nicotinamide Adenine Dinucleotide Phosphate - Reduced</b>
<b>nNOS</b>	<b>Neuronal Nitric Oxide Synthase</b>
<b>NO</b>	<b>Nitric Oxide</b>
<b>PBS</b>	<b>Physiological Buffered Saline</b>

<b>PCNA</b>	<b>Proliferating Cell Nuclear Antigen</b>
<b>PDGF-A</b>	<b>Platelet-derived Growth Factor-A Chain</b>
<b>PDGF-B</b>	<b>Platelet-derived Growth Factor-B Chain</b>
<b>PK-C</b>	<b>Protein Kinase-C</b>
<b>RNA</b>	<b>Ribonucleic Acid</b>
<b>SEM</b>	<b>Standard Error of the Mean</b>
<b>SMC</b>	<b>Smooth Muscle Cell</b>
<b>SNP</b>	<b>Sodium Nitroprusside</b>
<b>SSC</b>	<b>Standard Saline Citrate</b>
<b>SSRE</b>	<b>Shear Stress Response Element</b>
<b>TGF</b>	<b>Transforming Growth Factor</b>
<b>VEGF</b>	<b>Vascular Endothelial Growth Factor</b>
<b>WSR</b>	<b>Wall Shear Rate</b>

## CHAPTER I

### INTRODUCTION

Regulation of arterial tone, structure, and growth is accomplished through a variety of endogenous biochemical and biophysical factors. Vasoactive chemical mediators of vascular physiology include eicosanoid products, endothelial-derived relaxing and hyperpolarizing factors, mitogenic growth factors, angiogenic growth promoters and inhibitors, and autocrine and paracrine cytokines. Biophysical mechanical factors regulating vascular physiology include two primary hemodynamic forces: shear stress and circumferential wall stress. These various chemical factors and biomechanical forces help maintain normal vascular homeostasis as well as influence vascular growth and remodeling during angiogenesis, vasculogenesis, apoptosis, and vessel rarefaction. Alterations in these parameters, however, have been implicated in the development of vascular pathologies such as localization of atherosclerotic foci, pathogenesis of intimal and subintimal neoplasias, development of systemic hypertension, and diabetic microvascular disease. In an effort to further understand the contributions of biophysical mechanical forces and biochemical mediators on vascular pathophysiology, this research project characterizes the adaptive responses of rat small mesenteric arteries exposed to *in vivo* increases in blood flow under normotensive conditions. The relative contributions of the two primary flow-mediated hemodynamic forces in stimulating arterial remodeling will be assessed using a unique *in vivo* experimental model. Complete histologic and cellular analyses will be made of the gross morphological alterations induced by these stresses, and elucidation of the possible signal transduction and transmission pathways will be made through *in situ* hybridization and immunocytochemical approaches. The results from this

study will further characterize blood flow-associated stresses and their impact on biochemical signaling as endogenous stimuli capable of inducing arterial remodeling under *in vivo* conditions.

## CHAPTER II

### BACKGROUND AND LITERATURE REVIEW

#### Arterial Anatomy and Physiology

The arterial cross-section is composed of the intima, primarily an EC monolayer, the media, the muscular wall of the artery composed of SMC surrounded by an internal and external elastic laminae, and the adventitia, a dense collagenous structure containing bundles of collagen fibrils, elastic fibers, some SMCs and many fibroblasts. The EC layer is anatomically located between luminal blood flow and the underlying smooth muscle and extracellular components; therefore, the endothelium functions as a mechanically sensitive signal transduction interface between hemodynamic stresses and the vasoactive smooth muscle layer. On the basal aspect of the endothelium lies the extracellular matrix of the basement membrane, which is composed of four major classes of macromolecules: collagens, elastins, proteoglycans, and structural glycoproteins (89). The ECM functions to influence EC adhesion, spreading, migration, protein synthesis, proliferation, and differentiation (reviewed in 175). Other functions of the endothelium are maintenance of anticoagulant non-thrombogenic properties, control of lumen diameter and tissue perfusion, regulation of vascular permeability, metabolism of vasoactive substances, production of connective tissue and growth factors, and initiation of signal transduction cascades stimulated by acute inflammation, wound healing, and localization of atherosclerotic foci (35, 154).

The media is composed of SMCs oriented radially around the vessel circumference. Primary roles for the SMC layer include maintenance of arterial tone, synthesis of connective tissue and cholesterol, lipid metabolism, and reaction to vasoactive

agents through vasodilation or constriction (154). In both cell culture and the intact wall, SMCs can express two different phenotypes: a synthetic phenotype in which secretion is a primary function, and a contractile phenotype which is associated with vessel contraction and relaxation. Morphological alterations in the vascular wall from hypertension (95), atherosclerotic intimal thickening (54), and flow-mediated wall remodeling (179) primarily involve growth and proliferation of medial SMCs. Individual ECs and SMCs are surrounded by extracellular connective tissue, comprised of similar components as the ECM at the EC-SMC interface. The extracellular connective tissue is involved in cell-cell signal transmission and syncytial cellular coordination. The outlying adventitia contains many lymphatic channels and nerve fibers that help innervate the vessel wall. The adventitia is also highly vascularized and provides the vessel wall with nutrients as well as growth factor and cytokine production (154).

### Arterial Remodeling

Vessel wall remodeling can be broadly defined as any reorganization of wall components involving both increases and decreases in wall area. Remodeling can be viewed in terms of 1) gross network changes involving alterations in vessel length, vasculogenesis and/or angiogenesis, vessel arborization, and vessel rarefaction; or 2) organizational changes involving medial wall hypertrophy, intimal thickening, luminal enlargement, and ECM and/or connective tissue restructuring. Cellular mechanisms behind these gross morphological changes can include EC and SMC hyperplasia, cellular hypertrophy, cellular migration, cell lysis and death or apoptosis (32). Changes involving nuclear ploidy may also occur consistent with alterations in cell mass. Remodeling is an active process that enables the vessel to accommodate to changes in the local environment

in order to maintain normal vessel geometry and tissue perfusion (160). Control of arterial remodeling is multifactorial and depends on factors such as cytokines, growth factors, neurotransmitters, hormones, autacoids, and mechanical forces (32). This multifactorial control, however, predisposes remodeling to be incongruous throughout the vasculature. Inter- and intra-vascular heterogeneity of structural remodeling has been examined in experiments using whole animals, cultured cells and organs, and in models of arterial injury and hypertension (reviewed in 32).

### Biophysical Forces in the Vasculature

Biophysical forces in the vascular system can be described as stresses acting upon cellular and extracellular components of the vessel wall. Stress is defined as any force acting per unit area, and in the vasculature may be manifested as pressure and compression acting normal to a surface, frictional shear at the surface, and opposing tensile stresses acting outward from the surface (39). Circumferential wall stress, or hoop stress ( $\sigma$ ), acts normal to the cell surface and creates a force in a circumferential direction on the cross-section of the vessel. This compressive force is sensed primarily by the elastic, collagenous, and smooth muscle load-bearing components of the subendothelial wall. Using the LaPlace relation and assuming isotropic conditions exist in the vessel wall, circumferential wall stress is directly proportional to wall tension [the product of transmural pressure (P) and vessel inner radius (r)] and inversely proportional to vessel wall thickness (w). The equation for circumferential wall stress is  $\sigma = Pr/w$ ; therefore, under conditions of increased pressure, wall stress can be normalized through an increase in vessel wall thickness (36, 109). In addition, if local pressure is held stable, luminal enlargement concomitant with increases in medial wall thickness can offset any changes in

wall stress. Estimates for wall stress in arterioles and venules range between  $0.5 - 10 \times 10^5$  dynes (dyn) per square centimeter ( $\text{cm}^2$ ; ref. 165).

In comparison, shear stress ( $\tau$ ) is a frictional, tangential force exerted by blood flow on the luminal aspect of intimal ECs in the same direction as blood flow. This stress is sensed primarily by intimal ECs which can transfer this stimulus into internal stresses that may be transmitted to abluminal sites of attachment or to neighboring ECs through biochemical cascades or cytoskeletal activation. Transduction of these stresses to the underlying smooth muscle layer or to adjacent ECs may occur through mechanically-sensitive focal adhesion sites (38) and/or through metabolic and electrical coupling via gap junctions (36). In addition, medial SMCs have been found to be directly exposed to shear stress through interstitial fluid flow movement (3). Using the Poiseuille-Hågen relation and assuming complete laminar flow with a Reynold's number less than 2000, wall shear rate ( $\gamma$ ;  $\text{sec}^{-1}$ ) is directly proportional to fluid volume flow ( $Q$ ) and inversely proportional to the vessel radius ( $r$ ). The equation for WSR is  $\gamma = (m + 2)Q/\pi r^3$ . The dimensionless factor  $m$  depends on flow conditions:  $m = 2$  for laminar flow and  $m > 2$  for turbulent flow (145). For conditions of constant fluid viscosity ( $\mu$ ), shear stress is proportional to WSR. The equation for laminar shear stress, therefore, is  $\tau = 4Q\mu/\pi r^3$ , and is measured in  $\text{dyn}/\text{cm}^2$ . These equations indicate that under conditions of increased flow, a small increase in radius can restore WSR and shear stress to normal values. However, if vessel radius is held constant during periods of increased flow, a direct increase in shear stress occurs. Luminal shear stresses have been measured as negative values in regions of flow reversal,  $< 1 \text{ dyn}/\text{cm}^2$  in veins and in regions of flow separation, and  $> 100 \text{ dyn}/\text{cm}^2$  at bifurcations of larger arteries or during episodes of increased cardiac output or

hypertension (35, 36, 145). Shear stresses from interstitial fluid movement surrounds medial SMCs and have been calculated to range between 1 (188) and 10 dyn/cm<sup>2</sup> (2). Homeostatic arterial luminal mean shear stress is continuously regulated through endothelial-dependent vasodilation at approximately 15 dyn/cm<sup>2</sup> (109), which produces the lowest energy cost for propelling blood volume through a branched network.

In a homeostatic vascular system, blood flow is generally laminar with constant and predictable shear stresses. However, in areas of non-uniform geometry where arborization, bifurcations, and curved regions occur, flows tend to separate forming vortices and eddies characteristic of turbulent flow. In these regions, the frequency, magnitude, and direction of blood flow become chaotic, and shear stresses can fluctuate greatly and even form negative values in regions of flow reversal (36). Under transitional flow conditions, with Reynold's numbers between 2000 and 3000, disturbed laminar flow can occur with complex flow lines and a wide range of shear stresses. Consideration of these various forms of blood flow is necessary when studying shear stresses in different levels of the vasculature. In addition, large conduit arteries convey blood flow that is pulsatile, corresponding to systole and diastole of the cardiac cycle; therefore, large vessels are exposed to a range of shear stresses and stress gradients when compared to the steady flows found in the smaller arteries and in the microcirculation. Nevertheless, Barbee et al. (12), using atomic force microscopy to study the luminal surface of endothelial cells exposed to varying flow conditions, defines blood flow as "quasi-steady" and approaching laminar near the EC luminal plasma membrane even in pulsatile large artery flow.

### Studies on Flow-mediated Vascular Remodeling

The influence of blood flow on the vascular system has been studied for over a century. Thoma, in 1893, found a significant correlation between the diameter of a chick embryo vessel and the blood flow that it conveys (referenced in 59, 77). Thoma discovered that, during angiogenesis, blood vessels with the fastest blood flow rates became the dominant arteries while the vessels with slower flow rates constricted and eventually atrophied. Early works by Schretzenmayr, Fleisch, and Hilton (referenced in 166, 168) attributed flow-induced dilation during functional hyperemia in large arteries to a vascular reflex or to a conducted process through the vessel wall. Other early investigators studied the influence of blood flow on the state of constriction of vessels using various models such as arteriovenous fistulas (63, 144) and vasculogenesis and angiogenesis in the collateral circulation (100, 190). In 1975, Rodbard suggested that the endothelial layer of arteries senses increased blood flow and releases a vasodilating substance that acts on the medial smooth muscle to cause dilation (152). More recent studies using various *in vivo* and *in situ* models have determined that a significant correlation exists between blood flow and the extent of vessel dilation (67, 91, 92, 114, 139, 167, 168). More specifically, the degree of constriction of an artery has been determined to be inversely proportional to the blood flow conveyed through it.

Arterial ECs are the primary sensors for the fluid flow shear stress stimulus acting to regulate flow-induced vascular dilation. Smiesko et al. (167), using a canine femoral arteriovenous shunt model whereby femoral artery blood flow could be manipulated, showed a marked  $15.8 \pm 2.7\%$  increase in femoral artery diameter when blood flow increased from 10 to 293 ml-min<sup>-1</sup>. The response time for complete dilation was

approximately 80 seconds, and was preceded by an initial constriction of the vessel for approximately 15 seconds. After the luminal endothelium was removed by a balloon technique, the flow stimulus failed to cause any significant dilation response. The authors found that removal of the endothelium did not cause the artery to lose its basal tone, and concluded that based on their model using large conduit femoral arteries, an intact endothelium is necessary to permit flow-mediated arterial dilation. Similarly, Pohl et al. (137), using a canine femoral arteriovenous shunt model, induced approximately a 5-fold increase in femoral blood flow resulting in a transient latent response period followed by a significant vasodilation response in the presence of normal pressure. This response was completely abolished by both mechanical removal of the endothelium (via balloon catheter) and by chemical inactivation of the endothelium (via hydrogen peroxide treatment).

Hull et al. (67), using femoral-external jugular and saphenous artery-external jugular arteriovenous shunts in dogs, induced a 10-fold increase in blood flow causing significant 9% and 15% increases in femoral and saphenous artery diameters, respectively. These dilation responses consisted of transient decreases in arterial diameter corresponding to an initial drop in pressure, followed by rapid relaxation of the vessels in a manner proportional to the blood flow increase. A significant decrease in femoral arterial pressure occurred upon establishment of the arteriovenous shunt; however, this decrease in transmural pressure was found not to affect the dilation response. Also, an increase in pulse pressure was observed in this model, but this was also determined not to affect the response. Upon removal of the EC layer through mechanical rubbing, neither vessel dilated under increased flow conditions, suggesting a direct endothelial-dependent flow-

induced dilation in these large vessels. Inhibition of phospholipase A<sub>2</sub> by quinacrine attenuated the dilation response in a dose-dependent manner; however, cyclooxygenase inhibition through indomethacin treatment did not affect the response. These results indicate that the flow-mediated relaxation of large vessel smooth muscle is related to activation of phospholipase A<sub>2</sub>, and may involve a non-prostaglandin metabolite of arachidonic acid.

In a similar study, Kaiser and Sparks (76), using the same femoral-external jugular and saphenous-external jugular arteriovenous shunt model in dogs, further characterized the influence of the endothelium on flow-dependent arterial dilation. A cyclooxygenase and lipoxygenase blocker, 5,8,11,14-eicosatetraenoic acid (ETYA), caused irreversible inhibition of flow-induced dilation as well as significantly increasing the ED<sub>50</sub> for acetylcholine-induced relaxation; however, indomethacin did not affect the dilation response. Exposure of the femoral and saphenous arteries to methylene blue, an inhibitor of guanylate cyclase activation, caused a dose-dependent decrease in the dilation response to flow. These results suggested that both cyclic GMP and a non-prostaglandin lipoxygenase-dependent arachidonic acid metabolite are involved in the response to flow. Based on the results using an H-1 receptor antagonist tripeleminamine, these authors believe that increased blood flow stimulates a local increase in histamine which binds to the H-1 receptor and increases phospholipase A<sub>2</sub> activity. This initiates a cascade of events leading to endothelial production and release of a non-prostaglandin arachidonic acid metabolite. This metabolite, in turn, stimulates EDRF which activates a vascular smooth muscle guanylate cyclase to increase cyclic GMP resulting in large vessel relaxation.

Comparable studies have been performed investigating the significance of reduced blood flow on large vessels. Guyton and Hartley (58) used flow-restricting silver clips *in vivo* to alter unilateral carotid blood flow in juvenile rats. After 6 weeks of development, carotid arterial diameters increased 36% on the flow-restricted side and 62% on the contralateral control artery. After 12 weeks of development, changes were not significantly larger than at the earlier time point of 6 weeks. Overall flow reduction averaged 35% corresponding to an overall decreased diameter growth averaging -10.2% of the contralateral control carotids. Cross-sectional area of the tunica media was significantly reduced on the flow-restricted artery, yet the medial area to circumference ratio (which is proportional to vessel wall thickness) did not change. These results infer a direct relationship between blood flow, vessel dilation, and vessel wall growth in developing rats. Additionally, these authors found that the flow-induced changes correlated best with net changes in flow pulsatility and were not correlated with changes in mean flow velocity. They suggest that oscillatory shear stress is the primary force leading to flow-mediated arterial changes. Langille et al. (91) compared the adaptive responses of external carotid arteries following 70 - 80% flow reductions in weanling and mature rabbits. After 1 month of flow restriction (-79%) in the presence of normal arterial pressure, young rabbits experienced significant reductions in ipsilateral carotid artery DNA levels (-35%), elastin content (-38%), wall mass (-30%), and internal diameter (-31%) when compared to contralateral control carotid arteries. In mature rabbits, a decrease in intimal endothelial cell number (-15%) after 1 month and a decrease in internal diameter (-21%) of the ligated carotid artery was observed at 1, 2, and 4 weeks after flow obstruction, yet no significant differences were seen in medial or adventitial constituents.

These authors suggested that blood flow alterations occurring during weanling development may modulate proliferation of cellular and extracellular vessel wall components as well as normal flow-mediated dilatory responses. Pharmacologic interventions indicated that adult responses to decreased flow may involve two phases: a transient, papaverine-sensitive response, vasoconstrictor in origin, followed by a sustained, papaverine-insensitive structural reduction in diameter consisting of cellular remodeling. Treatment with indomethacin and captopril implied that neither prostaglandins nor a local renin-angiotensin system were involved in these responses. Also, manipulation of local flow conditions indicated that vessel responses were consistent only with changes in mean flow velocity, not pulsatile flow.

In a similar study by Langille and O'Donnel (92), ligation of the left external carotid artery yielded a 70% reduction in common carotid blood flow in rabbits with no significant change in flow through the contralateral common carotid. After 2 weeks of flow restriction, the reduced flow vessel exhibited a 21% decrease in lumen diameter when compared to the normal flow contralateral artery. Results from papaverine administration suggested that the reductions in carotid diameter after 2 weeks of flow reduction may reflect structural remodeling of the arterial wall rather than prolonged constriction of the medial smooth muscle. Complete abolition of the diameter reduction from diminished flow occurred upon removal of the intimal endothelial layer by both mechanical (balloon catheter) and chemical (Triton X-100) methods. These results support the vital role for intimal endothelium in sensing flow alterations and relaying the message for medial smooth muscle dilatory responses. In a more recent study from the same laboratory (186), common carotid artery ligation resulted in an 80% decrease in flow through the ligated

artery, corresponding to a 73% decrease in calculated shear stress. This reduced EC density by 33%, coincident with an 18% decrease in diameter after 5 days. This vessel also exhibited a substantial number of monocytes adhering to the endothelial surface at cell-cell junctions which appeared to be migrating across the endothelium into the subintimal space. This may be significant since monocyte adherence and transmigration, and subsequent differentiation into macrophages, are early events in the atherogenesis process. The contralateral carotid artery exhibited a 123% increase in blood flow, corresponding to a 170% increase in calculated shear stress. The contralateral carotid, despite these large increases in flow, did not significantly dilate after 5 days, and luminal EC density was not altered when compared to sham controls. Considering the studies discussed above, the vital role of luminal ECs in mediating the direct dilatory responses from high flow conditions in large conduit vessels is substantiated.

In addition to the investigations described above on large conductance and feed vessels, other studies have addressed the impact of flow on smaller microvascular arteries and resistance arterioles. Smiesko et al. (168), using rat mesenteric arcading arterioles (control lumen diameters 40 - 110  $\mu\text{m}$ ) exposed to increased blood flow velocity ( $\sim 570\%$ ) through collateral circulation *in vivo*, found a significant 70% flow-dependent vasodilation after a short latent period. The dilation response lasted for the duration of the experiment ( $\sim 10$  min), and was significantly correlated with red blood cell velocity, blood flow volume, and calculated WSR. Arcading arteriolar WSR increased from 722  $\text{sec}^{-1}$  to 5156  $\text{sec}^{-1}$  with establishment of the collateral circulation pathway. These authors proposed that there may not be a controlled stable set point for WSR in mesenteric arcading arterioles.

Koller and Kaley (84), using parallel occlusions in third-order arterioles of rat

cremaster skeletal muscle (mean control diameter 22.5  $\mu\text{m}$ ), induced a 230% increase in calculated arteriolar blood flow in the presence of normal arterial pressure. This resulted in an immediate 87% increase in calculated WSR and, following a brief (6 - 15 sec) latent period whereby diameter actually decreased, a significant 31% increase in arteriolar diameter. This increase in vessel diameter subsequently decreased the calculated WSR to approximately 46% over that of controls. In the presence of an intact endothelium under control flow conditions, the distribution of data was monotonic and calculated WSR was not correlated with arteriolar diameter. This suggests that during normal homeostatic conditions, WSR, and therefore shear stress (in the presence of stable blood viscosity), may be a controlled parameter in skeletal muscle microvascular networks. In addition, during periods of increased blood flow velocity, flow-dependent dilation occurs to regulate shear stress towards a pre-determined set point. Local impairment of the vasoactive functions of the endothelial layer through mercury light-sodium fluorescein (light-dye) treatment resulted in a slight decrease in control lumen diameter with a subsequent 36% increase in control calculated WSR when compared to control values with an intact endothelium. Arteriolar occlusion and increased flow showed complete abolition of the flow-induced dilation, corresponding to a highly significant 290% increase in calculated WSR. This increased WSR was not regulated or compensated for (through dilation) as when the endothelium was intact, supporting a role for endothelial regulation of WSR (and shear stress) in the microvasculature.

Comparison between flow-induced alterations in normal versus spontaneously hypertensive rats was performed by Qui et al. (139) on mesenteric conductance arteries (mean control diameter 500  $\mu\text{m}$ ). Using an *in situ* perfused mesenteric arterial tree, and

controlling mesenteric blood flows between 0.2 and 4.0 ml/min, intraluminal mesenteric pressure was found to increase linearly with flow in both normal and hypertensive rats, with absolute pressures for the hypertensive animals significantly higher. There was a mild trend for an increased diameter with flow in both normal (5%) and hypertensive (4%) rats, although no difference existed between the two populations. Removal of the luminal endothelium by CO<sub>2</sub> gas infusion resulted in increased arterial resistance in both rat strains, with a decreased lumen diameter only in the normal rats. Administration of L-NAME to inhibit NO synthesis did not alter mesenteric pressure in either strain. L-NAME significantly decreased conductance arterial diameter during flows of 0.2 and 2.0 ml/min in normal rats while not having any effect on diameters in the hypertensive rats. Results from this *in situ* model using both normotensive and hypertensive rats suggests that luminal endothelium plays similar roles in the control of mesenteric arterial resistance in both strains, and that conductance arteries from normal rats exhibit significant flow-diameter dependency which is adversely altered by both endothelium removal and NOS inhibition. In contrast, in hypertensive rats the diameter-flow relationship was not susceptible to alterations induced by L-NAME or by removal of the endothelium. In both strains, a positive interaction was discovered between flow-induced vessel dilation and increases in mesenteric transmural pressure.

Through establishment of a unique unilateral orchidectomy model in developing rats whereby blood flow was decreased subsequent to a decreased demand, Wang and Prewitt (187) analyzed microvascular cremaster arterioles during normal development and in the presence of reduced blood flow. Three weeks after performing the orchidectomy, and using arterioles of the intact contralateral cremaster muscle for controls, total

ipsilateral blood flow was reduced approximately 44%, yet flow per gram of tissue remained stable. The reduced flow yielded inhibition of normal vascular development as evidenced by the following: the lumen diameters of feeding (1A), arcading (2A), precapillary (3A), and transverse (4A) arterioles; the number of 4As per 3A; and the cross-sectional wall areas of 1A, 2A, and 3A arterioles, were all diminished when compared to controls. The authors speculated that the decreased blood flow resulted in a diminished shear stress, which alone or in combination with an altered production of metabolic growth factors, mediated the flow-dependent arteriolar growth retardation. In addition, a significant correlation was found between cross-sectional wall area and relaxed ( $10^{-3}$  M adenosine) internal diameters for all 4 orders of cremaster arterioles. In summary, results from these studies have substantiated the role of intimal ECs in sensing fluid shear stress and in mediating responses of the adjacent medial smooth muscle layer in both large and small vessels.

#### Mechanisms of Flow-mediated Vascular Remodeling

Considering the location of the endothelium and its vital role as a biomechanically responsive interface between flow-mediated shear stress and the medial wall, most experiments performed on shear stress have utilized cultured ECs from a variety of sources. These experiments generally use a cone-plate viscometer, a parallel-plate viscometer, or a capillary tube viscometer to expose the grown endothelial monolayer to controlled shear stresses (109, 148). The cone-plate viscometer has the advantage of not exposing ECs to a hydrostatic pressure component (in addition to shear stress). When the endothelium is exposed to increased shear stress, diverse responses occur ranging from immediate changes (msec) to prolonged chronic changes (hours to days). Rapid responses

include primarily biochemical and electrophysiological events such as changes in ionic conductance, inositol triphosphate generation, adenylate cyclase activity, activation of guanosine 3',5'-cyclic monophosphate (cGMP), elevation of intracellular free calcium, release of neurotransmitters including substance P, ATP, and acetylcholine, and the release of significant amounts of NO and prostacyclin necessary for smooth muscle-dependent dilation (12, 35, 37, 165). Evidence indicates these early responses to flow act primarily to initiate second messenger cascades, induce vasotonic adjustments, and start EC deformation as an auto-regulatory mechanism to decrease the amount of shear stress to which the endothelium is exposed (148, 166). Secondary intermediate responses are primarily biological growth responses associated with transcription factor activation, regulation of gene transcription, protein synthesis, and changes in cell cycle kinetics. Initiation of gene transcription for factors such as *c-fos*, *c-jun*, endothelin-1, nuclear factor kappa B, eNOS, tissue plasminogen activator, TGF- $\beta$ 1, monocyte chemotactic protein, bFGF, and PDGF all occur within minutes to several hours after onset of the stimulus (35, 148, 165). These secondary responses can also include stimulation of pinocytosis, initiation of cytoskeletal reorganization, focal adhesion rearrangement, and diverse cell-wide adaptive responses. Delayed responses represent chronic cellular adaptations to new hemodynamic conditions and include permanent cytoskeletal reorganization and cell alignment, organelle redistribution, normalization of mRNA levels, increased mechanical stiffness, and extracellular matrix restructuring with changes in thrombomodulin, collagen, and fibronectin synthesis (35, 37, 148).

Endothelial mechanotransduction of a shear stress stimulus generally operates via one of two mechanisms, or most likely through a combination of both, and involves many

of the factors cited above. The first pathway involves shear stress-generated force transmission through cytoskeletal components acting to distribute the sensed stimulus to the nucleus, to neighboring ECs, or to abluminal focal adhesion sites of attachment on the substratum. Luminal transmembrane proteins are stimulated by shear stress leading to conformational changes in vimentin-rich intermediate filaments and F-actin stress fibers (35). On the abluminal focal sites, conformational changes in these microfilaments can activate, through various linker proteins (talin, vinculin, paxillin,  $\alpha$ -actinin), membrane integrins associated with both the intracellular and extracellular environments. This could lead to rapid transmission of the stimulus through the substratum to the medial SMC layer and subsequent responses (37). The second pathway involves force signal transduction through the EC involving luminal membrane signaling and second messenger stimulation. This, in turn, initiates a biochemical signaling cascade leading to nuclear gene regulation and adaptive responses. The membrane signaling step entails sensing the shear stress stimulus through a shear stress-sensitive ion channel, possibly a non-specific stretch-activated antiport channel allowing sodium and calcium entry with potassium removal from the EC (93), or a shear-dependent opening of a potassium channel leading to hyperpolarization of the cell coincident with calcium entry (128, 131). This initial response can initiate a biochemical cascade involving phosphatidylinositol metabolism, cyclic GMP, protein kinase C, and activation of nuclear transcription factors such as nuclear factor kappa B, activator protein-1, and a shear stress-sensitive response element (34, 37). These, in turn, may regulate gene activation for such factors as PDGF, TGF- $\beta$ 1, immediate early genes (*c-fos*, *c-jun*, *egr-1*), tissue plasminogen activator, endothelin-1,

monocyte chemotactic protein-1, vascular cell adhesion molecule-1, intracellular adhesion molecule-1, and NOS (34, 35, 37).

In addition to these experiments aimed at analyzing the influence of shear stress on ECs, several investigators have recently discovered that medial SMCs in intact blood vessels can directly experience shear stress (3, 4, 188). These authors have shown that SMCs can be exposed to shear stresses up to  $10 \text{ dyn/cm}^2$  as a result of interstitial fluid flow driven by the transmural pressure gradient across the medial wall. The impact of shear stress on medial SMCs may stimulate similar biochemical factors as those cited above for the endothelium; however, further work needs to be done in examining the direct impact of shear stress on SMCs.

Through a derivation in the LaPlace relation, vasoactive flow-mediated luminal expansion can increase circumferential wall stress. Experiments analyzing the impact of wall stress on vessel remodeling have been performed on ECs and SMCs from a variety of experimental preparations (reviewed in 165). Both ECs and SMCs exposed to wall stress experience similar responses compared to those discussed above for shear stress. These include ion channel activation, protein phosphorylation, second messenger signaling, gene activation, growth factor induction, and cellular structural remodeling (165). Several recent reviews offer thorough comparisons of these and other mechanical stresses and their roles in vessel remodeling (46, 121, 165).

### Endothelial Nitric Oxide Synthase

Nitric oxide is an endothelium- and smooth muscle-derived vasoactive factor that was originally identified by Furchgott and Zawadzki in 1980 (49). Based on their

experiments using rat isolated aortic rings, results suggested acetylcholine stimulated ECs to release an “endothelium-derived relaxing factor” that induced vessel relaxation. This mediator was later identified as nitric oxide by Furchgott and others (47, 69). Nitric oxide contributes to the regulation of local and systemic vascular resistance, distribution of blood flow and oxygen delivery, electrolyte balance, and regulation of arterial pressure (178).

Nitric oxide is synthesized by vascular ECs and SMCs from one of the two terminal guanidino nitrogens of L-arginine following its conversion to L-citrulline by a nitric oxide synthase enzyme complex. Three isoforms of NOS have been identified which share <59% homology in terms of human amino acid sequences (43). Isoform I of NOS has been referred to as bNOS (brain) or cNOS (constitutive and/or  $\text{Ca}^{2+}$ -regulated), but is commonly termed nNOS (neuronal). Isoform I is constitutively expressed in neuronal and certain epithelial cells and is regulated by  $\text{Ca}^{2+}$  and calmodulin. Isoform I functions indirectly to regulate synaptic transmission of the CNS, mean arterial blood pressure, and smooth muscle relaxation and vasodilatation via peripheral nitrergic nerves (43). Isoform II is not constitutive but can be induced by various cytokines and bacterial lipopolysaccharide in a variety of cells. This isozyme is thus referred to as inducible NOS (also known as macNOS for the macrophage cell type). Isoform II is not dependent on  $\text{Ca}^{2+}$ -calmodulin. This isozyme acts to inhibit iron-containing enzymes and is involved in DNA fragmentation and in the pathophysiology of autoimmune diseases and septic shock (43). Both isoforms I and II are predominantly soluble enzymes, and both use molecular oxygen, NADPH as a cosubstrate, and FAD, FMN, and 6(R)-5,6,7,8-tetrahydrobiopterin as cofactors (178).

Isoform III of NOS normally accounts for both constitutive basal and stimulated NO synthesis in ECs throughout the vasculature (24, 43). This isozyme is more than 90% particulate (45); however, eNOS can be phosphorylated in response to certain agonists which induce translocation of the enzyme from the membrane-bound particulate fraction to the cytosolic subcellular fraction (116). Post-translational modifications of eNOS include palmitoylation and myristylation which, along with  $\text{Ca}^{2+}$ -calmodulin and intracellular pH, aid in its regulation. The addition of palmitic acid to eNOS has been shown to cause localization of the enzyme to endothelial caveolae (50), and depalmitoylation of eNOS was found to induce cytosolic translocation and subsequent phosphorylation (151). Sessa et al. (164) recently reported that eNOS is a Golgi-associated protein in cultured aortic and vein ECs and in intact vessels, and this membrane association is necessary for efficient synthesis of NO. Venema et al. (183), however, suggested that membrane association of eNOS functions to inhibit its catalytic activity by interfering with its calmodulin-binding domain. Isoform III of NOS uses heme, molecular oxygen, NADPH, FAD, FMN, and tetrahydrobiopterin as cofactors (178). Normal homeostatic conditions of the EC allow for basal levels of NO production through eNOS which continually regulates vascular resistance and maintains arterial tone. This occurs through stimulation of soluble guanylyl cyclase and modulation of cGMP in vascular SMCs (44, 70). Basal levels of NO produced from eNOS, as well as NO release through nitrergic nerves, serve to counterbalance the vasoconstriction normally produced by the renin-angiotensin system and the sympathetic nervous system. Basal release of endothelial NO also serves to maintain a nonthrombogenic vascular environment by inhibiting platelet aggregation and platelet and leukocyte adhesion to the vessel wall (5, 140, 141). Nitric

oxide has been found to stimulate DNA synthesis in microvascular ECs (198) as well as directly mediate angiogenesis and EC growth and migration (97, 199). In contrast, eNOS-mediated NO production has been shown by several investigators to inhibit DNA synthesis, mitogenesis, and proliferation of vascular SMCs (51, 52, 122). A negative feedback mechanism has been suggested for NO synthesis, as the addition of NO and NO donors non-competitively inhibit eNOS activity and endothelial NO production in response to receptor-dependent agonists and increased flow (8). Considering the role of hemodynamic stresses in regulating eNOS, the 5'-promoter region of eNOS contains a putative acute-phase shear stress response element similar to the SSRE found in PDGF and other shear stress-responsive genes (110).

Flow-induced increases in NO transcription and stimulation of NO production and release have been substantiated by numerous investigators using *in vitro*, *in vivo*, and isolated intact vessel preparations (27, 28, 62, 78, 87, 88, 103, 127, 130, 169); however, the regulation of eNOS by shear stress has only recently been investigated. This NO-dependent vasoactive relaxation in response to elevated blood flow acts as a feedback mechanism to restore wall shear stress towards normal homeostatic levels. Alternatively, any decrease in vessel diameter at constant flow would increase local shear stress, with subsequent endothelial NO-mediated vessel relaxation offsetting the original vasoconstriction (24).

Nishida et al. (126), in an initial attempt to characterize eNOS mRNA and protein expression, exposed BAECs to 15 dyn/cm<sup>2</sup> for 24 hours using a parallel plate viscometer. Northern and Western analyses revealed significant increases in eNOS mRNA transcript levels and eNOS protein expression in cells exposed to increased shear stress compared to

static controls. These increases in eNOS activity then, through production and release of NO, could have direct influence on shear stress-mediated endothelium-dependent vascular relaxation. A subsequent study by the same laboratory (177) attempted to characterize the mechanisms, time course, and dose response characteristics of these shear stress-induced increases in eNOS. In this study by Uematsu et al. (177), BAECs and HUVECs were grown on a parallel plate viscometer and exposed to shear stresses varying between 1.2 and 15 dyn/cm<sup>2</sup> for 1 to 24 hours. A 3 hour exposure to 15 dyn/cm<sup>2</sup> yielded an approximate 270% increase in eNOS mRNA versus static controls and directly increased eNOS mRNA levels in a dose-dependent manner. Results from administration of gene transcription inhibitors, potassium channel antagonists, and PK-C inhibitors suggested that shear stress-induced eNOS expression is dependent on *de novo* gene transcription, is regulated by potassium channel opening, and may not require PK-C activation. In addition, analysis of endothelial cell nitrite production indicated an increased capacity of the ECs to release NO upon exposure to shear stress.

Ranjan et al. (142) attempted to characterize the influence of shear stress on eNOS expression in BAECs and HUVECs. Using a parallel plate viscometer, eNOS peptide expression was elevated after a 3 hour exposure to 25 dyn/cm<sup>2</sup>. This increase remained through 12 hours of flow exposure. Shear stress exposure to 4 dyn/cm<sup>2</sup> did not elicit any significant increase in eNOS protein levels in either cell type. Endothelial NOS mRNA levels were found to be elevated 2- to 3-fold after 6 and 12 hours' exposure to both 4 and 25 dyn/cm<sup>2</sup>. Using dexamethasone to suppress the inducible function of eNOS, results indicated that all shear stress-mediated responses were specific for constitutive activation of eNOS. Results from various pharmacologic interventions suggested that flow-induced

NO was not involved in a positive feedback mechanism to cause an increase in eNOS, nor was PK-C activation necessary for the shear stress-mediated responses evidenced in this study.

The influence of cyclic strain on eNOS activity has recently been studied by Awolesi et al. (9, 10) using cultured BAECs. Endothelial cells subjected to deformation at 60 cycles/min with 6 and 10% strain exhibited upregulation of both eNOS transcripts and protein levels after 24 hours (9). In order to examine whether this upregulation was translated into functional activity, this same group analyzed ECs exposed to 10 and 24% strain for 24 hours (10). Nitric oxide production was indirectly assessed by measurement of L-citrulline accumulation and by measuring total nitrite in the media (according to the Greiss reaction). Results demonstrated that cyclic strain increases NO production through stimulated eNOS activity in cultured BAECs.

Recently, an interesting study was published considering the influence of NO on bFGF in inducing growth of aortic SMCs. Hassid et al. (61) exposed primary cultures of rat aortic SMCs to several agents capable of activating the cGMP pathway. These agents were found to stimulate bFGF-induced [<sup>3</sup>H]-thymidine incorporation by several-fold. These authors suggested that endogenous NO may act to amplify the mitogenic actions of bFGF *in vivo*. In addition, Morbidelli et al. (120) demonstrated that the mitogenic actions of VEGF on cultured coronary microvascular venular ECs are directly mediated by the presence of NO donors and inhibited by NOS antagonists. These results are supported by several investigators who found NO to be directly involved in cell replication and angiogenesis (97, 198, 199), but incompatible with the results indicating that NO alone inhibits growth and proliferation of aortic SMCs in culture (51, 52, 79, 122). Other

vasodilators, including ANF and calcium channel antagonists, also inhibit mitogenesis and proliferation of cultured vascular SMCs (2, 25).

### Platelet-derived Growth Factor

Platelet-derived growth factor is a 28 - 35 kD dimeric peptide secreted from SMCs, ECs, macrophages, and fibroblasts (155). PDGF exists as a disulfide-linked homo-(-AA or -BB) or hetero-dimer (-AB) which binds to specific high-affinity cell surface receptors on mesenchymal cells such as SMCs, ECs, fibroblasts, osteoblasts, and astrocytes (123, 16, 31). The PDGF receptors are composed of two complimentary subunits,  $\alpha$ - and  $\beta$ -, which bind in the presence of a PDGF dimer to form three distinct receptors:  $\alpha\alpha$ ,  $\alpha\beta$ , and  $\beta\beta$ . Ligand specificity of the receptors dictates that PDGF-AA binds only to  $\alpha\alpha$  receptors, PDGF-AB binds to  $\alpha\alpha$  or  $\alpha\beta$  receptors, and PDGF-BB binds to  $\alpha\beta$  or  $\beta\beta$  receptors (123). Upon ligand-receptor binding, all three forms of PDGF can bind heparin, stimulate vasoconstriction and SMC mitogenesis, and enhance chemotaxis in SMCs, monocytes, and neutrophils (153, 155). Much research has focused on characterizing these mitogenic and chemotactic properties of PDGF in various cell types under normal and stimulated conditions.

Under normal *in vivo* conditions, medial SMCs constitutively express low levels of PDGF-A mRNA (18), translated PDGF-AA protein (reviewed in 123), and PDGF- $\alpha$  and - $\beta$  receptors (113). PDGF-A, however, can also be expressed in microvascular endothelium (18). In comparison, under both normal *in vivo* conditions (18) as well as during atherogenesis (192) PDGF-B transcripts are localized primarily to the endothelium with lower levels found in the media (104). Several laboratories found cultured arterial SMCs capable of transcribing PDGF message in addition to the -A form (125, 163, 185).

Majesky et al. (104) found both PDGF-A and -B mRNA transcripts expressed in small amounts in normal newborn and adult rat aortic SMCs under *in vivo* conditions. In cell culture, PDGF-B transcripts accumulated in the SMCs of young rats with no PDGF-B expression observed in adult rat SMCs. Equal levels of PDGF-A mRNA were found in cultured SMCs in newborn and adult rats. These results suggested a differential expression of PDGF-B exists and may be related to the age of the animals. Barrett et al. (15) found a 3.7 kilobase RNA homologous to the *sis* (PDGF) gene expressed at extremely low levels in BAECs *in vivo*, at minimal levels in HUVECs *in vivo*, and at moderate levels in cultured human and bovine ECs. This implies that the PDGF gene may become activated under *in vitro* conditions, and the authors suggested that PDGF may be involved in vascular development of young animals and in maintenance of a homeostatic vascular system in adult animals.

The influence of physiologic stresses on PDGF transcription and protein translation has been performed on ECs and SMCs *in vivo* and in cell culture using models of hypertension (123), atherosclerosis (72), mechanical strain (193) and injury (30), flow reduction (85, 107) and flow elevation (64, 65, 66, 172). The remainder of this discussion focuses specifically on the effects of blood flow and its associated stresses on PDGF expression. Hsieh et al. (66), in 1991, investigated the effects of shear stress on PDGF-A and PDGF-B mRNA expression in primary HUVEC cultures. Under control conditions, the level of PDGF-A mRNA was negligible while a baseline level of PDGF-B mRNA expression was detected. Using a parallel plate flow viscometer and a physiologic level of shear stress (16 dyn/cm<sup>2</sup>), transient increases in PDGF-A (>10-fold) and PDGF-B (2- to 3-fold) mRNA occurred after approximately 1.5 hours and returned to baseline levels after

approximately 4 hours. Shear stress “dose-dependency” was analyzed using exposure levels from 0 to 51 dyn/cm<sup>2</sup> for 2 hours. Results showed a shear stress-dependent increase in both PDGF-A and PDGF-B mRNA between 0 and 6 dyn/cm<sup>2</sup>, with PDGF-A mRNA levels remaining elevated but steady between 6 and 51 dyn/cm<sup>2</sup>. PDGF-B mRNA levels subsequently declined between 6 and 31 dyn/cm<sup>2</sup>, then increased between 31 and 51 dyn/cm<sup>2</sup>. These results showed PDGF-A and -B expression can be enhanced through increased shear stress in HUVECs *in vitro*. In addition, these authors found that shear stress-induced PDGF-A exists as two major transcripts (~2.5 and 3.0 kb) and two minor transcripts (~1.7 and 3.8 kb), while shear stress-induced PDGF-B exists as a single transcript (~3.7 kb).

In 1992, Hsieh et al. (65) investigated the signaling mechanisms behind shear stress-induced PDGF expression in HUVECs. Using a similar protocol as in the experiment described above (66), and with the use of various pharmacologic agents, results suggested that shear stress-induced PDGF-A and -B mRNA expression is mediated by a calcium/phosphoinositide-dependent diacyl glycerol-activation of PK-C in which heterotrimeric G-proteins may also play a role. Basal levels of PDGF (primarily -B) expression were also determined to be PK-C-dependent. Protein kinase C, then, was hypothesized to activate nuclear gene transcription for PDGF. Prostaglandin synthesis, extracellular calcium, and cyclic AMP- and cyclic GMP-dependent protein kinases, however, were not involved in the shear stress-induced responses. In a subsequent study by the same authors (64), HUVECs were exposed to a physiologic level of shear stress (~16 dyn/cm<sup>2</sup>) in pulsatile (1 Hz) and steady flows on a parallel plate viscometer. Although PDGF-A mRNA levels were low in stationary cells, expression increased (>10-

fold) after 1.5 hours under both steady and pulsatile flows. PDGF-B mRNA levels were more abundant in stationary cells, and expression was also increased (<2-fold) after 1.5 hours under steady and pulsatile flows. Generally, steady flows elicited greater responses than pulsatile flows for both PDGF-A and -B transcripts. In this same study, hypothesizing that similar shear stress-induction mechanisms may exist for *c-fos* and PDGF, *c-fos* antisense technology was used to determine if *c-fos* regulates shear-induced PDGF induction. The antisense treatment completely abolished *c-fos* transcription without affecting PDGF mRNA induction, suggesting that flow-induced *c-fos* expression may not mediate flow-induced PDGF expression.

Further studies continued to elucidate the mechanisms of shear stress-induced PDGF expression. Mitsumata et al. (118) exposed BAECs to 30 dyn/cm<sup>2</sup> for periods up to 24 hours in a parallel plate viscometer in an attempt to examine the influence of PK-C in PDGF expression. PDGF-B mRNA expression was increased after 3 hours of exposure to shear stress, and significantly elevated 13-fold after 6 hours' exposure. PDGF-B mRNA levels remained significantly elevated for the duration of the experiment; however, control PDGF-A levels were quite low, and no significant changes in PDGF-A expression were observed at any time point during the experiment. Through the use of various pharmacologic agents that activate or inhibit PK-C, results suggested that both PK-C-dependent and PK-C-independent pathways exist that are capable of inducing PDGF-B mRNA expression in BAECs exposed to shear stress. In addition, these authors found an interesting result pertinent to the present study. Treatment of the ECs with TGF- $\beta$  (0.1 - 10 ng/ml) stimulated PDGF-B mRNA expression without affecting PK-C levels. In addition, in contrast to the results from Hsieh et al. (64) where *c-fos* mRNA expression

was significantly elevated after 30 minutes' exposure to shear, in this study 30 dyn/cm<sup>2</sup> did not alter *c-fos* expression at any time point.

Resnick et al. (147) used a cone-plate flow viscometer to expose BAECs to 10 dyn/cm<sup>2</sup> for 4 hours, and elicited a significant increase in PDGF-B mRNA. The promoter region of the human PDGF-B chain gene was found to contain the necessary elements for flow-responsiveness through use of a transfected reporter gene. Using a series of mutant human PDGF-B promoter (1.3 kb)-chloramphenicol acetyltransferase (CAT) reporter gene constructs transfected into ECs, these authors discovered a *cis*-acting component in the PDGF-B promoter region that is necessary for shear stress-responsiveness. This shear stress response element contains a six base pair core-binding sequence that binds to shear stress-induced transcription factors leading to gene expression. This transcription factor binding site (or its complement) has been found in the promoters of other shear stress-induced factors such as endothelin-1 (108), tissue plasminogen activator, the nuclear protooncogenes *c-fos* and *c-jun*, monocyte chemotactic protein, and intracellular adhesion molecule 1 (reported in 147). Halnon et al. (60) exposed BAECs to shear stress (10 dyn/cm<sup>2</sup>) in an effort to analyze the mechanism of PDGF-A mRNA induction. Shear stress elicited a several-fold increase in PDGF-A mRNA after 2 hours. CAT-reporter gene constructs transfected into ECs caused a two-fold increase in activity with exposure to shear stress, suggesting that shear stress-induced upregulation of PDGF-A mRNA is due in part to transcriptional activation. A SSRE specific for PDGF-A is thought to exist independent of the SSRE identified for PDGF-B, but this element has yet to be defined.

Considering the mechanisms of PDGF induction, Miano et al. (115) used a balloon injury model in rat aorta and found increased SMC *c-myc* and thrombospondin after 2

hours. This was followed by increased mRNA expression for PDGF-A, TGF- $\beta$ 1, and a bFGF receptor. Seven days after initiation of the injury, a spontaneous increase in *c-myc* and thrombospondin mRNA was detected again, followed 12 hours later by a significant increase in SMC DNA replication. These authors suggested that an autocrine mode of growth factor-stimulated SMC proliferation exists *in vivo*, and that immediate early genes act to regulate this process. This corroborates the findings of Reidy and coworkers (185) who demonstrated PDGF-induced SMC proliferation after arterial injury occurs *in vivo* through autocrine action affecting primarily intimal-associated SMC. In addition, Khachigian et al. (81) determined that *egr-1*, a serum-inducible phosphoprotein that acts as an “early growth response gene”, is stimulated through mechanical injury to displace the Sp-1 site on the PDGF-B promoter. This, in turn, upregulates PDGF-B in ECs exposed to mechanical vascular injury.

In contrast to the results discussed above concerning PDGF induction from exposure to shear stress, Malek et al. (107), using a cone-plate viscometer and cultured BAECs, found PDGF-B mRNA expression to decrease significantly 3.9-fold and 4.2-fold after 9 hours' exposure to steady laminar shear stress at levels of 15 and 36 dyn/cm<sup>2</sup>, respectively. This decrease, however, was preceded by a transient nonsignificant increase in PDGF-B mRNA at 30 minutes, followed by a return to control levels by 1 hour with subsequent decreases through 9 hours. PDGF-A mRNA expression was not detected in this cell line, consistent with the findings of Mitsumata et al. (118), yet contradictory to the results from Collins et al. (26) and Halnon et al. (60) on shear stress-induced ECs. No differences were observed between responses to steady and pulsatile flows (average ~15 dyn/cm<sup>2</sup>) or between laminar and turbulent flows, in terms of PDGF-B inhibition. These

authors suggested that the magnitude of shear stress is more important in growth factor regulation than the dynamic characteristics of the shear stress stimulus. In addition, temporal variation in the shear stress-regulation of PDGF mRNA expression may be evident considering the general trend for early PDGF induction (64, 65, 66, 147) followed by inhibition of PDGF mRNA expression (107). In a separate study by Kraiss et al. (85) using flow alterations in baboon aortoiliac prosthetic grafts, PDGF-A mRNA levels were significantly elevated in low-flow grafts compared to high flow grafts. Results from ICC and ISH indicated the increased PDGF-A protein and transcript levels were localized to the luminal endothelium and subjacent SMC layer. These authors proposed that abrupt reductions in blood flow induce accelerated neointimal thickening which may be temporally and anatomically regulated by PDGF-A. Similar results were found by Majesky et al. (106), who used a carotid balloon injury model and discovered both immediate and chronic elevation of PDGF-A transcripts and protein levels located preferentially on the neointimal SMCs.

Interactions between PDGF and other vasoactive peptides and growth factors have been studied using a variety of experimental protocols in various cell types. Stavri et al. (170) studied the roles of hypoxia and PDGF-B in inducing VEGF transcription in cultured rabbit aortic SMCs. Hypoxia alone strongly upregulated VEGF mRNA in a time- and concentration-dependent manner, reaching a maximum 30-fold increase after 12 - 24 hours. Exposure to PDGF-B caused only minimal increases in VEGF expression. The combination of hypoxia and PDGF-B administration, however, caused a synergistic increase in VEGF mRNA that was ~2-fold higher than the expected additive effect. These authors suggested that VEGF-mediated neovascularization may be mediated in part

through the synergistic interaction observed between hypoxia and PDGF-B in cultured SMCs. Bilato et al. (17) examined the interaction between bFGF and PDGF in mediating rat aortic SMC migration in cell culture. Basic FGF was weakly chemoattractant for SMCs but was required for PDGF-stimulated SMC migration. Further analysis demonstrated that bFGF exerted this effect through enhancing PDGF-mediated release of intracellular calcium and the subsequent activation of calcium-calmodulin-dependent protein kinase II. PDGF-B has also been suggested to upregulate FGF tyrosine kinase receptor mRNA and protein (90). Thommes et al. (174) found PDGF-A and IGF-1 to be weakly mitogenic for cultured rat aortic SMCs; however, co-administration of these factors resulted in significantly increased [<sup>3</sup>H]-thymidine incorporation and a strong increase in SMC number. These authors proposed that the synergistic actions of PDGF-A and IGF-1 might be due to differential activation of their intracellular signaling pathways. PDGF from extracts of human platelets has also been shown to rely on the presence of TGF- $\beta$ 1 and EGF in stimulating anchorage-independent transformation of neoplastic rat kidney fibroblasts (7). This oncogenic growth was found to depend on the presence of all 3 growth factors. Bonner et al. (19) determined that TGF- $\beta$ 1 causes downregulation of PDGF alpha receptors in fibroblasts during pulmonary fibrotic disease. These authors suggested that the proliferative and chemotactic influences of PDGF are dependent on the modulation of its receptor subtypes by other injury-induced cytokines such as TGF- $\beta$ 1.

#### Fibroblast Growth Factor

Basic fibroblast growth factor (bFGF) is a potent heparin-binding polypeptide mitogenic for vascular ECs and SMCs. Arterial and capillary ECs, SMCs, and fibroblasts can synthesize both aFGF and bFGF (18), while bFGF can also be produced in a wide

variety of tissues including brain, pituitary, retina, adrenal gland, kidney, corpus luteum, placenta, and in various tumors (162). Basic FGF has important chemotactic and angiogenic properties as well as vital roles in development of the vascular, nervous, and skeletal systems and in cellular differentiation (90). Lindner and co-workers found SMC proliferation in lesions resulting from endothelial denudation in rat carotid arteries to be bFGF-dependent (101, 102). Basic FGF has been shown to play a role in autocrine growth regulation for capillary ECs (162) and in autocrine migration of cultured ECs (117). Sakaguchi et al. (156) determined that bFGF acts in an autocrine fashion by binding to cell surface receptors from the cells where the factor was originally produced. Basal levels of transcription for both aFGF and bFGF are low; however, both proteins appear at relatively high levels in many tissues (124). This may be dependent on the fact that bFGF does not contain a signal sequence; therefore, release of bFGF peptides occurs through conjugation with carrier proteins (18), sequestration by ECM constituents (11), or through cell lysis in vascular injury (30). Newly synthesized bFGF can be secreted and become associated with the basement membrane and extracellular matrix components such as heparan sulfate (149). Saksela et al. (158) suggested that FGF conjugation with extracellular glycosaminoglycan heparan sulfate protects FGF from proteolytic degradation. In agreement, Baird and Ling (11) in their work on cultured BAECs, hypothesized that the neovascular response stimulated by bFGF is more regulated by the presence of heparinase-like enzymes than by the actual angiogenic or mitogenic activity of the growth factor. However, differential responses were observed by Yu et al. (196) in their work on cultured BAECs. These investigators discovered that cells cultured to subconfluency synthesized bFGF which became localized to the nucleus and exocytotic

vesicles, while confluent cells produced bFGF which became predominantly ECM-associated. Four distinct high affinity FGF receptors exist that exert tyrosine kinase activity and dimerize upon ligand-binding (124). FGF receptors have been identified on ECs, SMCs, myoblasts, and fibroblasts (18). Generally, most of these receptors have increased affinity for the basic form over that for the acidic form. For a thorough review of FGF receptors, please consult the articles by Schott and Morrow (161) or Bobik and Campbell (18).

Considering the angiogenic and growth-regulatory characteristics of bFGF and its role in mediating responses due to injury or in atherogenesis, bFGF has been proposed to play a role in the pathogenesis of shear stress-induced alterations. Sterpetti et al. (172) examined arterial SMCs exposed to varying degrees of shear stress, and found a “dose-dependent” release of bFGF into the medium that was still evident 24 hours after cessation of flow. Anti-bFGF antibody treatment verified the specificity of the mitogen, and results suggested shear stress stimulates SMCs to produce and release bFGF in direct proportion to the degree of flow in an *in vitro* system. Malek et al. (107) explored the effects of shear stress on induction of bFGF mRNA in BAECs cultured on a cone-plate viscometer. Steady laminar shear stress of 15 dyn/cm<sup>2</sup> elicited a significant 1.5-fold increase in bFGF mRNA between 30 minutes and 6 hours, declining to baseline levels after 9 hours. Steady laminar shear stress of 36 dyn/cm<sup>2</sup> caused a significant increase at 30 minutes, reached a 5-fold increase at 6 hours, and remained elevated 3-fold after 9 hours’ exposure. This elevated level of shear stress induced three bFGF mRNA species of approximate sizes 7.0, 4.0, and 1.9 kb. No differences were observed in bFGF mRNA expression between steady laminar and turbulent flows, or between steady laminar and

pulsatile laminar flows. These results suggest that the dynamic characteristics of the fluid flow do not play as important a role as the overall magnitude of the shear stress in terms of stimulating bFGF gene expression.

### Transforming Growth Factor

Transforming growth factor- $\beta$ 1 (TGF- $\beta$ 1) is a pleiotropic factor that has been shown to stimulate vascular SMC hypertrophy, inhibit mitogen-stimulated DNA synthesis, and has been suggested to be a mediator of SMC growth *in vivo* during atherogenesis and wound repair (6, 29, 105, 135). After synthesis, TGF- $\beta$ 1 is normally secreted from ECs, SMCs, and fibroblasts in a latent inactive form that is unable to bind to its cell surface mannose-6-phosphate/IGF II receptor (94). Certain factors such as angiotensin II, endothelin-1, and TGF- $\beta$ 1 itself are capable of activating the latent form and converting it into a biologically active form, which may then stimulate smooth muscle growth via hypertrophy or hyperplasia (18, 53).

Considering its bidirectional effects on SMC growth, TGF- $\beta$ 1 has been suspected as playing a role in shear stress-mediated vascular remodeling. Ohno et al. (131), exposing cultured BAECs to shear stress on a cone-plate viscometer, found expression of TGF- $\beta$ 1 mRNA to increase directly with increases in shear stress between 0 and 40 dyn/cm<sup>2</sup>. At constant exposure to 40 dyn/cm<sup>2</sup>, TGF- $\beta$ 1 mRNA levels increased several fold within 2 hours and remained elevated at 12 hours' exposure. These authors used a neutralizing TGF- $\beta$ 1 antibody to test for biologically active mature TGF- $\beta$ 1, which was found to increase significantly in conditioned medium. With use of channel blockers, results indicated that the shear stress-induced increases in TGF- $\beta$ 1 mRNA and TGF- $\beta$ 1 protein are mediated through an EC flow-activated potassium channel. In a subsequent

study (140) these same authors further examined the mechanism of shear stress-regulated TGF- $\beta$ 1 gene expression. Bovine aortic ECs exposed to 20 dyn/cm<sup>2</sup> on a cone-plate viscometer demonstrated a 3- to 5-fold increase in TGF- $\beta$ 1 gene transcription after exposure to shear stress for 2 hours. Using ECs transfected with TGF- $\beta$ 1 promoter-CAT reporter gene constructs, results indicated that shear-responsiveness of TGF- $\beta$ 1 gene expression is mediated by shear stress-responsive *cis* and *trans* elements activated through flow-regulated endothelial potassium channels.

In recent work by the same laboratory on shear stress-mediated TGF- $\beta$ 1 gene expression and protein secretion (128), cultured BAECs were subjected to varying levels of shear stress on a modified cone-plate viscometer. Low levels of flow (< 5 dyn/cm<sup>2</sup>) failed to induced significant alterations in TGF- $\beta$ 1 mRNA expression; however, between shear stresses of 5 and 40 dyn/cm<sup>2</sup>, TGF- $\beta$ 1 mRNA levels increased proportionately. In response to steady laminar shear stress of 20 dyn/cm<sup>2</sup>, ECs experienced a 3- to 5-fold increase in TGF- $\beta$ 1 mRNA levels after 2 hours' exposure, and produced a 4- to 10-fold increase in the amount of biologically active TGF- $\beta$ 1 protein as measured in the conditioned medium after 24 hours' exposure to increased flow. Using ECs transfected with the TGF- $\beta$ 1 promoter-CAT reporter gene constructs, results indicated that the shear stress responsiveness of TGF- $\beta$ 1 mRNA production is dependent on activation of the promoter region and involves transcriptional regulation. Results from channel blockade provided further evidence for dependency on a flow-activated endothelial potassium channel for increased TGF- $\beta$ 1 mRNA expression. These authors speculated that the mechanotransduction of a shear stress stimulus through ECs leading to increases in TGF-

$\beta 1$  involves regulation between potassium and calcium fluxes, with potassium-induced hyperpolarization possibly inducing calcium influx and calcium-dependent kinases and signaling cascades.

## CHAPTER III

### HYPOTHESIS

The general hypothesis for this research project is that elevated flow induces growth and remodeling of small systemic arteries in the presence of normal arterial pressures under *in vivo* conditions. These arterial adaptations are believed to be mediated by several endogenous flow-induced biochemical factors. In addition, considering the model established herein, we expect the primary mechanical stimulus experienced by the local vasculature to be flow-mediated shear stress with minimal contribution from stretch-induced wall stress.

Specifically, we believe that elevated shear stress will stimulate arterial remodeling primarily in a radial direction resulting in significant luminal enlargement. We expect this will involve a combination of cellular hypertrophy and hyperplasia for both the endothelial and smooth muscle layers between 1 and 7 days. We expect a restructuring of the extracellular connective tissue as well as early involvement of flow-induced NO (assessed through eNOS expression). We hypothesize that flow-induced shear stress will stimulate the expression of several mechanosensitive genes. Principally, we believe that endothelial PDGF-B mRNA and medial PDGF-A mRNA expression will be elevated and contribute to enhanced endothelial and SMC proliferation. Secondly, we believe that shear stress may act to regulate endothelial and/or smooth muscle bFGF mRNA and endothelial TGF- $\beta$ 1 mRNA expression. We expect detection of these changes in gene expression within 1 day after onset of increased flow and persisting possibly through 3 days.

## **CHAPTER IV**

### **RESEARCH DESIGN, MATERIALS, AND METHODS**

#### **Rat Mesenteric Flow Model**

All experimental protocols in this research project complied strictly with the guidelines instituted by the Animal Care and Use Training Program, Eastern Virginia Medical School, Norfolk, VA. The Animal Care Facility at EVMS is AAALAC approved and is directed by Thomas Sheehan, DVM. Three groups of ten male Wistar rats weighing approximately 300 grams each were anesthetized with Na<sup>+</sup>-pentobarbital (60 mg/kg IM, Anpro Pharmaceutical, Arcadia, CA) and given 0.1 cc penicillin G potassium (10,000 units IM, Marsam Pharmaceutical, Cherry Hill, NJ). Supplemental IM injections of Na<sup>-</sup>-pentobarbital were provided as needed in order to maintain a surgical level of anesthesia. Once surgical anesthesia was obtained, the abdomens were shaved clean and swabbed with a topical antiseptic/antimicrobial agent (Hibiclens, Wilmington, DE). The rats were placed supine on a warm heating pad (~ 37°C) and covered with a sterile surgical drape so that only the shaved abdominal wall was exposed. Using sterile technique, a midline laparotomy was made spanning the length of the abdomen from below the diaphragm to above the testis. The cecum, adjoining section of the small intestine, and supporting mesenteric membranes and vasculature were gently exteriorized and placed on the sterile drape. The cecum, intestines and mesentery were kept moist throughout the entire surgery with pre-warmed, sterile physiological saline (pH 7.4). The intestines and supporting vasculature were gently arranged in order to examine the fourth, fifth, and sixth ileal arteries (and veins) proximal to the ileocecal junction for any pre-

existing vascular anomalies. This section of the rat mesenteric vasculature was subjected to altered blood flow. In addition, the ninth ileal artery (and vein) proximal to the ileocecal junction was examined for any abnormalities and acted as the control section for the rat. If pre-existing vascular anomalies were present in these regions, appropriate vascular sections were found between the second and eighth ileal arteries proximal to the ileocecal junction for the treatment group, and between the ninth and the twelfth ileal arteries for the control group. If no anomalies were found, arterial ligations were made using sterile 10-0 Ethilon monofilament nylon suture (Ethicon, Inc., Somerville, NJ) on the following arteries as depicted in Figure 4-1: (1) the parent fifth ileal artery proximal to the ileocecal junction; (2) the second-order branch of the fourth ileal artery leading in the direction towards the fifth artery; and (3) the second-order branch of the sixth ileal artery leading in the direction towards the seventh ileal artery. In addition, any transverse marginal artery in the ligated arteriolar arcade that connected two second-order arterial branches was ligated to form a true barrier to collateral blood flow (4). Ileal arteries are defined as pre-branching first-order parent vessels leading from the superior mesenteric artery to the ileum, where each divides into two second-order branches. A marginal artery is defined as a transverse vessel segment joining two adjacent small arterial arcades. Marginal and second-order arteries give rise to first-order (1A) arterioles that directly feed the bowel wall.

Ligations at these specific sites allows various vessels to be subjected to four different scenarios: (A) high flow, normal pressure in a large ileal artery; (B) high flow, normal pressure in a smaller second-order artery; (C) no flow, normal pressure in a smaller

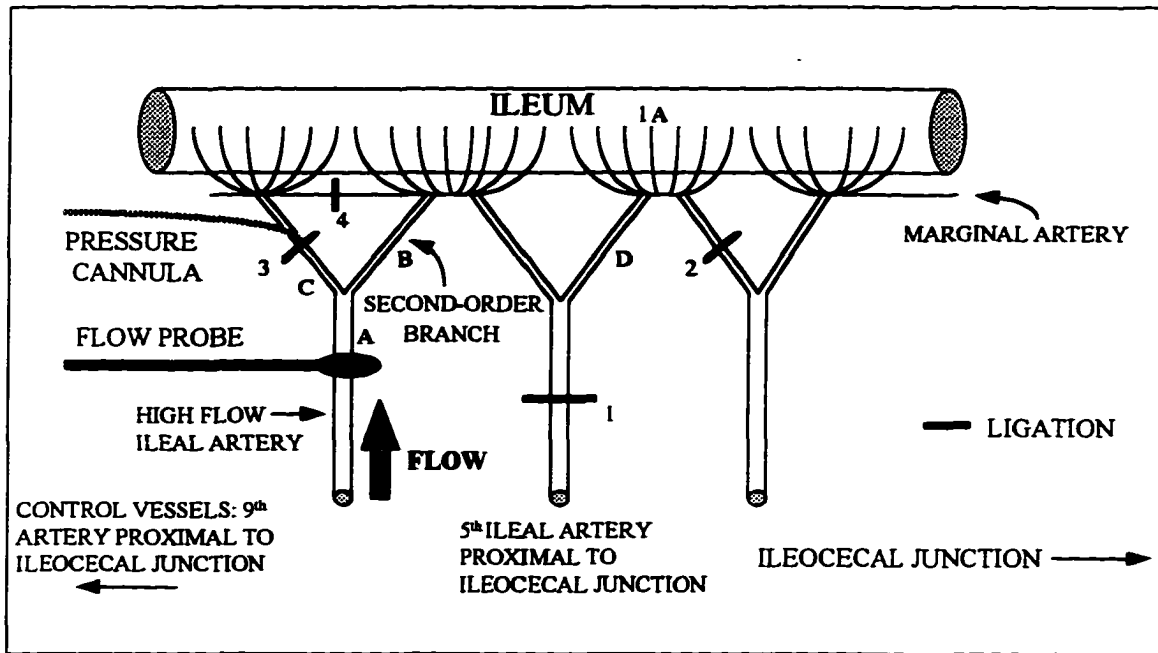


**Figure 4-1. Rat Mesenteric Flow Model.** This diagram illustrates the general mesenteric arterial arrangement with sites of ligation, placement of pressure cannula, and flow probe used for both acute hemodynamic measurements and chronic morphological assessments. In the chronic studies, the proximal branch of the high flow sixth ileal artery was ligated. Results showed significantly increased blood flow and calculated wall shear rates in the high flow ileal artery and second-order branch with no significant changes in mean aortic or mesenteric arterial pressures. This is a paired design model with control and high flow vessels in the same animal. Control vessels were obtained from the ninth ileal artery and second-order branch proximal to the ileocecal junction and are not included in the illustration.

artery; and (D) low flow, normal pressure in a smaller artery (under the possible influence of ischemia-induced metabolites). A fifth possible scenario involves first-order arterioles (1-A) of the intestinal wall located between the fourth and fifth ileal arteries proximal to the ileocecal junction where ischemia may occur. These sites are illustrated in Figure 4-1.

The focus of this study was on the high flow ileal artery and second-order branch (denoted on Fig. 4-1 as A and B, respectively) and their matching control vessels. Arterial ligations were made by first identifying the best site on each vessel branch for the ligation, and then carefully and gently clearing away surrounding adipose tissue to correctly identify the artery and adjacent vein. Tremendous care was taken during dissection in order not to stretch or injure the vessels, and unnecessary manipulation of the vessels was kept to a minimum. A short piece of suture was cut, gently wrapped around the artery, and tied twice. Because of the delicacy of this surgical technique, if the artery was punctured during the procedure, ligations were made directly above and below the site of damage in order to ensure cessation of blood loss. Once bleeding stopped, the procedure continued as normal. Generally speaking, the ligation around the fifth ileal artery was made first, followed by the ligation around the second-order branch of the fourth artery, and then the second-order branch of the sixth artery. During the surgery, the level of consciousness of the rat as well as the patency of the airway were constantly observed.

Once all ligations were complete, the number of 1-A arterioles feeding the intestinal wall in the flow-dependent region was counted and the length (in mm) of the flow-dependent region measured. The flow-dependent region is considered to be the section of bowel receiving blood flow from the feeding sixth ileal artery (corresponding to section A in Fig. 4-1) proximal to the ileocecal junction. The 1-A arterioles counted were

those that spanned at least 50% of the distance across the radial bowel axis. The cecum, intestines, and supporting vasculature were then gently placed back into the abdominal cavity. The muscular abdominal wall was closed and sutured with sterile 4-0 Plain Gut (Ethicon, Inc.). The abdominal skin was closed using sterile surgical clips, and the area around the incision swabbed with an antiseptic/microbicidal solution (Pharmadine Solution, Sherwood Pharmaceutical Co., Mahwah, NJ). The rat was placed in a prone position on a separate warm heating pad with the upper thorax and head raised to aid breathing. Ear notches were made for identification. Detailed diagrams of the individual vessel arrangement and actual sites of ligation were made immediately after the surgery for each animal. Once fully recovered from anesthesia, rats were placed into appropriate cages and returned to the Animal Care Facility. Several hours after each surgery, as well as the next day after surgery, observations were made on each rat to ensure full recovery. Animals were provided water and standard rat chow *ad libitum* for 1, 3, or 7 days.

After the appropriate number of days, each rat was anesthetized with Na<sup>-</sup>-pentobarbital (60 mg/kg, IM), and supplemental injections of Na<sup>-</sup>-pentobarbital were given as needed throughout the remainder of the procedure. Once a surgical level of anesthesia was reached, MAP was measured through tail artery cannulation for purposes of establishing pressure for perfusion-fixation. The ventral portion of the tail just below the testis was shaved and cleaned. The animal was placed supine on a warm heating pad, and a midline incision was made on the proximal ventral portion of the tail to expose the underlying tissue and sheath covering the tail artery. The surrounding tissue was carefully dissected away, and the sheath opened to expose the tail artery. Two sutures were placed under the artery, the distal suture tied twice, and the proximal portion of the artery

adjacent to the proximal suture clamped with micro-forceps. Lidocaine HCl (10 mg/ml, Astra Pharmaceutical Products, Inc., Westborough, MA) was administered topically on the artery to induce dilation. Using microsurgical Castroviejo scissors, a small incision was made in the tail artery, and a polyethylene catheter (0.28 mm ID) inserted into the artery and advanced until it reaches the micro-forceps. Both proximal and distal sutures were tied around the catheter to secure it. The forceps were released, and a heparin solution (1000 units/kg BW, Elkins-Sinn, Cherry Hill, NJ) slowly injected into the artery. The catheter, attached to a calibrated Statham pressure transducer and a Gould Brush 2200 recorder (Cleveland, Ohio), enabled precise and immediate recordings of tail artery pressure. The chart speed was set at 5 mm/sec, and a MAP was recorded once stabilized (approximately 5 minutes).

After a stable pressure was recorded, the rat was gently moved from the heating pad and placed supine in a collecting pan. A midline laparotomy was made, followed closely by a pneumothorax as the method for sacrifice. Since several of the internal organs demand large blood flows, ligation of the arteries feeding these organs allowed a more accurate estimate of pressure during perfusion through the thoracic aorta. The abdominal cavity was further opened to allow access to the internal organs. First, the left renal artery was ligated, followed by ligation of the left and right femoral arteries. The right renal artery was not ligated as the right kidney served as control for cellular proliferation. The inferior vena cava below the kidneys was isolated and severed to allow an outflow for perfusion-fixation. The thoracic aorta above the diaphragm was isolated and cleared of surrounding tissue. Two long sutures were placed under the thoracic aorta, and a small cut made in the thoracic aorta using microsurgical Castroviejo scissors. A 14

G catheter was gently inserted into the vessel, and the catheter secured with the sutures and attached to a heated dual reservoir setup containing a vasodilator mixture [100  $\mu$ M sodium nitroprusside (Sigma, St. Louis, MO), 100  $\mu$ M verapamil hydrochloride (Sigma), 100  $\mu$ M papaverine hydrochloride (Aldrich Chemical Co., Milwaukee, WI), 1 liter 0.9% physiological saline] and 10% buffered formalin phosphate (Fisher Scientific, Fair Lawn, NJ). The tubing was cleared of air bubbles, and the vasodilator mixture pumped through the thoracic aorta catheter and isolated mesentery and right kidney at approximate MAP (as recorded on the pressure transducer). After approximately 5 minutes, the system was switched to formalin to allow fixation of the tissues at approximate MAP. After the mesentery and right kidney were completely perfuse-fixed, the appropriate tissues were carefully extracted from the rat and placed in 10% buffered formalin phosphate until ready for microsurgical dissection. Chart recordings of MAP and perfusion pressure were appropriately labeled and saved.

#### Hemodynamic Parameter Measurements

In a duplicate series of experiments hemodynamic parameters were measured before and initially after creation of the model by arterial ligation. These measurements were made by our collaborator, Joseph L. Unthank, Ph.D., in the Department of Surgery, Indiana University School of Medicine. The left common carotid artery was cannulated in order to measure MAP. Following a medial laparotomy and surgical protocol as described above, a perivascular ultrasonic flow probe (0.5V probe and Model 206 Flowmeter, Transonics Systems Inc., Ithaca, NY) was placed on the sixth ileal artery proximal to the ileocecal junction (Fig. 1). The proximal second-order branch off the fourth ileal artery proximal to the ileocecal junction was ligated, followed by cannulation

of the proximal branch of the sixth ileal artery proximal to the ileocecal junction. The cannula was oriented away from the flow-dependent region and was inserted for purposes of obtaining a local mesenteric arterial pressure. The cannula was constructed from 31 gauge MicroFil tubing (World Precision Instruments, Sarasota, FL) sealed in PE 10 and PE 50 tubing. The fifth ileal artery proximal to the ileocecal junction was then ligated. The sites of arterial cannulation and ligations are included in Figure 1. Measurements of blood flow, arterial pressure, and internal diameters of the sixth ileal artery and its distal second-order branch were made prior to and after each cannulation or ligation as described above. Ileal artery blood flow measurements were corrected for zero offsets, and measurements of internal diameters were made through videomicroscopy. Before accepting each pressure measurement, the stopcock connecting the cannula to the pressure transducer was opened to the atmosphere to verify that the cannula was patent as demonstrated by the entrance of blood into the cannula. Finally, vessels were completely relaxed through topical administration of a dilator cocktail ( $10^{-4}$  M adenosine,  $10^{-5}$  M sodium nitroprusside), with subsequent measurement of flow, pressure, and diameters. Wall shear rate was calculated from these data using the formula:  $WSR = (4Q)/(\pi r^3)$  where Q is blood flow (ml/sec) and r is the vessel radius (cm).

#### Tissue and Slide Preparation

The right kidney was cleared of surrounding adipose tissue and perirenal fascia, divided into three cross-sections, and fixed in formalin. The intestines and supporting mesenteric vasculature were closely examined under the dissection microscope (StereoZoom 4, Bausch & Lomb). Arteries of interest and the section of intestinal wall containing one or more I-A arterioles were carefully extracted and placed in formalin.

Control vessels and a control section of the intestinal wall were taken from the appropriate location and placed in formalin.

All tissues were fixed in formalin for 4 hours, after which each was placed in a small section of Kimwipe paper (Kimberly-Clark Corp., Roswell, GA) and labeled. Keeping the tissues moist throughout this procedure, a maximum of three tissues were loaded per processing cassette, which was also labeled according to the tissues inside. The tissues were then placed in the processing unit (Autotechnicon Duo, Technicon Corp., Tarrytown, NY) for a 13½ hour cycle in the following baths: 70% ethanol, 95% ethanol, 100% ethanol, xylene, paraffin (Paraplast Plus Tissue Embedding Medium, Oxford Labware, St. Louis, MO). If a prolonged amount of time was expected before tissues were able to be processed, they were placed in the Kimwipe paper, labeled, and placed in 0.9% physiological buffered saline (PBS), pH 7.4, at 4 °C, until ready for processing.

After the tissues completed processing, they were transferred to the heating unit of the tissue embedding center (Tissue Tek II, Lab Tek Products, Division Miles Laboratories, Inc., Westmont, IL). The tissues were embedded in liquid paraffin in molded plastic cassettes, labeled, and allowed to solidify on the cold unit of the embedding center. The tissue blocks were stored at room temperature in an ordered fashion until ready for use.

Tissue sections were cut from paraffin blocks at a thickness of 4 µm using a rotary microtome (American Optical 820, Conneaut Lake Scientific, Conneaut Lake, PA). The tissue sections were placed immediately in 30% RNase-free ethanol (30% absolute ethanol, 70% DEPC-H<sub>2</sub>O). Sections were transferred to a heated dH<sub>2</sub>O bath to allow for

adequate spreading of the tissue. Precleaned Superfrost/Plus microscope slides (Fisher Scientific, Pittsburgh, PA) were used for all protocols. For slides used in histologic staining, vessel sections were placed approximately in the middle of each slide, with only a single vessel type per slide. For *in situ* hybridization experiments, control vessels were placed above same animal treatment vessels on the bottom third of the slide. Also, for *in situ* hybridization experiments, duplicate slides per vessel pair were made for sense and antisense probes. Slides were labeled appropriately on the frosted end in pencil and stored in slide boxes at room temperature.

#### Morphological Analysis

Toluidine blue stain was prepared by adding 1 gram sodium borate and 1 gram toluidine blue O dye (Eastman Kodak Co., Rochester, NY) to 100 ml dH<sub>2</sub>O. The was mixed, filtered, and stored in the dark in a light-proof container. Prepared slides were deparaffinized in xylene (3 min x 2) and rehydrated in 100% ethanol (10 dips x 3), 95% ethanol (10 dips), and dH<sub>2</sub>O (5 min) at room temperature. Slides were placed on a 37 °C slide warmer (Fisher Scientific) and stained with toluidine blue for 45 seconds. The slides were rinsed with dH<sub>2</sub>O, dehydrated in 95% ethanol (10 dips), 100% ethanol (10 dips x 3), and xylene (3 min x 2) at room temperature. Slides were coverslipped with Accumount 60 mounting medium (Baxter Health Care Corp., McGraw Park, IL).

Microscopic measurement and quantitation of morphological parameters were performed using JAVA Video Image Analysis Software System (Jandel Scientific, Jandel Corp.) linked to a Zeiss 25 binocular microscope (Carl Zeiss, Oberkocken, W. Germany). Pixel gray level thresholds were set for optimum contrast, and inside and outside

circumferences were automatically traced and digitized. Data transformations provided values for lumen area, wall area, and inside and outside diameters.

### Immunocytochemistry Protocols

#### Proliferating Cell Nuclear Antigen

The protocol used for immunocytochemical localization of PCNA is modified from that of Vector Laboratories (Vector Laboratories, Inc., Burlingame, CA) for use with paraffin-embedded formalin-fixed tissues. Two slides per sample were used, one positive and one negative control. Prior to starting the protocol, tissue sections were outlined using a diamond pencil, and the slides were labeled according to the primary antibody used (or negative control). Except for the initial incubation step or unless otherwise specified, all reactions took place at room temperature.

Slides were incubated in a 55 °C oven for 1 hour or until the paraffin was completely dissolved. Tissues were deparaffinized and rehydrated in xylene (4 min x 3), 100% ethanol (2 min x 3), 95% ethanol (2 min x 2), 70% ethanol (2 min), and dH<sub>2</sub>O (5 min). Endogenous peroxidase activity was blocked with 0.4% hydrogen peroxide in methanol for 10 minutes. Slides were washed in PBS for 20 minutes, followed by a 20 minute treatment in a humidified chamber with 5% normal goat serum (Vector Laboratories) as a blocking agent. The positive slides were treated with the primary antibody mouse monoclonal anti-PCNA clone PC-10 (Boehringer Mannheim Corp., Indianapolis, IN) in a 1:200 dilution with PBS in a humidified chamber for 2 hours. Negative slides received 5% normal goat serum only, and positive and negative slides were kept in separate chambers. Slides were then washed with PBS for 20 minutes. All slides received the secondary antibody biotinylated goat anti-mouse IgG (Vector Labs) in

a 1:400 dilution with PBS in a humidified chamber for 30 minutes. Slides were washed in PBS, and treated with Vectastain Elite Avidin-Biotinylated Complex immunoperoxidase system (Vector Laboratories) for 30 minutes. Slides were rinsed in PBS and incubated in a diaminobenzidine tetrahydrochloride (DAB, Sigma) chromagen solution for 5 minutes in a humidified chamber. The DAB solution contained 0.1 M imidazole, 0.2% DAB, hydrogen peroxide, and PBS. Slides were washed under running tap water for 5 minutes, followed by counterstaining with hematoxylin (Gill's Formulation #1, Fisher Scientific) for 5 minutes. Slides were again washed under running tap water for 5 minutes, dehydrated and cleared in the following washes: 70% ethanol (2 min), 95% ethanol (2 min x 2), 100% ethanol (2 min x 2), and xylene (2 min x 2). Slides were air dried and coverslipped with Accumount 60 Mounting Medium (Baxter Health Care Corp.). Unless otherwise specified, all treatments took place at room temperature.

#### Endothelial Nitric Oxide Synthase

The ICC protocol for eNOS is similar to that described above for PCNA but with several exceptions. The endogenous peroxidase blocking step with hydrogen peroxide was extended to 30 minutes instead of 10 minutes, followed by a 20 minute wash in PBS. The tissues were then permeabilized with a 20 minute wash in 0.15% Triton X-100 (Sigma) in PBS, followed again by a 20 minute PBS wash. Blocking serum (5% NGS) was added as stated above for PCNA. The primary antibody was a mouse affinity-purified monoclonal IgG-1 against eNOS (Transduction Laboratories, Lexington, KY) used in a 1:1000 dilution. The immunospecificity of this monoclonal antibody has been validated through both Western blot and preadsorption immunohistochemistry (195). Primary antibody incubation proceeded overnight at 4 °C in a sealed humidified chamber. The next

day slides were washed briefly with PBS and treated to the secondary antibody (Biotinylated Goat Anti-Mouse IgG) in a 1:200 dilution for 30 minutes. The procedure then proceeded as described above.

Analysis of positive and negative tissues and quantitation of ICC results were performed through direct microscopic measurement (Zeiss 25 binocular microscope; Carl Zeiss) and by utilizing the JAVA Video Image Analysis Software System (Jandel Scientific). For PCNA slides, the total number of medial SMC nuclei, as well as the number of PCNA-positive and negative SMC nuclei, were systematically counted. For analysis of ECs, the absolute number of intimal EC nuclei were counted. These nuclear counts were subsequently normalized to wall area and luminal perimeter, respectively. For eNOS analysis, slides were blindly scored according to a 0 - 4 grading scale for positive stain specific to the endothelial luminal lining. A score of 0 denoted negative staining while a score of 4 indicated excellent specific stain.

#### Extracellular Connective Tissue Staining

Tissue cross-sections were stained for extracellular connective tissue using a modification of the protocol included in Masson's Trichrome Stain kit (Sigma). Slides were deparaffinized and rehydrated in xylene (3 min x 2), 100% ethanol (2 min x 2), 95% ethanol (2 min x 2), 70% ethanol (2 min), and dH<sub>2</sub>O (5 min). Tissues were treated with Bouin's histological reagent solution (Sigma) for 15 minutes at 56 °C as a general fixative and to intensify the final coloration step. Slides were washed under running tap H<sub>2</sub>O for several minutes and treated with the nuclear stain hematoxylin (Gill's #1 formulation, Fisher Scientific) for 5 minutes. After a short dH<sub>2</sub>O rinse, slides were treated with Biebrich-Scarlet acid fuchsin solution for 2 minutes to stain muscle fibers and cytoplasm.

Slides were rinsed in dH<sub>2</sub>O and treated with a phosphotungstic-phosphomolybdic acid solution for 5 minutes, followed by collagen staining in aniline blue solution for 8 minutes. Coloration was intensified through exposure to a 1% acetic acid solution for 2 minutes, and the slides were dehydrated and cleared in the following washes: 70% ethanol (2 min), 95% ethanol (2 min x 2), 100% ethanol (2 min x 2), and xylene (2 min x 2). Slides were air dried and coverslipped with Accumount 60 Mounting Medium (Baxter Health Care Corp.). Unless otherwise specified, all reagents were included in the kit (Sigma) and all treatments took place at room temperature. Microscopic evaluation of these slides was performed using the video image analysis system Image-1 (Universal Imaging Corporation, West Chester, PA) linked to a Sony DXC-151 CCD camera (Sony, Japan) and Nikon Optiphot-2 microscope (Nikon, Japan). Quantitation of percent connective tissue in vessel medial wall cross-sections was achieved using established stereologic methods (56). Quantitative stereology provides an efficient and unbiased method for directly estimating the areal fraction of profiles (in this study the stained connective tissue) in a standardized area of a structure (the medial wall) through the use of a fixed test grid system (56).

### cDNA Subcloning

The following is a general description of cDNA subcloning techniques that were used for preparing linearized DNA used in synthesizing <sup>35</sup>S-CTP labeled riboprobes. Details are then given concerning subcloning specifications for the following factors: PDGF-A, PDGF-B, bFGF, and TGF-β1.

For consistency purposes, and to allow use of standard RNA polymerases T<sub>3</sub> and T<sub>7</sub>, all cDNAs were subcloned into pBluescript SK+ (Stratagene, La Jolla, CA) if

originally located in a different plasmid. If in a plasmid other than pSK<sup>+</sup>, the cDNA was cut out of the original plasmid using appropriate restriction endonucleases and buffers, and the fragment ligated into an appropriate site in pSK<sup>+</sup> using DNA ligase. The DNA fragment in pSK<sup>+</sup> was used to transform XL1-Blue cells (Stratagene) which were plated on LB-ampicillin agar plates and grown overnight. Appropriate clones with cDNA inserts were picked according to the integrity of the  $\beta$ -galactosidase gene and blue/white color detection. The cDNA was amplified and purified using Qiagen Plasmid purification systems (Qiagen Inc., Chatsworth, CA). Appropriate linearized sense and anti-sense strands were constructed using restriction endonuclease digestion. The linearized DNA strands were diluted to 0.5  $\mu\text{g}/\mu\text{l}$  and stored at  $-20\text{ }^{\circ}\text{C}$  in TE buffer, pH 8.0, until ready for riboprobe synthesis. Throughout this process, PC/Gene Software was utilized for verifying restriction sites with restriction maps, and 1% agarose gel electrophoresis used to verify the efficiency of cutting, proper fragment lengths, and orientation of the fragment.

#### PDGF-A:

The genomic sequence for PDGF-A chain was identified by Collins and co-workers (20). The cDNA for PDGF-A was available in our laboratory as a pBluescript SK<sup>+</sup> insert in a Sal I/Sac II site. Sal I and T<sub>3</sub> make a 368 bp sense strand, and Sty I and T<sub>7</sub> make a 321 bp antisense strand.

#### PDGF-B:

The original genomic sequence was identified by Aaronson and co-workers (143). In our laboratory, the PDGF-B cDNA was initially cut out of pUC-13 and oriented into a Xba I/Sma I site in pBluescript SK<sup>+</sup>. The original length was 272 bp; however, Xba I did

not give complete digestion when trying to linearize the DNA. An alternate Bst XI site was found that provided proper cutting, but gave 3'-overhangs. Treatment of this antisense chain with DNA polymerase I Klenow fragment prior to probe synthesis provided blunt ends through exo- and endonuclease activity (another possibility for antisense chain linearization is to use Not I which leaves acceptable 5' overhangs). The final length of both sense and antisense chains was 265 bp. Sma I and T<sub>3</sub> make sense while Bst XI and Klenow fragment (or Not I) and T<sub>7</sub> make antisense.

#### bFGF:

The original nucleotide sequence of bFGF was identified by Abraham et al. (1). In our laboratory, the cDNA for bFGF was available in pSK+ in an Eco RV site. The 704 bp segment was linearized with Xho I and T<sub>3</sub> to make sense and Bam HI and T<sub>7</sub> to make antisense.

#### TGF-β1:

The original cDNA sequence was described by Qian et al. (138). In our laboratory, the cDNA was available in pBluescript II KS+ as a 985 bp fragment in a Sma I/Bam HI site. The restriction sites between the promoters are reversed in pKS+ when compared to the pSK+ positions. Treatment with Eco RI (or Sma I) and T<sub>7</sub> make sense, while Bam HI and T<sub>3</sub> make antisense.

#### <sup>35</sup>S-CTP Riboprobe Synthesis

All enzymes and buffers for <sup>35</sup>S-CTP riboprobe syntheses were purchased from Promega Corporation (Madison, WI). Linearized sense and anti-sense cDNA strands were transcribed in the presence of 90 μCi <sup>35</sup>S-CTP (Dupont de Nemours, Boston, MA) in a standard 20 μl transcription reaction containing transcription buffer (5x), 100 mM DTT.

RNAse inhibitor, ATP, UTP, CTP, GTP, 1  $\mu$ g linearized cDNA, and the appropriate RNA polymerase T<sub>3</sub> or T<sub>7</sub>. If a 3' overhang existed on the cDNA, it was treated with DNA polymerase I Klenow fragment (5 units/ $\mu$ g DNA) for 15 minutes at room temperature. Transcription proceeded for 2 hours at 37 °C, and the reaction stopped with DNase. Radionucleotide incorporation was measured using PEI cellulose-F chromatography paper (EM Industries, Inc., Gibbstown, NJ) and phosphorimager analysis (Molecular Dynamics). The samples were then purified on a Sephadex G-50 spin column (5 Prime  $\rightarrow$  3 Prime, Inc., Boulder, CO). The DNA was eluted, treated with 10 mg/ml tRNA and 100 mM DTT, and if probe length exceeded 800 bp, subjected to limited alkaline hydrolysis for a final length of 150 bp. Alkaline hydrolysis consisted of incubation at 60 °C in 0.2 M Na<sub>2</sub>CO<sub>3</sub> and 0.2 M NaHCO<sub>3</sub> for a calculated amount of time. The time for alkaline hydrolysis was determined according to the following calculation: initial length of probe (in kb) - 0.15 kb  $\div$  0.11 kb-min<sup>-1</sup> x initial length of probe x 0.15 kb. Small volume aliquots were prepared, the pH was neutralized, and the probe precipitated in cold 100% ethanol (2.5 x volume) and 3 M NaOAc, pH 7.5 and stored at -70 °C until use. On the day of use, an aliquot was centrifuged, the supernatant removed, and the pellet treated with cold 70% ethanol for 5 minutes. The solution was centrifuged again and the supernatant removed. The probe pellet was dried down and resuspended in 20 mM DTT and formamide. Prior to use for *in situ* hybridization, a 1  $\mu$ l sample of the probe was added to 6 ml scintillation cocktail in order to measure radioactivity (desired results 10<sup>6</sup> CPM/ $\mu$ l).

### *In situ* Hybridization

The *in situ* hybridization methods used in this laboratory are primarily based on those described by Wilcox (191) for formalin-fixed, paraffin-embedded tissues. All

equipment used on day 1 of this protocol was treated with either 3% hydrogen peroxide or 0.5M NaOH to destroy RNase enzyme. Also, all solutions made for day 1 were prepared with RNase-free materials and diethyl pyrocarbonate (DEPC; Sigma) treated dH<sub>2</sub>O. Slides were cleared and deparaffinized in xylene and graded alcohols. The slides were washed in 0.5 x SSC for 10 minutes, deproteinated with a 5 µg/ml solution of proteinase K tritirachium album (Amresco, Solon, Ohio) for 10 minutes at room temperature, and rinsed 3 times in PBS. The slides were post-fixed in 4% paraformaldehyde (Sigma) for 10 minutes at 4 °C, and rinsed 3 times in PBS. The were then covered with 200 µl prehybridization stock containing 50% dextran sulfate, 50x Denhardt's solution, EDTA, Tris, NaCl, DEPC-H<sub>2</sub>O, and formamide in a humidity chamber for 2 hours at approximately 40 °C. The prehybridization solution was allowed to drip off, and the tissues were incubated with 100 µl hybridization solution containing 1 M DTT, 10 mg/ml yeast tRNA, and radioactive probe at 10<sup>6</sup> CPM/slide in the humidity chamber (Isotemp Incubator, Fisher Scientific) at 55 °C overnight.

Solutions and equipment used on day 2 of this protocol were not RNase-free. The slides were removed from the incubator after the hybridization step and washed in a low stringency solution of 2 x SSC and 10 mM β-ME-EDTA for 20 minutes. Slides were treated to a 40 µg/ml RNase A solution (Sigma) for 30 minutes at room temperature to digest unhybridized probe. Slides were washed again in the low stringency solution for 20 minutes, followed by four 1 hour washes in a high stringency solution of 0.1 x SSC and 10 mM β-ME/1 mM EDTA at 55 °C. Slides were rinsed in 0.5 x SSC for 20 minutes, and then serially dehydrated in graded alcohols containing 0.1 x SSC and 1 mM DTT. Slides were allowed to air dry overnight.

### Emulsion, Developing, and Counterstaining

Kodak NTB-2 emulsion (Eastman Kodak Co.) was heated at 42 °C for several hours prior to dipping. All slides were placed inverted in specially designed slide holders. In absolute darkness, emulsion was gently mixed with an equal amount of warmed dH<sub>2</sub>O and poured into a glass slide holder immersed in a pre-heated H<sub>2</sub>O bath. Slides were dipped into the emulsion mixture for approximately 1 second, removed and placed inverted in an incubator box containing dessicant. After all slides were dipped, the box was sealed shut and the slides allowed to air dry overnight. The next day, in absolute darkness, slides were transferred to individual black boxes (containing dessicant), which were wrapped in aluminum foil, labeled, and stored in a separate incubator box at 4 °C for 10 weeks.

After the appropriate amount of time, the slides were brought to room temperature. Kodak Dektol Developer (Eastman Kodak Co.) was prepared (17 g. developer to 250 ml dH<sub>2</sub>O at 32 - 38 °C) and diluted with an equal amount of dH<sub>2</sub>O. Kodak Fixer (Eastman Kodak Co.) was also prepared (45 g. fixer to 250 ml dH<sub>2</sub>O). In absolute darkness, slides were removed from the black boxes and placed in slide holders. Slides were dipped in developer for 4 minutes, dH<sub>2</sub>O for 30 seconds, and fixer for 5 minutes, after which they were placed in room temperature dH<sub>2</sub>O until all slides were completed. Slides were washed under slowly-running tap water for 15 minutes and allowed to air dry overnight.

The next day slides were cleared in xylene and rehydrated in graded alcohols. Slides were counterstained in hematoxylin dye (Surgipath Harris Formula, Surgical Medical Laboratories, Inc., Richmond, IL) for 2 minutes, followed by a 2% glacial acetic

acid rinse for 30 seconds. Slides were soaked in dH<sub>2</sub>O and treated with a bluing agent (sodium bicarbonate, lithium carbonate in dH<sub>2</sub>O) for 30 seconds. Slides were soaked in dH<sub>2</sub>O, 95% ethanol, and treated with eosin-y stain (Surgipath, Surgical Medical Laboratories, Inc.) for 1 minute. Slides were dehydrated, cleared, air dried, and coverslipped with Accumount 60 Mounting Medium (Baxter Health Care Corp.).

Microscopic evaluation of *in situ* hybridization slides was performed using the Image-1 system linked to a Sony DXC-151 CCD camera and Nikon Optiphot-2 microscope. Pixel threshold intensity gray levels were set, and secondary filters were established to cover a narrow range of silver grain size. A region of interest was made covering approximately 50  $\mu\text{m}^2$ . Automatic silver grain counts were performed in both the endothelial and medial layers in vessel cross-sections. Data from duplicate samples were averaged, and mean values for sense were subtracted from those for anti-sense to provide an overall value for specific signal. Data were represented as number of grains per 50  $\mu\text{m}^2$  of tissue for wall area measurement, and as number of grains per 15  $\mu\text{m}$  luminal perimeter for endothelial measurements.

#### Statistical Analysis

Data were stored and analyzed on personal computers using Instat 2 (Graphpad Software, v. 2.02), Excel (Microsoft, v. 5.0), and Sigma Plot (Jandel Scientific, v. 2.0). Morphological data were analyzed using a two-way ANOVA with post-hoc Bonferroni-corrected paired and unpaired T-tests. This two-way ANOVA allows analyses of between- (time) and within- (treatment) subjects and considers interaction effects. Flow, WSR, and pressure data were analyzed using a repeated measures one-way ANOVA (a two-way ANOVA without replication) with post-hoc Bonferroni and Student-Newman-

Keuls tests. Subjective eNOS scores were analyzed using the non-parametric Wilcoxon signed rank test for data from non-Gaussian populations. All other data were analyzed using a two-tailed paired Student's T-test. All data means and variances were tested for normality using ANOVA-associated Normality tests. Unless otherwise specified, data were presented as mean values  $\pm$  SEM, and the null hypothesis was rejected at an uncorrected  $\alpha$  level of 0.05. Paul Kolm, Ph.D., and members of the Lewis Hall computer center were available for consultation.

**CHAPTER V**  
**RAT MESENTERIC FLOW MODEL INDUCES SIGNIFICANT INCREASES**  
**IN SHEAR STRESS WITH POSSIBLE CONTRIBUTION FROM**  
**WALL STRESS**

**Introduction**

Vascular homeostasis is continuously influenced by the mechanical forces created by transmural pressure and blood flow. Arterial pressure is directly related to circumferential wall stress and affects primarily medial and adventitial components of the vessel wall. Blood flow exerts tangential shear stress acting predominantly on the luminal aspect of intimal ECs. This shear stress can also affect underlying SMCs through interstitial fluid flow (3, 4, 188). These biophysical forces have been implicated in the pathophysiology of various vascular disorders such as localization of atherosclerotic foci and formation of intimal, subintimal, and medial neoplasias. A primary concern in studies of the pathophysiology of hemodynamic stimuli is the inability to completely separate the influence of wall stress from that of shear stress. Even when transmural pressure is held constant, the influence of flow-induced vasodilation leading to increased wall stress through cell stretch warrants consideration. The aim of the experiments in this chapter was to characterize a unique rat mesenteric flow model in order to differentiate the roles of wall stress and shear stress in mediating vascular remodeling under *in vivo* conditions.

## Results

Control and post-ligation hemodynamic parameter data are summarized in Table 5-1. Eight rats were successfully evaluated for this part of the study. Neither mean arterial (carotid artery) nor local mesenteric pressures changed significantly post-ligation. Prior to any ligations, ileal artery blood flow averaged  $65 \pm 0.08$  ml/min. After ligation of only the proximal branch off the sixth ileal artery, ileal artery blood flow decreased  $35 \pm 5\%$  (data not shown). For control conditions before any ligations, it was assumed that flow through the second-order branch artery was equal to half of the flow through the parent ileal artery. This assumption seems reasonable considering that the *in vivo* inner diameters of the two branches were similar under control conditions ( $220 \pm 18$   $\mu\text{m}$  distal vs.  $213 \pm 13$   $\mu\text{m}$  proximal branch). After ligation of the proximal branch, the flow through the ileal artery and the only remaining branch would be equal. Given this assumption, after ligation of the proximal second-order branch of the sixth ileal artery and ligation of the adjacent fifth ileal artery, blood flows through the supplying ileal artery and distal branch were increased  $36 \pm 13\%$  ( $p < 0.01$ ) and  $170 \pm 25\%$  ( $p < 0.001$ ), respectively, relative to pre-ligation control conditions. Significant flow-induced dilation was demonstrated in the ileal artery ( $\sim 7\%$ ;  $p < 0.001$ ), while the second-order artery did not experience a significant increase ( $\sim 5\%$ ) in internal diameter post-ligation. The ileal artery exhibited a nonsignificant ( $\sim 10\%$ ) increase in calculated average WSR, while average WSR in the second-order branch increased  $118 \pm 27\%$  ( $p < 0.001$ ). Measurements of completely dilated vessels indicate that control ileal arteries possess  $\sim 6\%$  tone while control second-order arteries have  $\sim 9\%$  tone under resting conditions (data not shown).

**TABLE 5-1: Control and post-ligation hemodynamic parameters**

Parameter:	Control	Post-ligation
MAP (mm Hg)	111.8 ± 4.3 (8)	119.4 ± 3.4 (8)
Second-order branch pressure (mm Hg)	91.0 ± 2.6 (6)	88.3 ± 5.7 (6)
Ileal artery blood flow (ml/min)	0.65 ± 0.08 (8)	0.83 ± 0.07 (8)**
Second-order branch blood flow (ml/min)	0.33 ± 0.04 (8)	0.84 ± 0.07 (8)***
Internal radius (µm): ileal artery	150.3 ± 6.3 (8)	160.7 ± 7.3 (7)***
Internal radius (µm): second-order branch	130.2 ± 8.9 (7)	136.8 ± 6.0 (7)
WSR (sec <sup>-1</sup> ): ileal artery	4125 ± 468 (8)	4545 ± 630 (8)
WSR (sec <sup>-1</sup> ): second-order branch	3832 ± 647 (7)	7618 ± 1193 (7)***

Data represent control and post-ligation mean ± standard error of the mean for arterial pressure, blood flow, vessel internal radius, and calculated wall shear rate (WSR):  $[(4Q)/(\pi r^3)]$  where Q = blood flow (ml/sec) and r = vessel radius (cm)]. Sample size is indicated in parentheses. Data were analyzed using a repeated measures ANOVA with a post-hoc Student-Newman-Keuls test and an  $\alpha = 0.05$ . \*\* p < 0.01; \*\*\* p < 0.001 versus pre-ligation values.

## Discussion

This chapter attempts to characterize a modification of an existing mesenteric collateral flow model established by Unthank et al. (181) that utilizes a series of arterial ligations (Fig. 4-1) which force a supplying ileal artery to feed the arterial arcade and bowel in the flow-dependent section. Upon setting the ligations, blood flow through the feeding ileal artery and its second-order branch increased significantly (Table 5-1). Acute flow-induced dilation exhibited in the ileal artery (~7%) offset any significant increase in calculated WSR for this vessel. The second-order artery, however, did not significantly dilate resulting in a highly significant doubling of its calculated WSR. Considering the acute flow-induced dilation experienced by the high flow ileal and second-order branches (+7%; +5.4%, respectively) and the acute changes observed in WSR in these vessels (+10%; +100%, respectively), we believe the primary stimulus for both ileal and branch vessels is shear stress; moreover, the ileal artery may be exposed to acute flow-induced cell stretch and its associated wall stress which may contribute to the remodeling evidenced in this vessel. After administration of a vasodilator cocktail, the ileal artery demonstrated ~6% tone while the second-order branch possessed ~9% tone under control conditions. Based on measurements of wall area, the assumption of conservation of wall area during active dilation, and surgical manipulation perhaps injuring the response, we believe that the maximum change in acute wall stress that could have occurred in these vessels would be ~10%. This may be an adequate stimulus to induce acute arterial remodeling in these vessels. Co-existence of these flow-induced stresses and their combined influence on local vasculature accurately portrays normal conditions

experienced by blood vessels *in vivo*. As discussed in Chapter 6, chronic wall stress appears to remain stable (as measured through wall thickness:lumen diameter ratios), suggesting that flow-induced stresses are temporally normalized by vascular adaptations involving luminal enlargement and wall hypertrophy.

A primary concern in developing this model was abolition of any influence of altered arterial pressure, since pressure-induced wall tension alone can stimulate an array of biochemical and molecular signals (33, 118, 146). In addition, the influence of pressure-induced myogenic tone contributing to alterations in wall stress must be considered. In this model, neither mean carotid nor local mesenteric arterial pressures changed significantly post-ligation (Table 5-1). In a recent paper by Unthank et al. (181), 3 to 4 sequential ileal arteries were ligated creating a region containing 44-55 1A arterioles subject to collateral flow through the two boundary ileal arteries. Collateral blood flow increased approximately 274% through the supplying ileal arteries; however, local mesenteric pressure at the center of the collateral-dependent region decreased approximately 53%. A reduction in the passive diameters of both arteries and arterioles from the decrease in pressure at this location could alter wall stress and shear stress and potentially influence their growth response. The model used in the current study allows specific examination of flow-induced stresses without the influence of pressure-mediated stimuli.

This model allows high flow and control arteries for both ileal and second-order branches to be studied in the same animal. This greatly reduces the individual variation inherent when using different animals for control and treatment groups. Standardization

of the exact site for vessels to be ligated, as well as the sites to obtain unligated control vessels, also decreases individual variation. In addition, for purposes of maintaining consistency, diagrams of the mesenteric artery arrangement were made during the surgeries for each rat. The length of the collateral flow-dependent region was measured and the number of 1A arterioles feeding the intestinal wall in the region was counted. The practicality of performing the surgeries to establish this model also offers several advantages. Through the use of Na<sup>+</sup>-pentobarbital (60 mg/kg IM) as our choice of anesthetic, rats generally achieve a surgical level of anesthesia within 30 minutes, maintain this level of anesthesia for the duration of the surgery (approximately 45 minutes), and recover completely after an additional 1 to 2 hours. Only on rare occasion was supplemental anesthetic given during the surgeries. After performing the medial laparotomy, the cecum and adjacent ileum were easily identified and exteriorized. Through the use of a dissecting microscope, the overall architecture of the mesenteric vasculature was easily visualized and the exact location for setting the ligations was easily and rapidly determined. Separating the artery from its adjacent vein proved troublesome, but by using a curved suture needle ligating only the artery was made easier. These various factors specific to this model help establish it as a unique and useful experimental tool that can be used to address hemodynamic forces and their effects on vascular physiology under *in vivo* conditions.

In conclusion, this chapter details a novel experimental model that allows manipulation of hemodynamic parameters under *in vivo* normotensive conditions. The primary stimulus for the ileal and second-order arteries was determined to be flow-induced shear stress, with possible contribution from stretch-induced wall stress for the larger

vessel. Considering the arterial remodeling discussed in the following chapters, this rat mesenteric flow model permits an exclusive flow stimulus leading to significant *in vivo* growth regulation in small mesenteric arteries and allows continued analyses of possible signaling factors involved.

## CHAPTER VI

### **FLOW INDUCES ARTERIAL LUMINAL ENLARGEMENT AND MEDIAL WALL HYPERTROPHY THROUGH ENDOTHELIAL AND SMOOTH MUSCLE NUCLEAR REPLICATION AND CELLULAR HYPERPLASIA**

#### Introduction

Arterial remodeling from hemodynamic stresses has been demonstrated using various experimental preparations on a variety of cell types. Unthank and co-workers showed elevated collateral flow stimulates luminal enlargement (179) and medial wall hypertrophy (181) in rat small mesenteric arteries. Langille and co-workers found blood flow directly regulates developmental proliferation of cellular and extracellular vessel wall constituents in young rabbits (91) in addition to stimulating remodeling of the vessel wall in adult rabbits (92, 186). In contrast, Kraiss et al. (86) showed SMC proliferation to be inversely correlated with shear stress using polytetrafluoroethylene graft implants in baboons. Other models of experimental atherogenesis (197), *in situ* perfused organ culture (13), and arteriovenous shunts (111) have revealed differential results concerning the influence of hemodynamic stresses on arterial wall restructuring. In terms of cellular mechanisms behind structural remodeling of the arterial wall associated with changes in lumen diameter, EC and SMC hyperplasia and/or cellular hypertrophy, reorganization of existing wall components, cellular migration, alterations in ECM constituents, cell death and removal, or combinations of all of these may be involved.

As discussed in the previous chapter, the primary stimulus in the experimental model presented here is flow-induced shear stress with possible contribution of acute wall

stress in the ileal artery. The aim of the experiments in this current chapter was to characterize the remodeling response of small mesenteric arteries exposed to elevated blood flow *in vivo*. Flow-induced arterial remodeling in terms of luminal enlargement and medial wall hypertrophy was analyzed for both treatment and time effects over a 7 day period. The endothelial and smooth muscle cellular mechanisms contributing to these gross morphological alterations were examined through immunocytochemical approaches and nuclear profile analyses.

## Results

### *Rat Mesenteric Flow Model*

Thirty rats were successfully analyzed for this part of the experiment. During establishment of the arterial ligations according to the mesenteric flow model (Figure 4-1), several parameters were measured for purposes of maintaining consistency throughout the experiment. The mean length of the flow-dependent region, defined as the section of the intestinal wall subject to blood flow from the unligated ileal artery, was  $41.83 \pm 0.88$  mm. The number of IA arterioles that fed the intestinal wall in the flow-dependent region was  $19.3 \pm 0.67$ , while the MAP (measured for purposes of setting individual pressures for perfusion-fixation) was  $89.3 \pm 1.52$  mm Hg.

### *Morphological Analysis*

Figures 6-1 and 6-2 graphically illustrate flow-induced alterations in inside lumen diameter and medial wall area, respectively, for ileal and second-order arteries after 1, 3, and 7 days of increased blood flow. The 2-way ANOVA shows there is no significant interaction ( $p = 0.11$ ) between flow and duration of exposure for changes in ileal artery lumen diameter. Significant increases in lumen diameters were observed in both control ( $p$

< 0.002) and high flow ( $p < 0.005$ ) ileal arteries with time. Post-hoc Bonferroni-adjusted statistics indicated a significant increase (+13%) in lumen diameter for ileal arteries exposed to high flow for 7 days when compared to same animal control vessels. The 2-way ANOVA demonstrated a significant ( $p = 0.004$ ) interaction between flow and the duration of exposure for changes in lumen diameter in the second-order arteries. Lumen diameters for control second-order arteries did not change significantly with time. Post-hoc independent comparisons revealed +14% and +38% increases in lumen diameter for high-flow second-order vessels when compared to same animal controls after exposure to flow for 3 and 7 days, respectively. The 2-way ANOVA for flow-induced changes in medial wall area (Fig. 6-2) suggested significant interactions between flow and time exist for both the ileal artery ( $p = 0.014$ ) and the second-order artery ( $p = 0.005$ ). Post-hoc analysis indicated that after 7 days of increased flow, ileal artery wall area was significantly (+58%) elevated compared to its same animal control. Similarly, post-hoc analyses showed that high flow second-order arteries exhibited significant medial wall area enlargement compared to corresponding control vessels after 3 (+53%) and 7 (+120%) days of elevated flow. Medial wall areas for control ileal and second-order arteries did not change significantly with time.

Figure 6-3 compares the sensitivity of the ileal artery to that of the smaller second-order branch in terms of flow-induced changes in inside diameter and medial wall area (as a percent change compared to relative control vessels). These data clearly show a

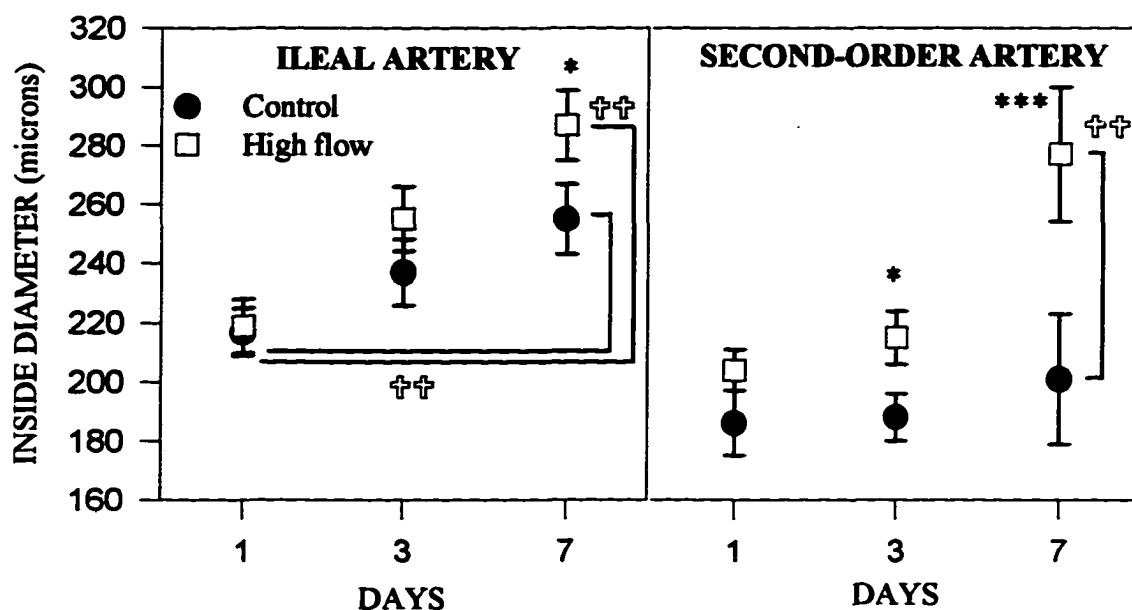


**Figure 6-1. Flow-Induced Alterations in Lumen Diameter.** Flow-induced alterations in lumen diameter for ileal and second-order vessels show no interaction between high flow and time for ileal artery luminal enlargement, with both control and treatment vessels experiencing significant increases with time. Significant interactions between flow and time were demonstrated for the second-order artery lumen diameter. Post-hoc independent comparisons of control versus treatment for each time point are indicated. Data were evaluated with a 2-way ANOVA using post-hoc Bonferroni-corrected T-tests. Values represent mean  $\pm$  SEM, and  $n = 10$  for each group. \*  $p < 0.05$ , \*\*  $p < 0.01$ , \*\*\*  $p < 0.001$  versus control; †  $p < 0.05$ , ††  $p < 0.01$  versus day.

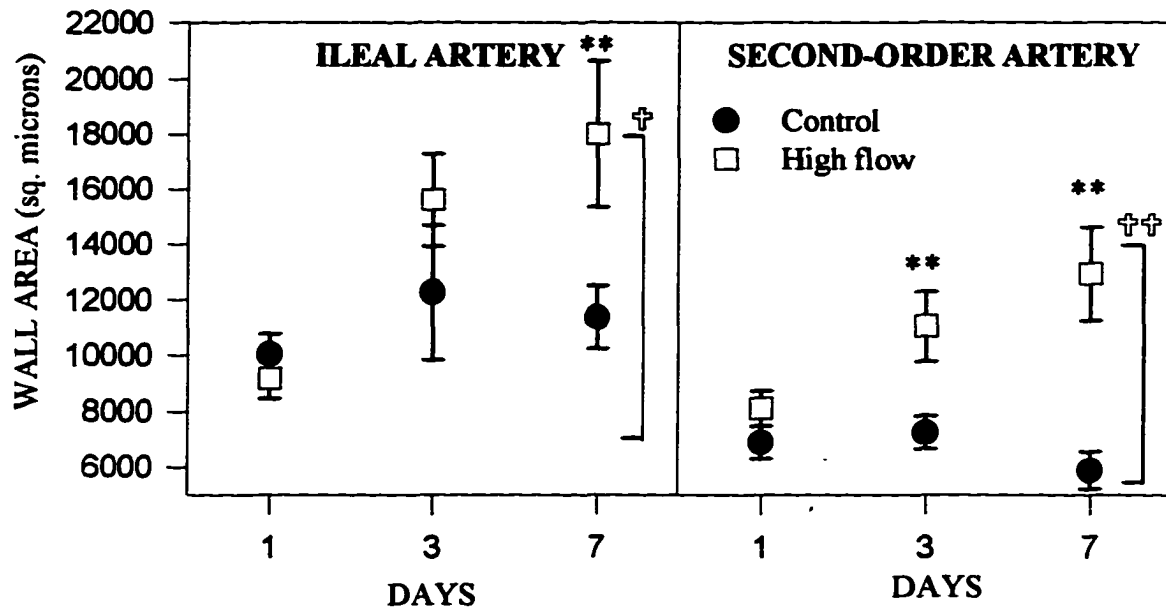


**Figure 6-2. Flow-Induced Alterations in Medial Wall Area.** Flow-induced alterations in medial wall area for ileal and second-order vessels. Significant interactions between flow and time were demonstrated for changes in ileal and second-order artery wall area. Post-hoc independent comparisons of control versus treatment for each time point are indicated. Data were evaluated with a 2-way ANOVA using post-hoc Bonferroni-corrected T-tests. Values represent mean  $\pm$  SEM, and  $n = 10$  for each group. \*  $p < 0.05$ , \*\*  $p < 0.01$ , \*\*\*  $p < 0.001$  versus control; †  $p < 0.05$ , ††  $p < 0.01$  versus day.

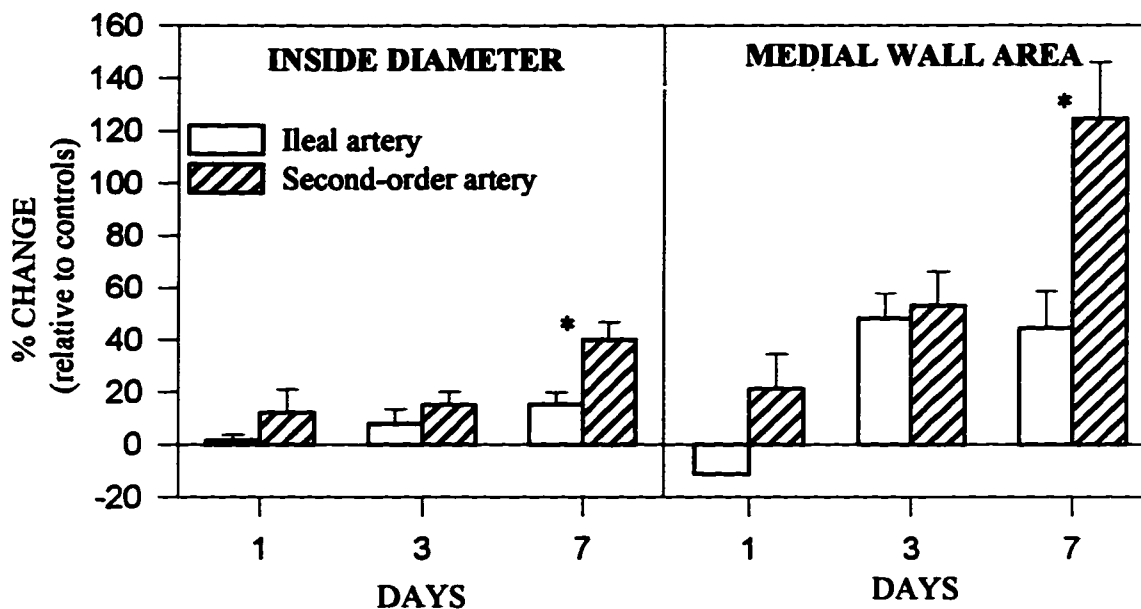


**Figure 6-3. Percent Change in Lumen Diameter and Medial Wall Area.** The percent change in lumen diameter and medial wall area between control and high flow vessels suggest a “dose-dependency” in terms of the magnitude of the flow-induced response. The percent changes in medial wall area far exceed those evidenced for luminal expansion in both vessels in response to flow. Values represent mean  $\pm$  SEM, and  $n = 10$  for each group. \*  $p < 0.05$ .

significantly heightened response for the second-order artery compared to the larger ileal artery for flow-induced alterations after 7 days in both lumen diameter and wall area. Figure 6-3 also indicates that the relative increases in medial wall area far exceed the changes observed in inside diameter after exposure to elevated flow. Figures 6-4 and 6-5 respectively illustrate medial wall thickness:lumen diameter ratios and medial wall area:lumen area ratios. No significant differences were detected for high flow vessels compared to same animal control vessels at any time.

#### *ICC Results for PCNA/SMC Nuclear Profile Analysis*

In order to determine the ratio of medial SMCs undergoing active DNA replication and cell division, ICC was performed for PCNA and medial SMC nuclei were counted. Figure 6-6 illustrates the percent PCNA-positive medial SMC nuclei for high flow vessels divided by those for control vessels. Data were best represented in this fashion to account for elevated basal PCNA counts, which averaged between 7% and 21% in both ileal and branch arteries. These data clearly indicate ileal artery medial SMCs undergo significant DNA synthesis after 3 and 7 days of elevated blood flow (+189%, +179% compared to same animal controls, respectively), while significant DNA synthesis occurs in the second-order arterial branch after 7 days (+407% compared to control).

In the case of polyploidy whereby cells undergo DNA replication without cell division, cells can stain positive for PCNA without a change in cell number (14). Figure 6-7 shows absolute medial nuclear counts with significant SMC hyperplasia indicated in

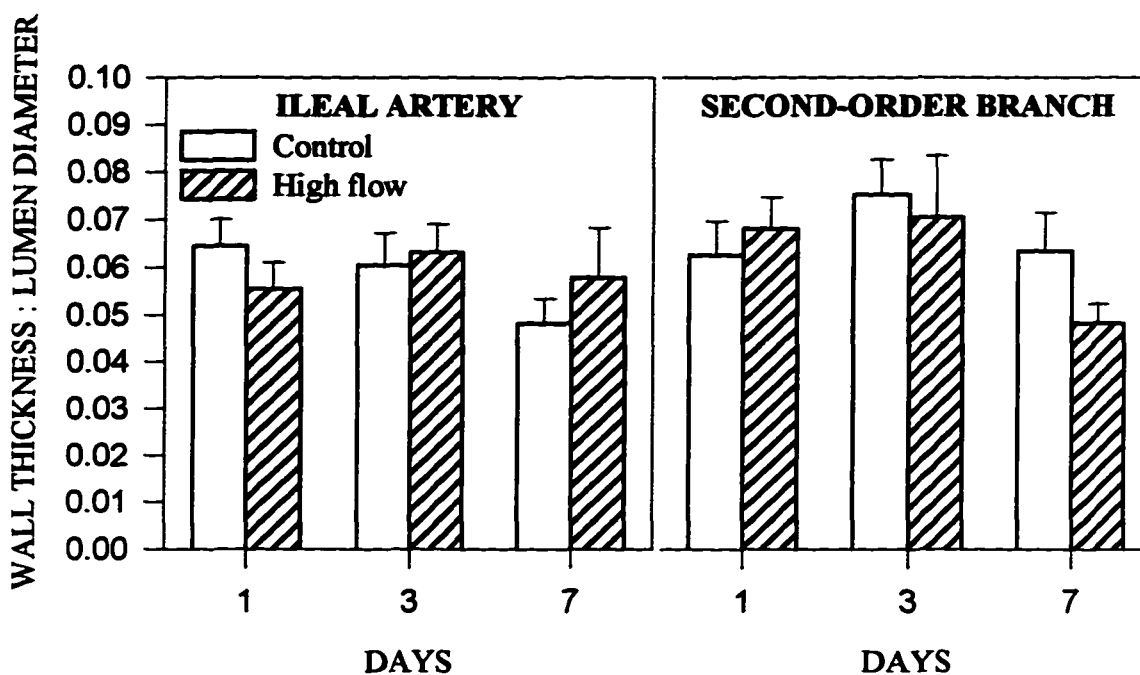


**Figure 6-4. Medial Wall Thickness:Lumen Diameter Ratio.** Medial wall thickness:lumen diameter ratios for ileal and second-order arteries show no significant differences between high flow and control vessels. These data show that similar increases are observed in wall thickness when compared to luminal expansion, indicating that chronic wall stress is stabilized in the presence of normal arterial pressure. Values represent mean  $\pm$  SEM, and  $n = 10$  for each group.

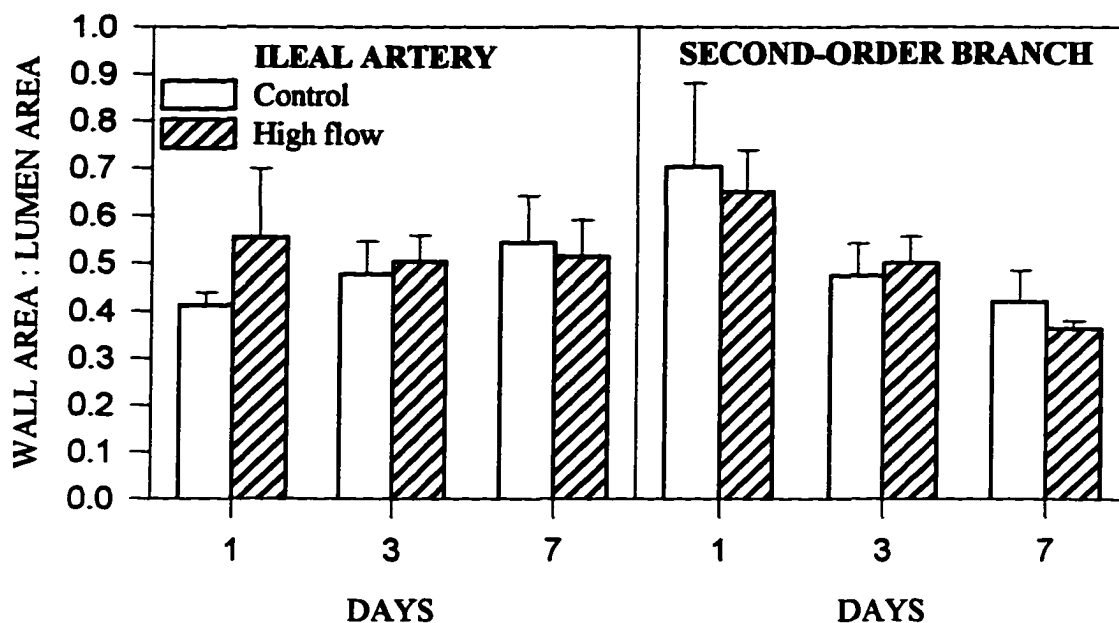


**Figure 6-5. Medial Wall Area to Lumen Area Ratio.** Medial wall area:lumen area ratios for ileal and second-order arteries show no significant differences between high flow and control vessels. These data show that similar increases are observed in medial wall hypertrophy when compared to luminal area and indicate that chronic wall stress is stabilized in the presence of normal arterial pressure. Values represent mean  $\pm$  SEM, and  $n = 10$  for each group.

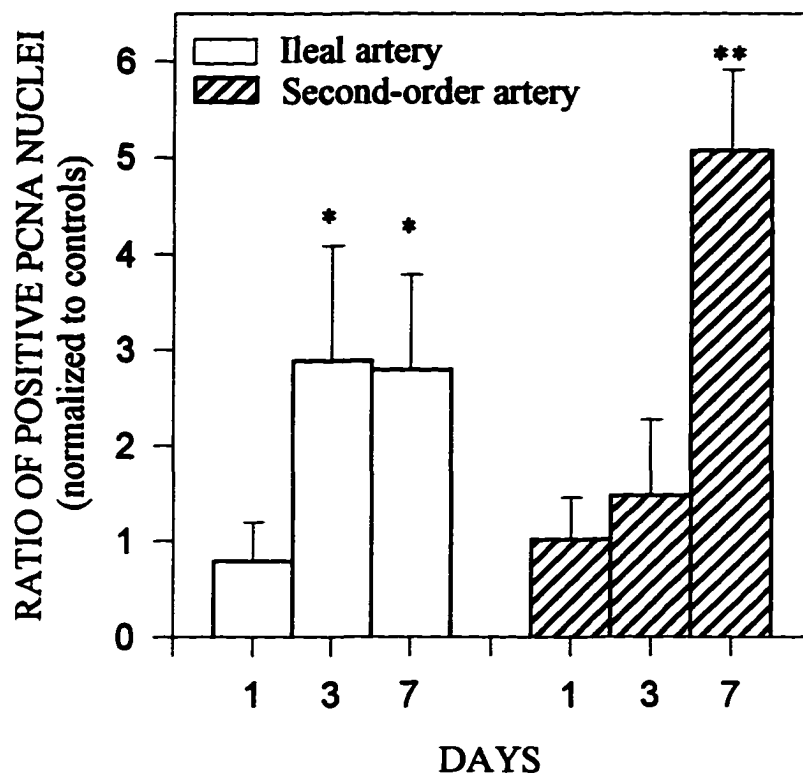


**Figure 6-6. Medial Wall SMC PCNA Ratio.** Immunocytochemical results for medial SMC PCNA in ileal and second-order arteries. Data represent percent PCNA-positive medial SMC nuclei for high flow vessels divided by those for control vessels for both the ileal artery and second-order branch. Data suggest significant DNA synthesis in the media of SMCs after exposure to elevated flow for 3 and 7 days. Values represent mean  $\pm$  SEM, and  $n = 6$  for each group. \*  $p < 0.05$ , \*\*  $p < 0.01$  versus control.

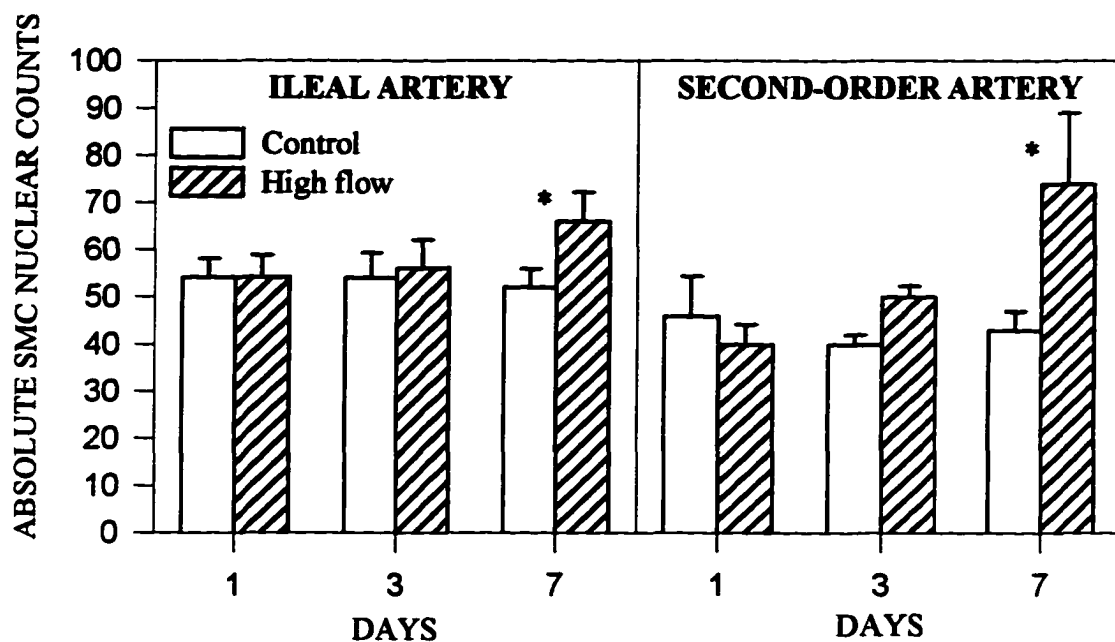


**Figure 6-7. Absolute Medial Wall SMC Nuclear Counts.** This data indicate significantly increased cell division after *in vivo* exposure to flow for 7 days for both ileal and second-order arteries. Significant differences in absolute nuclei number were not detected between control and high flow vessels after 1 or 3 days. Values represent mean  $\pm$  SEM, with  $n = 6$  for each group. \*  $p < 0.05$  versus control.

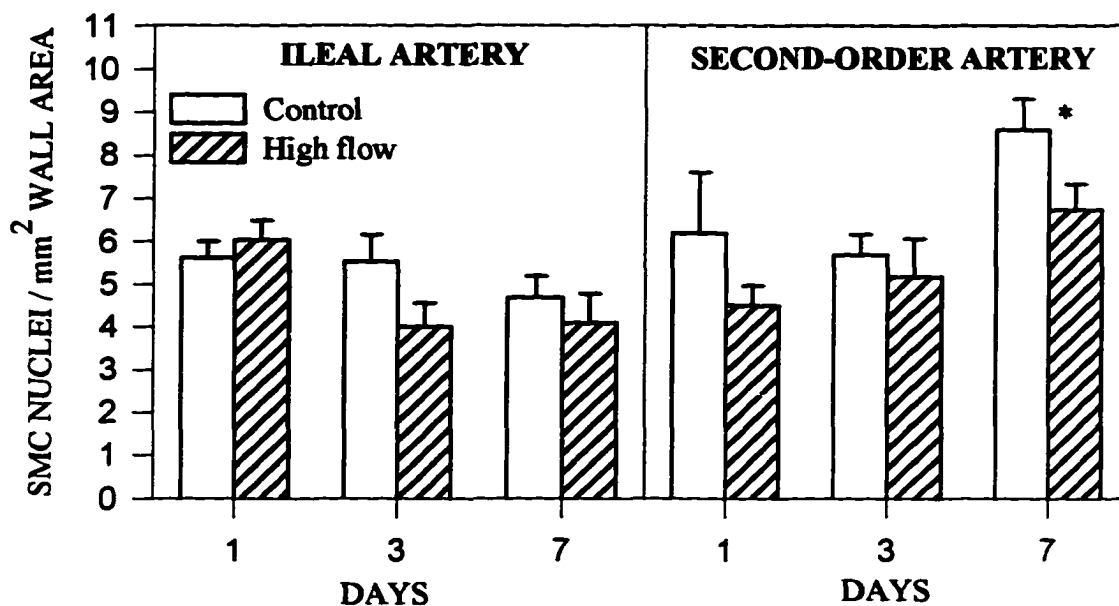


**Figure 6-8. Normalized Medial Wall SMC Nuclear Counts.** This data suggest that, at almost all time points, increased cell division is proportional to increased medial wall area to maintain a constant SMC density. The second-order vessel demonstrates a significant decrease in cell density upon exposure to elevated flow after 7 days, suggesting that cellular hypertrophy and perhaps nuclear polyploidy may be involved in this vessel at this time point. Alternatively, SMCs in this vessel may be actively engaged in the cell cycle prior to cytokinesis. Values represent mean  $\pm$  SEM, with  $n = 6$  for each group. \*  $p < 0.05$  versus control.

both high flow ileal (+30%;  $p < 0.04$ ) and second-order (+73%;  $p < 0.05$ ) arteries after 7 days. When data were normalized to medial wall area (Fig.6-8), SMC nuclear density remains constant in the presence of enlarged wall areas for almost all time points in both the ileal and second-order arteries. However, data indicate that the second-order artery experienced significant SMC hypertrophy after exposure to elevated flow for 7 days, as shown by a decreased (-22%;  $p < 0.02$ ) medial nuclear density concomitant with an increased wall area. These results imply that flow-mediated vessel wall remodeling *in vivo* occurs primarily through SMC hyperplasia with some contribution of cellular hypertrophy in small branching mesenteric arteries. Additionally, the second-order branch may be experiencing nuclear polyploidy after exposure to flow for 7 days, as suggested by increased nuclear replication in the presence of a decreased nuclear (and cellular) density.

#### *EC Nuclear Profile Analysis*

Figures 6-9 and 6-10 illustrate absolute and normalized intimal EC nuclear counts, respectively. At 1, 3, and 7 days of increased flow, absolute EC nuclear counts were significantly elevated in both the ileal (+17%, +50%, +65%; respectively) and second-order (+33%, +89%, +81%; respectively) arteries when compared to same animal control vessels. When data were normalized to 100  $\mu\text{m}$  luminal perimeter, only in the 1 day second-order vessels did the increase in EC counts not reach significance ( $p = 0.07$ ). Percent changes for normalized data for the ileal and second-order artery at 1, 3, and 7 days were +17%, +38%, and +44%, and +23%, +67%, and +36%, respectively. These results suggest that after 24 hours of increased blood flow *in vivo*, rat mesenteric arterial ECs are stimulated to undergo significant cellular replication leading to increased EC

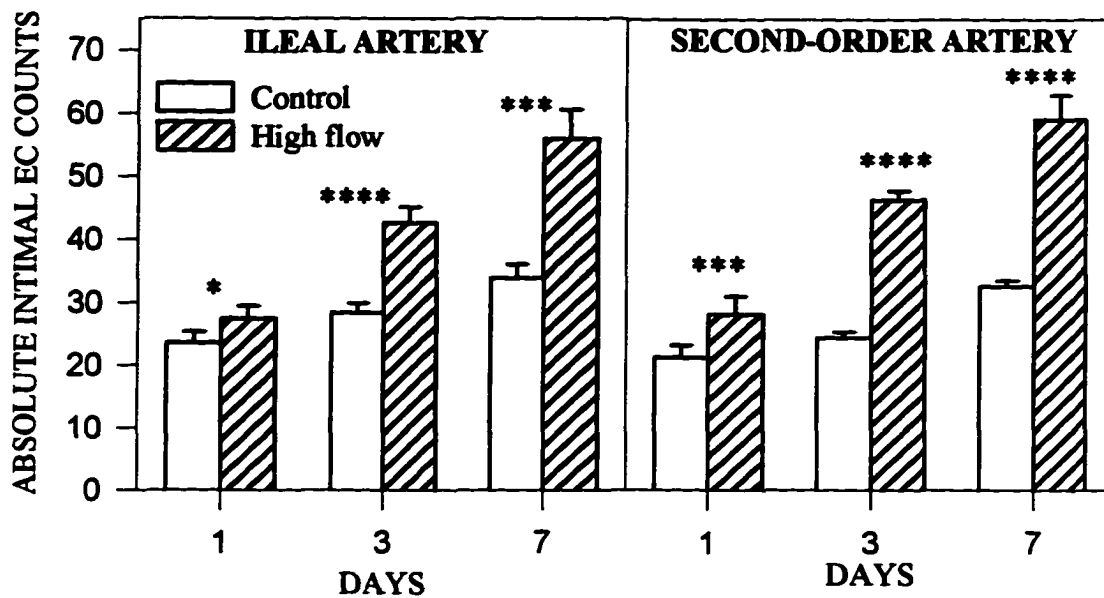
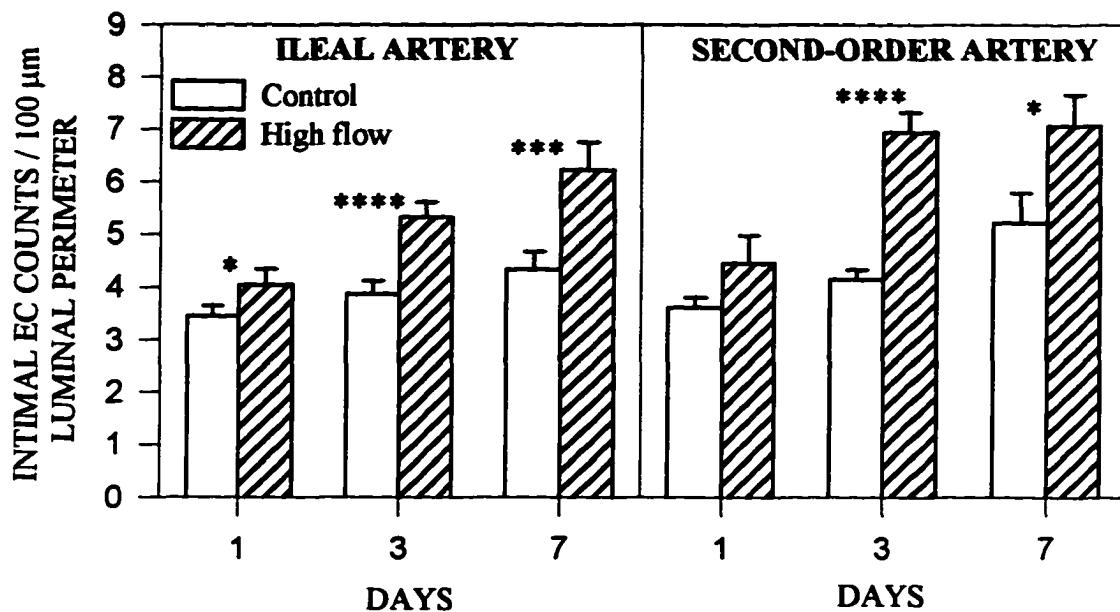


**Figure 6-9. Absolute Intimal EC Nuclear Counts.** These results indicate that once blood flow is increased, flow-mediated stresses are rapidly sensed by intimal endothelium leading to EC replication after 24 hours continuing through 7 days. Values represent mean  $\pm$  SEM, with  $n = 10$  for the ileal artery group and  $n = 8$  for the second-order branch group. \*  $p < 0.05$ , \*\*\*  $p < 0.001$ , \*\*\*\*  $p < 0.0001$  versus control.



**6-10. Normalized Intimal EC Nuclear Counts.** These data represent intimal EC nuclear counts normalized to 100  $\mu\text{m}$  luminal perimeter. The flow-mediated stress stimulus is rapidly sensed by the endothelium, leading to significant EC replication in the ileal artery after 24 hours, and in the second-order vessel after 3 days. Values represent mean  $\pm$  SEM, with  $n = 10$  for the ileal artery group and  $n = 8$  for the second-order branch group. \*  $p < 0.05$ , \*\*\*  $p < 0.001$ , \*\*\*\*  $p < 0.0001$  versus control.

densities. This exaggerated EC hyperplasia persists through 7 days of increased flow.

### Discussion

In this model, significant adaptations occurred in terms of luminal enlargement and medial wall hypertrophy in the ileal and second-order arteries after exposure to elevated flow (Figs. 6-1, 6-2). Generally, these morphological alterations were dependent upon the duration of *in vivo* flow exposure between 1 and 7 days. Ileal artery lumen diameters of both control and high flow vessels increased significantly with time. This implies that significant developmental growth in terms of luminal enlargement may be occurring in normal ~10 week old rat mesenteric ileal arteries over a 7 day period. Considering the significant interactions between day and treatment for all other morphological data, however, the authors believe that age was not a major factor influencing the results of this study. In agreement, Unthank et al. (180) found minimal bowel growth occurs in normal Wistar-Kyoto rats from 10 to 20 weeks of age.

Several important points should be mentioned when analyzing these flow-induced morphological data. A heightened adaptive response of the smaller second-order artery is noticed when compared to that of the larger ileal artery (Fig. 6-3). Percent changes in lumen diameter of high flow ileal arteries compared to same animal controls range between 1% and 13%, while the same changes for the second-order vessels range between 10% and 38%. Similarly, percent changes in medial wall area of high flow ileal arteries compared to same animal controls range between -9% and 58%, while the same changes for the second-order vessels range between 18% and 120%. Considering that the increase in blood flow and calculated WSR were significantly higher in the smaller second-order

branch compared to the parent ileal artery, the degree of flow-mediated vascular remodeling is suggested to be dependent on the magnitude of the flow stimulus in mesenteric vasculature. Another important observation concerns the greater changes observed in medial wall area compared to those found in luminal diameter. This suggests that a more dramatic adaptive response occurs affecting the circumferential component as opposed to the radial component of the vessel wall, supporting a role for wall stress in mediating these events. This is somewhat counter-intuitive, considering that the normal adaptation to increased blood flow is luminal enlargement to restore shear stress towards normal. In this model, highly significant increases in wall area, more consistent with changes in transmural pressure or wall stress, occur in the presence of unaltered arterial pressures. These results support a role for wall stress in addition to shear stress in contributing to flow-induced vascular remodeling. However, these results also raise questions concerning the signal transduction pathways that might be stimulated from increased blood flow *in vivo*. A possible role for flow-regulated growth factors in mediating *in vivo* vascular growth is addressed in the subsequent chapters.

The flow-mediated growth alterations evidenced in this study are structural rather than functional, because all vessels were maximally relaxed when formalin-fixed. This represents forms of vascular remodeling, as proposed by Langille and O'Donnell (92) in their work with rabbit common carotid arteries. These authors found a 21% decrease in lumen diameters in arteries subject to 70% flow reduction after 2 weeks. Based on the results that papaverine did not attenuate the response, they suggested that the decreased lumen diameters were the result of chronic flow-dependent structural modifications

occurring in the arterial wall. Results from the current study indicate that structural modifications from increased flow occur rapidly in the arterial wall and become statistically significant after exposure to elevated flow for 3 days.

Through a derivation of the Laplace relation for wall tension, if arterial pressure is held constant, a stable wall thickness:lumen diameter ratio implies a normal wall stress. In the current model, a constant wall thickness: diameter ratio between 1 and 7 days (Fig. 6-4) suggests that long-term wall stress remains constant. Luminal enlargement with medial wall hypertrophy coincident with a normal wall thickness:diameter ratio has been found by several other investigators using models of experimental atherogenesis in monkey iliac arteries (197) and collateral flow in rat mesenteric (179) and rabbit basilar arteries (96). In addition, a stable medial wall area:lumen area (Fig. 6-5) is shown for both vessels at all time points, indicating that the relative increases in wall area are similar to those for luminal enlargement. However, Price and Skalak (147) used a computational arteriolar network model based on a rat spinotrapezius transverse arteriole-collecting venule arcade and suggested wall stress to be a primary determinant for arteriolar remodeling and terminal arteriolar growth. Computed arteriolar shear stresses did not correlate with arteriolar remodeling in their model, but increased capillary shear stress did stimulate formation of arterio-venous shunts. The relative contributions of shear stress versus flow-stimulated wall stress in regulating vascular growth and remodeling in arterioles and small arteries necessitates further studies. Based on the assumptions and results from the current study as discussed in Chapter 5, we believe the primary stimulus for these vessels is shear stress with possible influence of acute flow-dependent wall stress in the ileal

artery. These flow-induced forces, then, can stimulate arterial remodeling as evidenced in this study.

Analysis of SMC and EC nuclei can provide insight into the cellular mechanisms governing structural remodeling of the arterial wall. Immunocytochemical results for PCNA (Fig. 6-6), a cell cycle-dependent cyclin (112), suggest ileal and second-order branch medial SMCs undergo DNA replication after 3 days of *in vivo* exposure to increased shear stress. Polyploid cells with DNA replication in the absence of cytokinesis, however, can erroneously be counted positive according to PCNA data (14). Absolute medial wall SMC nuclear counts (Fig. 6-7) suggest cellular hyperplasia after 7 days of elevated flow in both the ileal and second-order arteries. These combined data imply that elevated flow stimulates DNA replication and cellular division in medial SMCs under *in vivo* conditions. Normal SMC nuclear densities for the ileal and second-order arteries (Fig. 6-8) indicate that as medial wall hypertrophy occurs in response to elevated flow, SMC hyperplasia maintains a constant SMC density. After exposure to high flow for 7 days, however, the second-order artery exhibited a slightly significant ( $p = 0.046$ ) decrease in SMC density. Medial wall hypertrophy in this vessel at this time point may involve a combination of cellular hypertrophy and hyperplasia. Considering the PCNA data, nuclear polyploidy may be involved also. This would be in agreement with the findings of Owens (134) that large vessel SMC hypertrophy is often accompanied by development of nuclear polyploidy in hypertensive animals. Owens suggested that polyploidy may act as a gene amplification adaptive mechanism commensurate with an increased transcriptional requirement of an enlarged cell. Another interpretation of the data for this vessel at this

time point is that numerous SMCs may be actively engaged in the cell cycle prior to cytokinesis. Once the remodeling process becomes complete, cellular hyperplasia and diploidy would result.

These results characterizing medial wall growth in response to increased blood flow are in concordance with the results from previous studies on developing animals. Langille et al. (91) found significant decreases in lumen diameter and arterial wall mass with significantly decreased DNA levels in flow-restricted carotid arteries in juvenile rabbits. Wang and Prewitt (187) established a unique unilateral orchidectomy model in developing rats and analyzed microvascular cremaster arterioles during normal or reduced blood flow. After 3 weeks of flow reduction due to a decreased demand, lumen diameters and cross-sectional wall areas were significantly reduced when compared to the arterioles of the control contralateral cremaster. In recent work by Unthank et al. (179) on collateral flow in rat mesenteric arteries, medial SMC hypertrophy was indicated after 1 week and SMC hyperplasia after 4 weeks contributing to medial wall expansion during luminal enlargement. In contrast to these findings, Sterpetti et al. (171) found an inverse relation between SMC growth rate and the magnitude of shear stress between 0 and 9 dyn/cm<sup>2</sup> in cultured bovine aortic SMCs. In addition, DNA synthesis was significantly reduced after 24 hours exposure to all levels of shear. However, direct exposure of the underlying SMCs to shear stress is not a factor in the current study. Kraiss et al. (86), through the use of vascular prostheses implanted in baboons, elicited a doubling of aortic blood flow with a resulting decrease in neointimal cross-sectional area, SMC proliferation, and total SMC volume. The authors noted, however, that by using rigid prosthetic aortic grafts, shear stress-induced vasoactive agents could not influence vessel diameter as would

normally occur in an *in vivo* situation. Lumen diameter, therefore, was altered only through changes in neointimal thickness which implies flow-mediated wall stress as the primary stimulus.

In the current study, intimal ECs were found to be rapidly and significantly affected by exposure to increased blood flow as shown by dramatic EC hyperplasia after 24 hours (Fig. 6-9). This may be part of an adaptive process coincident with increasing lumen diameters to maintain a stable EC density along the lumen perimeter; however, normalized EC counts in the high flow vessels indicate a dramatic endothelial replication leading to increased EC densities in all vessels at almost all time points (Fig. 6-10). These results are consistent with the results of Unthank et al (179), who found the number of EC nuclei in high flow collateral vessels ~90% greater than those observed in control vessels after both 1 and 4 weeks. Walpola et al. (186) discovered a 33% decrease in EC number in ligated rabbit carotid arteries after 5 days exposure to an ~80% decrease in blood flow. Masuda et al. (111) found EC density significantly elevated in high flow canine carotid arteries after 4 weeks; however, a corresponding increase in lumen diameter was not detected. The results from these studies, along with the present work, illustrate a significant direct influence of blood flow and shear stress on intimal EC replication. However, several investigators (28, 99, 119, 200) have found an inverse relation exists between blood flow and EC division in cultured aortic ECs. In cell culture, however, flow and shear stress stimulate a phenotypic change from a proliferative cell to a differentiated cell. In addition, cultured cells are usually not pre-conditioned to flow, as is the case with an *in vivo* preparation. Under culture conditions, the influence of growth factors is dramatically increased compared to the *in vivo* environment (104). These variables must

be considered and caution used when comparing results between *in vivo* and *in vitro* experiments.

In conclusion, the experiments described in this chapter examined the influence of flow-associated stresses on arterial remodeling in an *in vivo* experimental model. Significant luminal expansion and medial wall hypertrophy occurred in a time-dependent fashion over a 7 day period in both ileal and second-order branching arteries. These adaptations involved early and dramatic EC hyperplasia after 24 hours with subsequent medial SMC DNA replication and cellular hyperplasia after 3 days.

## **CHAPTER VII**

### **INCREASES IN EXTRACELLULAR CONNECTIVE TISSUE CONTRIBUTE TO FLOW-INDUCED VESSEL WALL HYPERTROPHY**

#### Introduction

Results from the previous chapters demonstrated that significant luminal enlargement and medial wall hypertrophy occurred in arteries exposed to flow-mediated stresses between 1 and 7 days. Further examination revealed EC and SMC nuclear and cellular replication as mechanisms contributing to the gross morphological changes observed. In order to completely analyze flow-mediated alterations in the medial wall, the contribution of extracellular connective tissue components must be considered. Most work in this area has focused on the endothelium and the ECM of its basement membrane. Ookawa et al. (133) determined that cultured aortic ECs were dependent upon the presence of underlying ECM components type IV collagen, heparan sulfate, chondroitin sulfate, and dermatan sulfate for shear stress-induced cytoskeletal rearrangement. Wilson et al. (194) found strain-stimulated DNA synthesis in cultured SMCs was dependent on the composition of the underlying matrix. Cyclical strain increased DNA synthesis in cells grown on collagen I, fibronectin, and vitronectin, but did not affect cells grown on elastin or laminin. In addition, the responses to strain were dependent on the interactions between  $\beta_3$  and  $\alpha_v\beta_5$  integrins and the specific matrix proteins. The extracellular components fibronectin, laminin, collagen type IV, and vitronectin have been found to redistribute in terms of fibril orientation and thickness (175, 176, 189) and to both increase and decrease in response to shear stress (57, 132, 175, 176) and cyclic stretch (173). The

aim of the present chapter is to characterize alterations in extracellular connective tissue of the vessel wall after exposure to elevated blood flow and to determine its contribution to flow-induced vessel wall hypertrophy under *in vivo* conditions.

### Results

Figure 7-1 shows the percent extracellular connective tissue present in the medial vessel wall for control and high flow ileal and second-order arteries. No significant differences were observed between control and high flow vessels at any time. The percent of medial wall occupied by extracellular connective tissue in control arteries ranged from 29% to 34%, while in the high flow arteries ranged from 34% to 41%. These results indicate that as the vessel wall hypertrophied in response to elevated flow, a concomitant increase in medial extracellular connective tissue occurred. Figure 7-2 shows photomicrographs of trichrome-stained extracellular connective tissues for same animal control and high flow vessels. The photo for the 7 day control animal contains a grid used for stereologic assessment.

### Discussion

The vessel medial wall is comprised of both cellular and extracellular components. As discussed in Chapter 6, exposure to elevated blood flow stimulated DNA replication and cellular hyperplasia in medial SMCs, thus contributing to significant medial wall hypertrophy. As the medial wall remodeled in response to elevated flow, synthesis of medial extracellular connective tissue was stimulated resulting in a constant percent connective tissue in the medial wall at all times (Fig. 7-1). This increase in connective

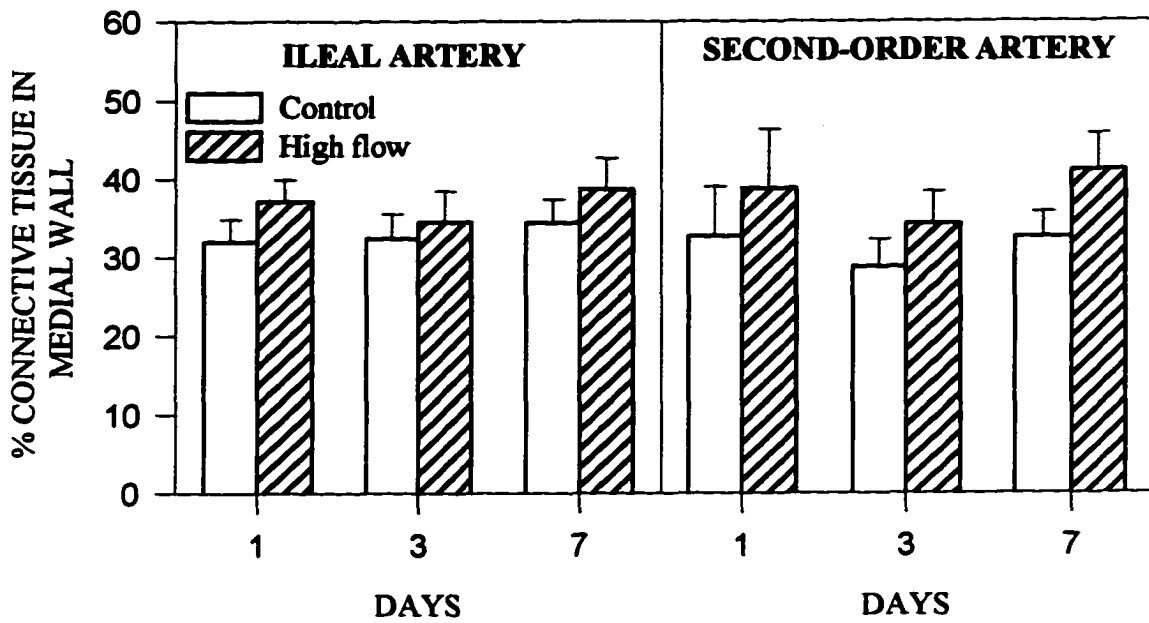


**Figure 7-1. Percent Extracellular Connective Tissue in Medial Wall.** A stable percent extracellular connective tissue in the medial wall indicates that as the medial wall hypertrophies, increased synthesis of medial connective tissue occurs to maintain a normal medial wall environment. Values represent mean  $\pm$  SEM, and  $n = 8$  for each group.

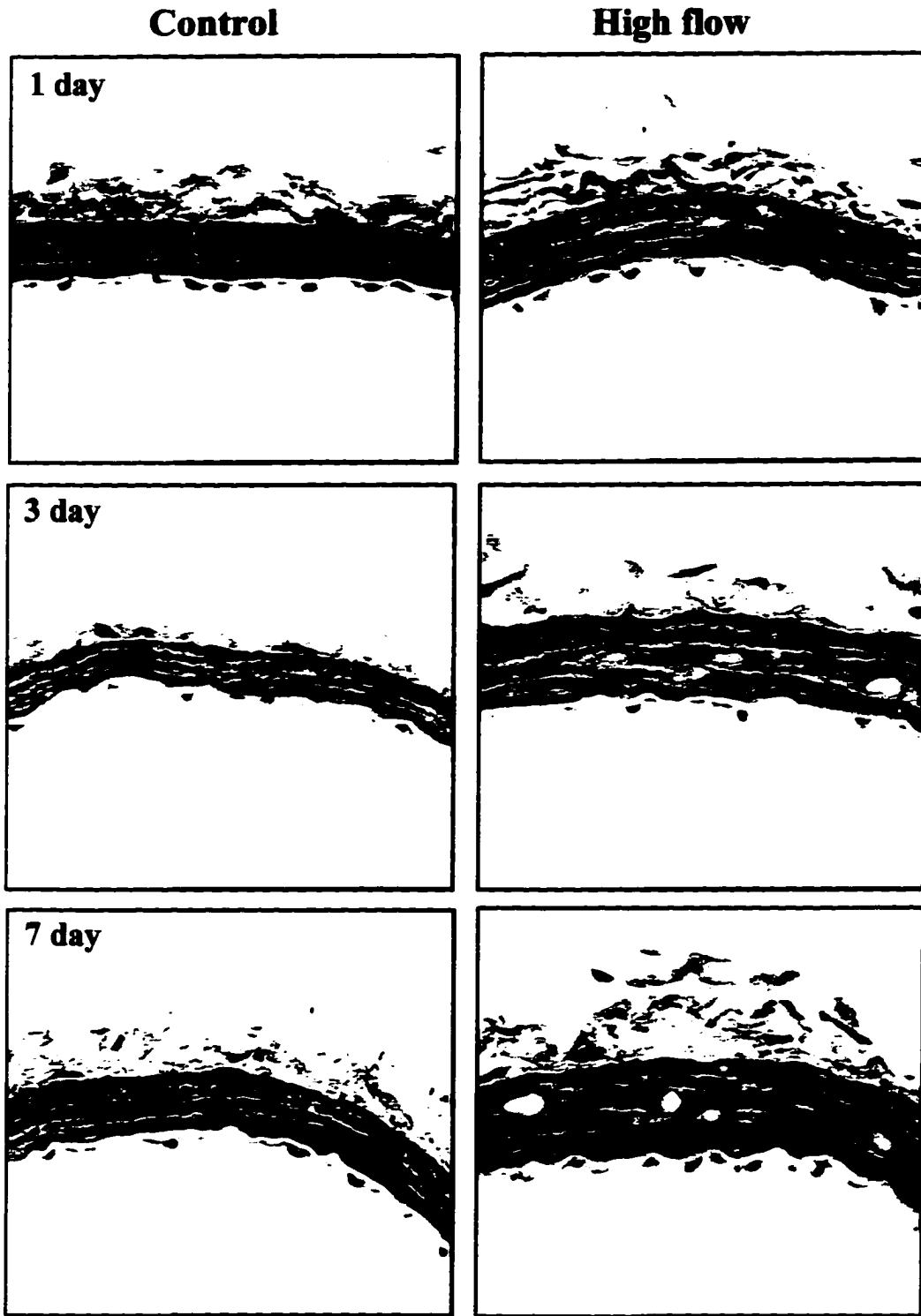


**Figure 7-2. Photomicrographs of Trichrome-Stained Extracellular Connective Tissue.**

tissue acts to maintain normal cell-cell contact concomitant with an enlarged wall area. If the extracellular components do not increase coincident with an enlarged wall area, disruption of the local micro-environment could occur. Physiologic roles for these ECM components include regulating EC adhesion, cellular spreading and migration, protein synthesis and EC proliferation, and cellular differentiation (reviewed in 175). Alterations in extracellular anatomy concomitant with altered SMC replication is essential for proper maintenance of vascular homogeneity and regulation of vascular physiology. In addition, upregulation of various growth factors can directly influence the proliferation of extracellular components. Ross (154) determined that PDGF can stimulate synthesis of ECM components under *in vitro* conditions. The findings of Sankar et al. (159) and Roberts et al. (150) established a role for TGF- $\beta$ 1 in inducing *in vitro* fibronectin expression and collagen formation, respectively. Ignatz and Massague (71) found TGF- $\beta$ 1 to increase expression of both fibronectin and collagen and to increase their incorporation into the surrounding ECM. In the current study, TGF- $\beta$ 1 transcription was not altered by elevated flow; however, elevated levels of PDGF-A mRNA were detected in the high flow ileal artery after 24 hours (Fig. 9-1). This increase in PDGF-A could possibly enhance synthesis of extracellular connective tissue as observed in this study.

One important role that has been proposed for the ECM is that it can act as an extracellular store for various growth factors. Kelly et al. (80) found that the alternatively spliced long-form of PDGF-A produced by cultured CHO cells was primarily localized to the underlying matrix, the short-form of PDGF-A predominantly secreted, and PDGF-B distributed between cells, ECM, and cell supernatant. Subsequent work by the same laboratory (41) found that plasmin released a mitogenically-active form of PDGF from

underlying ECM in a variety of cell types. The ECM has also been identified as a storage site for other growth factors including TGF- $\beta$  and bFGF (21, reviewed in 41). Basic FGF peptide has been found to localize to ECM-associated heparan sulfate proteoglycans, where it can be released through the actions of plasmin (157). This raises the possibility of shear stress inducing EC-derived plasminogen activators and inhibitors, which could then enzymatically release bFGF from the ECM through plasmin formation. Diamond et al. (40) found TPA secretion to be significantly increased over control levels in cultured HUVECs exposed to arterial levels of shear stress. In addition, release of these factors from the ECM often occurs in a regulated fashion and may be mediated by specific extracellular proteases such as chondroitin lyase (80) in addition to plasmin (22). This ability of the ECM to sequester growth factors is pertinent to the present study, as our results show upregulation of PDGF-A chain mRNA in SMCs and ECs surrounded by extracellular connective tissue. Even if transcription of a certain factor is increased and elevated protein levels result, physiologic activity may be significantly influenced by storage in the ECM.

In conclusion, this chapter illustrates that as the medial wall hypertrophies in response to elevated flow and its associated stresses *in vivo*, a concomitant increase in extracellular connective tissue synthesis occurs to maintain normal vessel architecture. This increase in ECM tissue could be directly stimulated by increased flow or, more likely, involves stimulation from local action of flow-induced growth factors.

## **CHAPTER VIII**

### **ENDOTHELIAL-DERIVED NITRIC OXIDE MAY MEDIATE FLOW-INDUCED VASCULAR REMODELING**

#### Introduction

The ability of NO to mediate numerous aspects vascular function has been well substantiated. Flow-induced increases in NO transcription, translation and release have been demonstrated by numerous investigators using *in vitro*, *in vivo*, and isolated intact vessel preparations (27, 28, 88, 103, 130, 169). The feedback mechanism of NO-dependent vasoactive relaxation in response to elevated blood flow acts to influence arterial tone and regulate blood supply to downstream tissues. Shear stress regulation of the endothelial isoform of NOS has been investigated at the transcript (126, 177) and protein (126, 142) levels. In addition, the influence of cyclic strain on eNOS mRNA, protein translation, release, and activity has been studied (9, 10). The aim of this current chapter is to determine the influence of flow-associated stresses on arterial eNOS levels in our *in vivo* rat mesenteric flow model and to characterize the possible role of NO in mediating flow-induced arterial remodeling.

#### Results

Immunocytochemical results for eNOS in control and high flow vessels are depicted in Figure 8-1. Blind scoring of the specific eNOS signal was performed using a 0 - 4 grading scale, and scores were assessed using appropriate non-parametric statistics. Data show significantly elevated eNOS scores in the high flow ileal artery at all time points. After 1, 3, and 7 days of elevated flow, eNOS scores were increased 49%, 55%,

and 70%, respectively, in the high flow ileal arteries compared to controls. Only after 7 days of elevated flow did the eNOS scores reach significance for the second-order vessels (+69%;  $p < 0.05$ ). Endothelial NOS scores for 1 and 3-day high flow second-order vessels were still elevated over controls (+28%, +24%, respectively), although statistical significance was not reached. Photomicrographs of eNOS-immunostained cross sections are shown in Figure 8-2 with same animal control and high flow vessels.

### Discussion

The role of NO in mediating many aspects of vascular homeostasis is well documented (24, 42, 82, 178). The importance of NO in regulating vascular tone in the mesenteric circulation has also been characterized by several investigators (48, 68, 73). In addition, flow-dependent alterations in NO transcription and translation have been elucidated using a variety of experimental conditions (23, 62, 87, 88, 177); however, studies analyzing shear stress regulation of eNOS are somewhat limited. Shear stress-induced increases in eNOS mRNA, protein, and release have been documented in cultured BAECs and HUVECs (126, 127, 136, 142). In addition, cyclic strain has been found to upregulate eNOS mRNA and protein expression in cultured BAECs (9, 10). However, the influence of shear stress on eNOS upregulation under *in vivo* conditions has yet to be substantiated.

Results from the current study suggest that eNOS protein was elevated in arteries exposed to increased blood flow after 24 hours (Fig. 8-1). As discussed in Chapter 5, the influence of flow-mediated wall stress in these vessels was lower than that of shear stress. These results are consistent with previous studies demonstrating

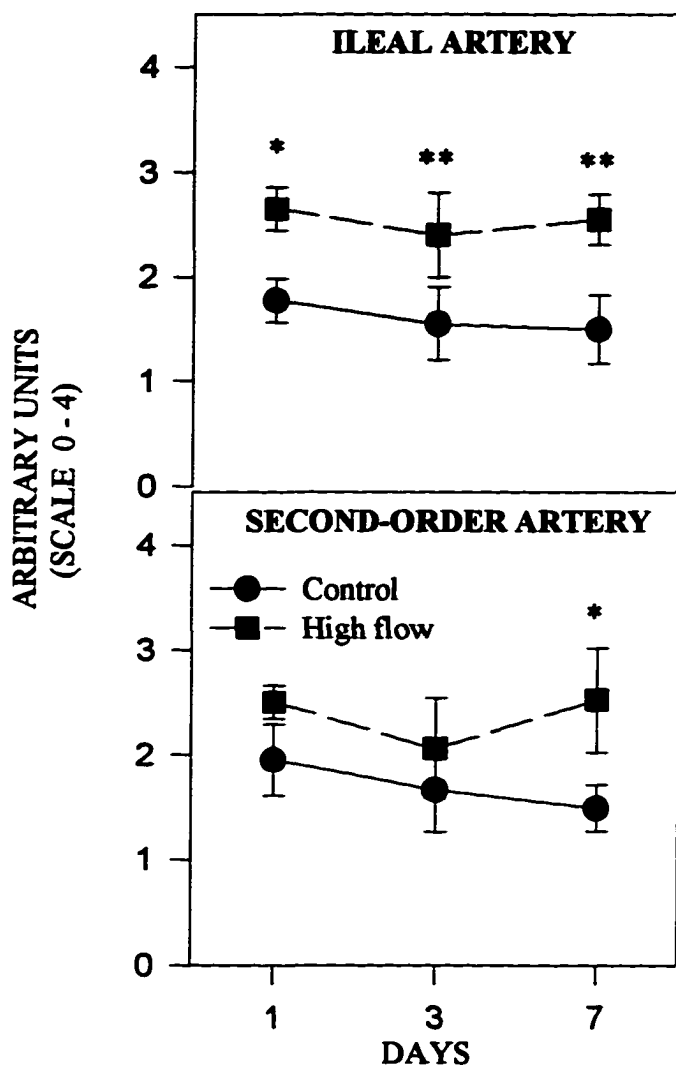


**Figure 8-1. Endothelial NOS Protein Levels.** Immunocytochemical results for eNOS in control and high flow vessels indicate significantly elevated peptide levels in the ileal artery after 1, 3, and 7 days of elevated flow, and significantly elevated levels in the second-order artery after 7 days. Blind scoring of the specific eNOS signal was performed using a 0-4 grading scale, and statistical analysis was performed using a paired replicate Wilcoxon signed rank test. Values represent mean  $\pm$  SEM, with  $n = 10$  for the ileal artery group and  $n = 7$  for the second-order artery group.

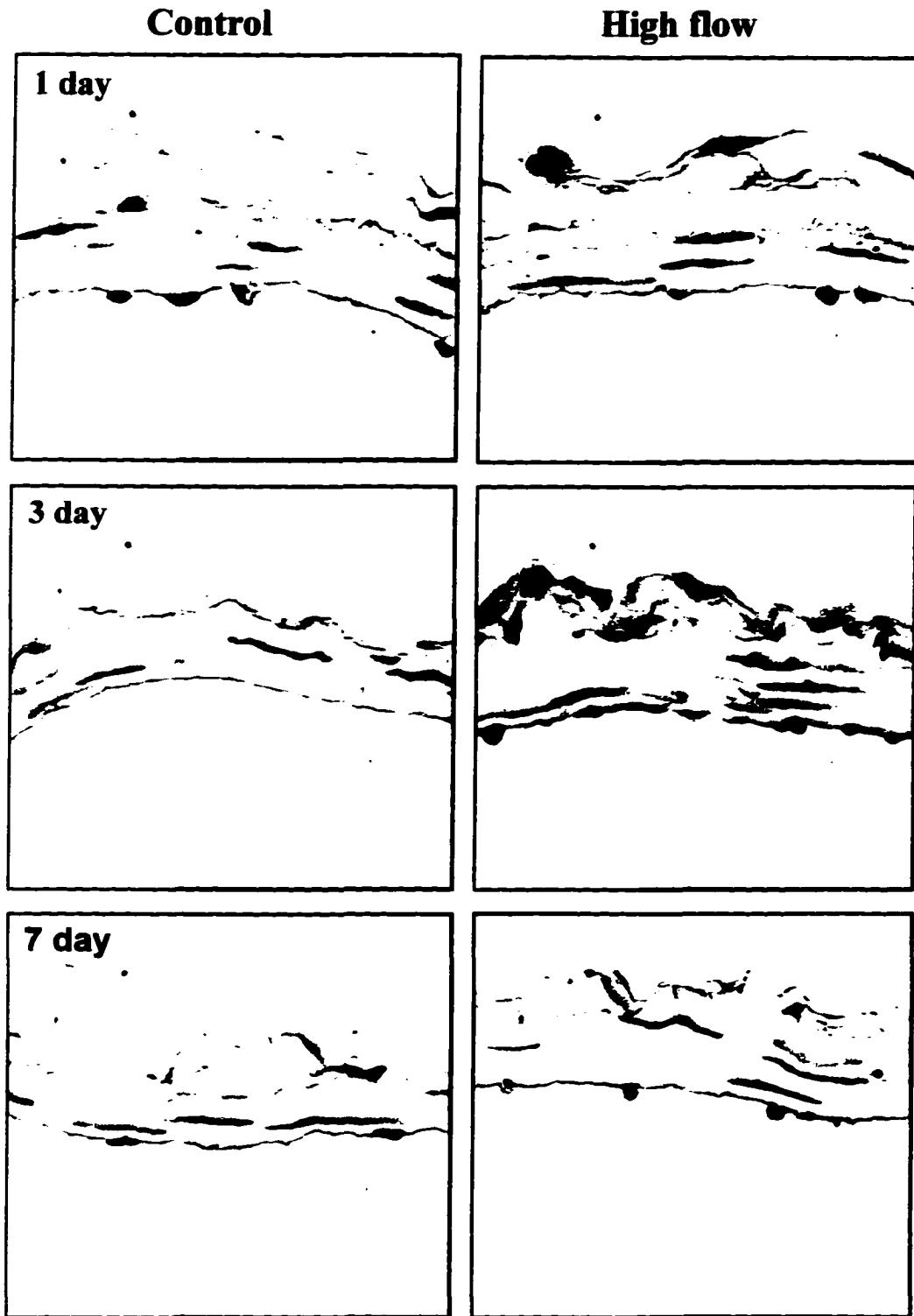


**Figure 8-2. Photomicrographs of ICC Slides for eNOS.**

that flow upregulates eNOS protein levels in cultured ECs (126, 142). Several investigators have found eNOS-mediated NO to be anti-mitogenic and inhibitory for DNA synthesis in vascular SMCs (51, 52, 122). Our results showing increased eNOS protein concomitant with early EC hyperplasia and luminal enlargement and medial wall hypertrophy after 3 and 7 days, then, seem rather counter-intuitive. However, several investigators have recently found that NO mediates the mitogenic effects of VEGF on cultured microvascular venular ECs (120) and amplifies bFGF-induced mitogenesis in primary rat aortic SMCs (61). In addition, Ziche et al. (198) found that the NO-generating agents SNP, ISDN, and GTN stimulated DNA synthesis in cultured ECs isolated from coronary postcapillary venules. Results from treatment of cells with L-NMMA and methylene blue suggested endogenous NO can directly modulate EC proliferation in the microvasculature. Subsequent work from the same laboratory (199) demonstrated that substance P-induced angiogenesis *in vivo* in rabbit cornea and *in vitro* in ECs isolated from coronary postcapillary venules were both potentiated by administration of SNP, ISDN, and GTN. Nitric oxide donation was found to significantly enhance EC thymidine incorporation, cell number, and migration *in vitro*. Leibovich et al. (97) determined that LPS-stimulated human monocyte-induced angiogenesis required an L-arginine/NOS-dependent effector mechanism, as assessed *in vivo* in rat corneas and *in vitro* by chemotaxis of HUVECs. Indeed, the results cited here, as well as those from the present study, identify crucial roles for NO in mediating various vascular mechanisms including cell migration and chemotaxis, cellular proliferation and nuclear replication, angiogenesis, and synergism and potentiation with other vasoactive agents.

In conclusion, this chapter suggests NO as a possible signaling factor in flow - mediated vascular wall remodeling under *in vivo* conditions. Elevated eNOS levels 24 hours through 7 days after initiation of the flow stimulus imply that NO, probably in combination with cytokines or growth factors, is involved in the cellular changes leading to flow-induced luminal enlargement and/or medial wall hypertrophy.

## CHAPTER IX

### **EARLY MEDIAL AND SUBSEQUENT ENDOTHELIAL PLATELET-DERIVED GROWTH FACTOR-A CHAIN MAY BE INVOLVED IN FLOW-MEDIATED VASCULAR REMODELING *IN VIVO***

#### Introduction

Platelet-derived growth factor is an important regulator of the vasculature that influences cell migration, proliferation, chemotaxis, angiogenesis, cell-cell adhesion, and cellular metabolism (155). PDGF exists as both the homo-dimers -AA and -BB or as the heterodimer -AB. Upon binding to and dimerization of the receptor, PDGF can stimulate vasoconstriction, mitogenesis, chemotaxis, and other functions in a variety of cells (153, 155). Various mechanical perturbations including shear stress have been found to stimulate transcription (64, 65, 66, 115), translation (85), and release (30) of the -AA homodimer in both endothelial and smooth muscle layers. Shear stress-mediated PDGF-A induction and subsequent migration and proliferation of SMCs and fibroblasts corroborates with the “response to injury hypothesis of atherogenesis” proposed by Ross (154). Increased shear stress may be sensed as an insult by the endothelial and smooth muscle layers, which can respond by synthesizing and secreting growth factors contributing to atherogenesis and formation of intimal and medial neoplasias. As discussed in previous chapters, the experimental model employed in the current study induces an increase in *in vivo* blood flow leading to EC and SMC hyperplasia and vessel wall remodeling. The aim of this and subsequent chapters is to determine the role of

various biochemical growth factors in this flow-mediated vascular remodeling. Specifically, this chapter examines PDGF-A mRNA expression in control and high flow vessels using *in situ* hybridization approaches.

### Results

*In situ* hybridization data for medial wall SMC PDGF-A mRNA expression are illustrated in Figure 9-1. A highly significant (+215%) increase in medial PDGF-A mRNA is indicated for the high flow ileal artery after 24 hours. This increase becomes non-significant after 3 (+122%) and 7 (+42%) days as the values decline towards control levels. An elevated basal expression of medial PDGF-A mRNA in the ileal artery remains constant with time. No significant differences between control and high flow vessels were detected for the second-order artery at any time. Figure 9-2 shows *in situ* hybridization data for endothelial PDGF-A mRNA expression. The ileal artery shows a non-significant (+39%) increase in EC levels after 24 hours which becomes significant after 3 (+129%) and 7 (+182%) days. No significant differences were detected between control and high flow second-order arteries; however, data for this vessel were somewhat noisy and resulted in irregular control values. Figure 9-3 contains autoradiographs for PDGF-A mRNA expression for same animal sense and anti-sense control and high flow vessels.

### Discussion

The most obvious result from this chapter is the highly significant upregulation of ileal artery medial PDGF-A expression after exposure to increased blood flow for 24 hours (Fig. 9-1). According to the results discussed in previous chapters, once the flow stimulus was established in this model, significant EC hyperplasia occurred after 24

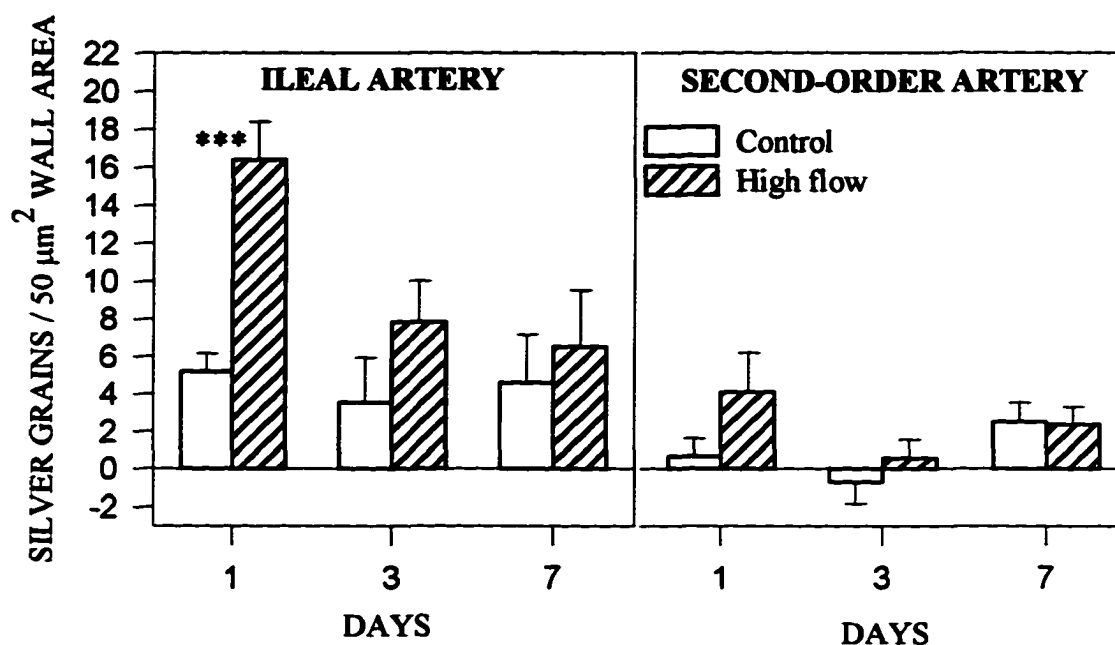


**Figure 9 - 1. Medial SMC PDGF-A mRNA Expression.** Medial wall SMC PDGF-A mRNA expression for control and high flow ileal and second-order branch vessels after *in situ* hybridization with  $^{35}\text{S}$ -CTP riboprobe and development of silver grain emulsion after 10 weeks. PDGF-A mRNA expression is significantly elevated in the ileal artery after 24 hours, and then gradually declines towards normal levels by 3 and 7 days. Basal levels of PDGF-A mRNA expression are evident in the control ileal artery. No significant differences were detected between control and high flow second-order arteries, and control level of expression in these vessels was low. Values represent mean  $\pm$  SEM, and  $n = 9$  for the ileal artery group and  $n = 7$  for the second-order artery group.

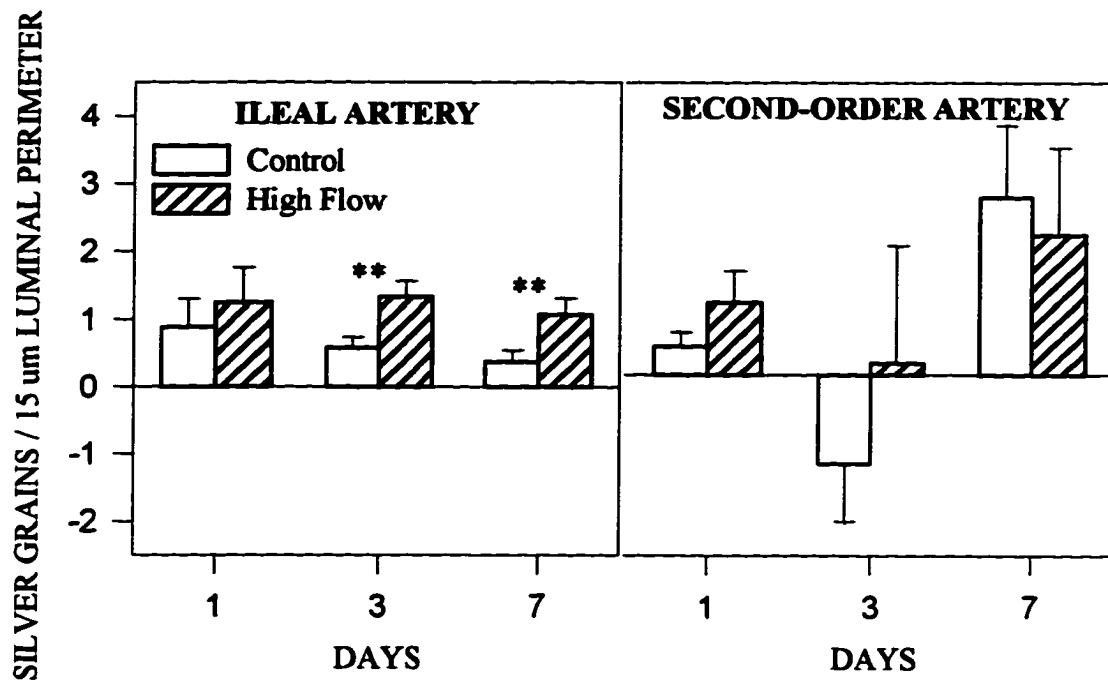


**Figure 9-2. Endothelial PDGF-A mRNA Expression.** Endothelial PDGF-A mRNA expression for control and high flow ileal and second-order branch vessels after *in situ* hybridization with  $^{35}\text{S}$ -CTP riboprobe and development of silver grain emulsion after 10 weeks. PDGF-A mRNA expression is significantly elevated in the ileal artery endothelium after exposure to high flow for 3 and 7 days. No significant differences were detected between control and high flow second-order arteries, with specific signal similar to background levels. Values represent mean  $\pm$  SEM, and  $n = 10$  for the ileal artery group and  $n = 7$  for the second-order artery group.

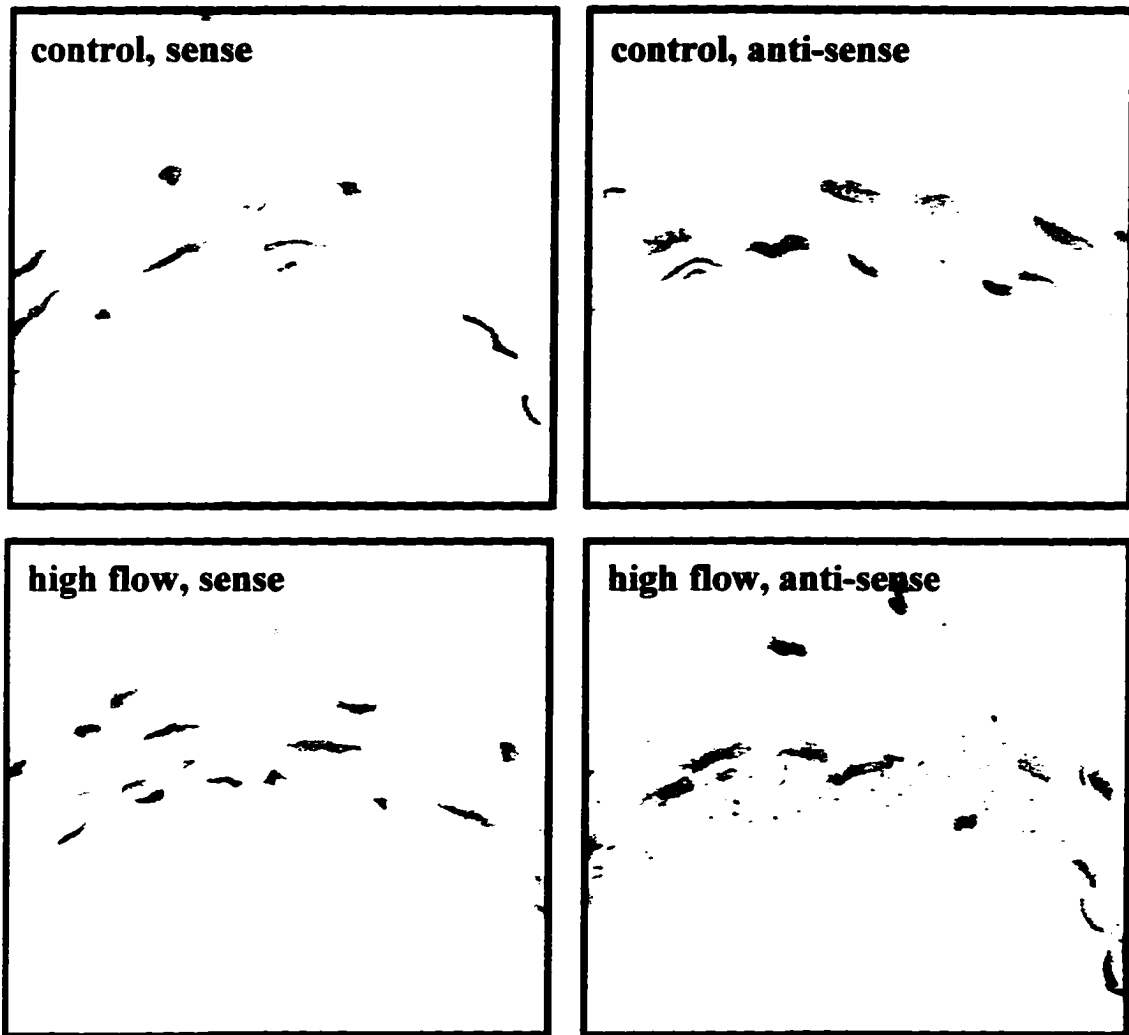


**Figure 9-3. Autoradiographs for PDGF-A mRNA Expression.**

hours with subsequent SMC hyperplasia and luminal and medial wall remodeling after 3 and 7 days. The significant upregulation of PDGF-A mRNA in the ileal artery media after 24 hours strongly suggests its involvement in flow-mediated vascular remodeling. Autocrine growth stimulation by PDGF has been characterized by several investigators (115, 154, 185). Indeed, autocrine mitogenicity from PDGF-A seems to be involved in the current model, as early medial expression precedes subsequent medial SMC DNA synthesis, cellular hyperplasia, and medial wall hypertrophy. An opposing proposal was offered by Vlodavsky et al. (184), who suggested that PDGF exerts its mitogenic action in a paracrine mechanism to affect neighboring cells within the vessel wall. In the current model, perhaps elevated medial PDGF-A is stimulating neighboring ECs to multiply. Although not specifically analyzed in this study, medial PDGF-A protein levels are most likely elevated after 3 and 7 days of elevated flow. Results showing no significant differences between control and high flow second-order branches are somewhat confusing, although heterogeneity in vascular growth responses between different orders of vessels as well as between components of a single vessel has been characterized by Daemen and De May (32) and Bobik and Campbell (18).

Basal levels of PDGF-A mRNA expression are evident in this study for the ileal artery media. This would corroborate the findings of Majesky and coworkers (104, 106) who found PDGF-A mRNA constitutively expressed in quiescent normal newborn and adult rat aortic and carotid artery SMCs. In addition, Majesky et al. (106) found basal levels of transcripts for PDGF receptor subunits, indicating that the normal vessel wall has the potential to synthesize and respond to both basal and increased levels of PDGF.

Endothelial PDGF-A mRNA expression was detected preferentially in the high flow ileal artery after 3 and 7 days (Fig. 9-2). This result is interesting considering that rapid EC replication occurred after 24 hours (Figs. 6-10, 6-11). If the flow-mediated stress stimulus was sensed immediately by the endothelium and transferred to subjacent medial SMCs through cell-cell contacts (matrix proteins, focal adhesion sites), then medial expression of PDGF-A could occur after 24 hours as shown. Then, through an autocrine positive feedback loop (154), endothelial expression could subsequently be stimulated by 3 and 7 days resulting in EC hyperplasia. Alternatively, this delayed increase in EC PDGF-A transcription could indicate repair of a shear stress-injured endothelium, as suggested by Majesky et al. (106) who showed increased SMC PDGF-A mRNA 2 weeks after arterial balloon injury. However, this does not account for the relatively small increase (+39%) in EC PDGF-A mRNA observed after 24 hours. Perhaps the cellular machinery involved in initially sensing the stimulus and starting the signaling cascade leading to nuclear transcription was delayed, as the percentage of PDGF-A mRNA steadily increases at 3 and 7 days.

PDGF-A may act through an autocrine mechanism to induce synthesis of medial ECM evidenced in this study (Chapter 7). Ross (154) suggested that growth factors induce synthesis of underlying extracellular connective tissue components *in vitro*. The ECM is capable of regulating storage and release of growth factor peptides (referenced in 41); therefore, enhanced expression of medial PDGF-A evidenced in this study could reasonably translate into elevated protein levels, followed by sequestration in the ECM and subsequent autocrine stimulation of cellular and extracellular factors.

An early catalyst for SMCs to proliferate when exposed to an injuring stimulus involves increased PDGF-A transcription, as determined by Majesky et al. (106) using a rat carotid balloon catheter injury model. PDGF-A mRNA levels were elevated 10- to 12-fold 6 hours after balloon injury in carotid SMCs. This transient increase in SMC PDGF-A mRNA directly preceded entry into the synthetic phase of the cell cycle. Interestingly, 2 weeks after wounding neointimal SMCs expressed elevated PDGF-A transcripts and protein levels while expression in subjacent SMCs had returned to normal. This suggests that PDGF-A plays dual roles in response to arterial injury: first, an immediate upregulation occurs in order to mediate chemotaxis and cellular and extracellular proliferation directly in response to the injury, and second, a chronic elevation of PDGF-A occurs as part of the regeneration process and arterial repair.

In conclusion, early medial and subsequent endothelial expression of PDGF-A mRNA in ileal arteries exposed to flow-associated stresses *in vivo* may contribute to the cellular replication and vessel wall remodeling observed in this study. Temporal and autocrine regulation of this growth factor is implied, as significant medial expression after 24 hours contributed to subsequent endothelial expression after 3 and 7 days. Basal transcription of PDGF-A was observed in the media of the ileal artery, supporting the findings of previous investigators. However, characterizing the *in vivo* regulation of this growth factor, in terms of shear stress responsiveness and interaction with other factors, cytokines, and extracellular components, necessitates further examination.

## CHAPTER X

### PLATELET-DERIVED GROWTH FACTOR-B CHAIN IS NOT INVOLVED IN FLOW-INDUCED VASCULAR REMODELING

#### Introduction

The physiologic actions of PDGF in the vasculature are well established. Expression of the PDGF-B chain has been associated with medial SMC proliferation and migration leading to intimal thickening (74), chemotaxis and vasoconstriction (124), and stimulation of other growth-regulatory genes and mesenchymal cells producing extracellular components (18). In normal arteries, a low level of basal expression exists for PDGF-B in the media with higher levels found in the endothelium (192). The influence of physiologic stresses such as vascular injury and repair (81, 106), cyclic strain (193) and shear stress (66, 107, 118, 147) can significantly alter PDGF-B transcription and translation. Shear stress upregulation of PDGF-B mRNA has been shown in cultured ECs from several sources (64, 66, 118, 147). Elevated levels of PDGF-B peptide were also found in cultured SMC exposed to cyclic strain (193). In contrast, Malek et al. (107) found that shear stress significantly downregulated PDGF-B mRNA in cultured BAECs. In this same study, however, cyclic strain was found to have no effect on PDGF-B expression.

In the current study as discussed in the previous chapter, early medial and subsequent endothelial expression of PDGF-A mRNA was significantly upregulated after exposure to elevated blood flow. The aim of this current chapter is to further analyze the

contribution of PDGF in flow-induced vessel wall remodeling through *in situ* hybridization analysis of PDGF-B mRNA transcription.

### Results

Figure 10-1 illustrates data from *in situ* hybridization for medial PDGF-B mRNA expression. An elevated baseline level of medial PDGF-B expression is noted especially in the ileal artery. No significant differences were detected between control and high flow vessels at any time in both ileal and branch arteries. Expression of PDGF-B in the ileal artery media after 7 days is elevated in both the control and high flow vessels when compared to 1 and 3 day vessels. Figure 10-2 shows data for endothelial expression of PDGF-B. Significant increases (+62%) are evident in the ileal artery after 7 days. No other significant differences were detected between control and high flow vessels. Again, a basal level of endothelial PDGF-B expression is shown, especially in the ileal artery endothelium. Basal levels in the second-order artery are relatively low. Figure 10-3 illustrates autoradiographs for PDGF-B mRNA expression for same animal sense and anti-sense control and high flow vessels.

### Discussion

As discussed in Chapter 5, the primary flow-induced stimulus in this model was determined to be shear stress with possible involvement of stretch-induced wall stress in the ileal artery. These flow-associated stresses had no impact on medial wall expression of PDGF-B mRNA (Fig. 10-1), suggesting that medial wall PDGF-B is not involved in the flow-regulated arterial remodeling observed in this study. However, a significant upregulation of endothelial PDGF-B mRNA was apparent after exposure to elevated flow for 7 days (Fig. 10-2). This is in agreement with the findings of several other investigators

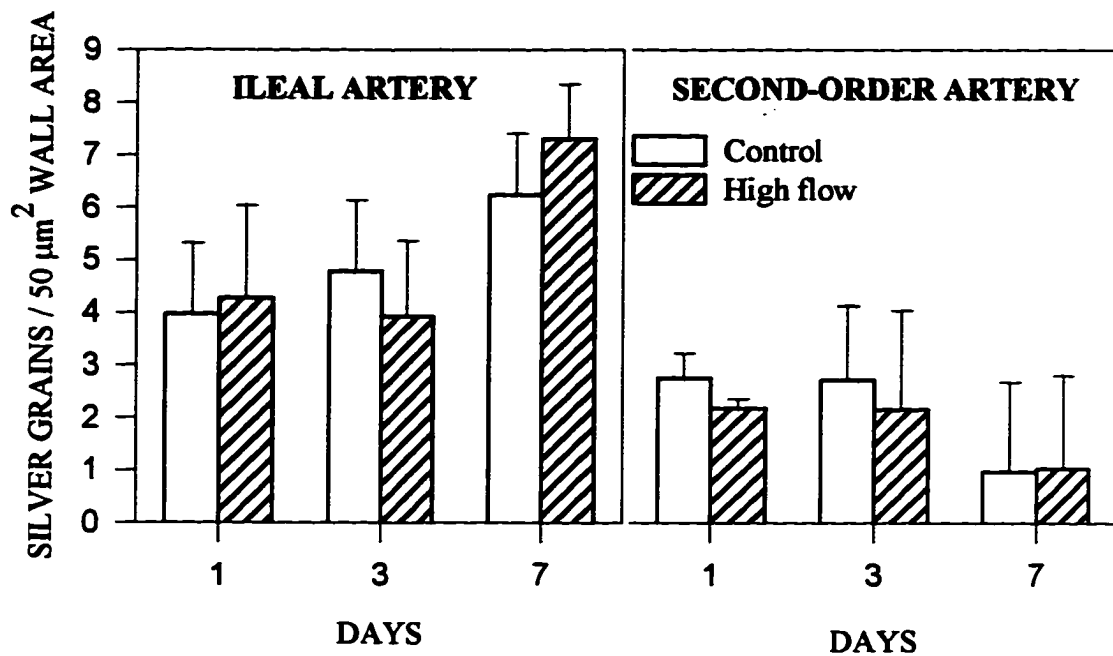


**Figure 10-1. Medial SMC PDGF-B mRNA Expression.** Medial wall SMC PDGF-B mRNA expression for control and high flow ileal and second-order branch vessels after *in situ* hybridization with <sup>35</sup>S-CTP riboprobe and development of silver grain emulsion after 10 weeks. No significant differences were detected between control and high flow vessels at any time. Transcript levels of both control and high flow ileal arteries were elevated after exposure to elevated flow for 7 days. Basal production of PDGF-B mRNA is noted for both the ileal and second-order arteries. Values represent mean  $\pm$  SEM, and  $n = 8$  for the ileal artery group and  $n = 6$  for the second-order artery group.

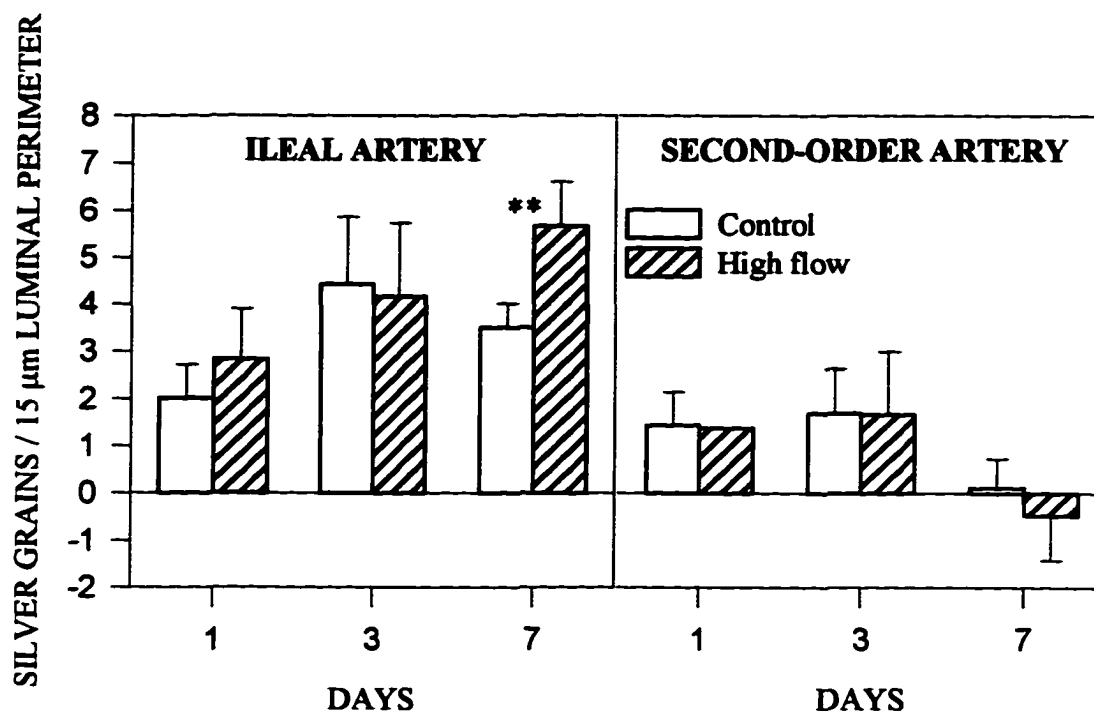


**Figure 10-2. Endothelial PDGF-B mRNA Expression.** Endothelial PDGF-B mRNA expression for control and high flow ileal and second-order branch vessels after *in situ* hybridization with  $^{35}\text{S}$ -CTP riboprobe and development of silver grain emulsion after 10 weeks. A significant increase in ileal artery PDGF-B mRNA occurred after exposure to flow for 7 days, while no other significant differences were detected at any time. An elevated basal level of PDGF expression is obvious in the ileal artery endothelium. Values represent mean  $\pm$  SEM, and  $n = 8$  for the ileal artery group and  $n = 6$  for the second-order artery group.

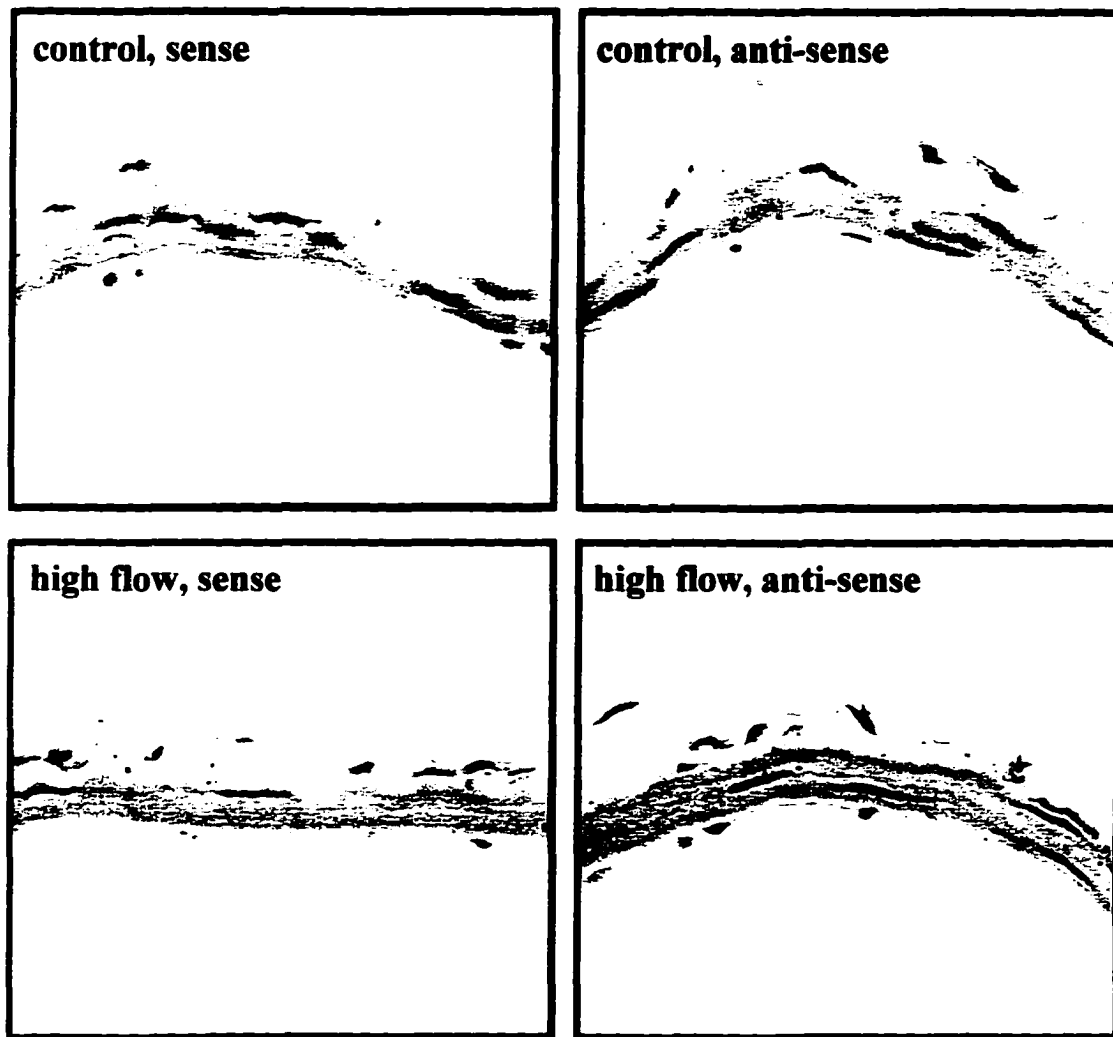


**Figure 10-3. Autoradiographs for PDGF-B mRNA Expression.**

who demonstrated shear stress increased the endothelial expression of PDGF-B in cultured cells (64, 66, 118, 147). In comparison, these studies were generally short-term, and PDGF-B upregulation was transient with a subsequent reduction towards basal levels. In the current study, only chronic exposure to flow-associated stresses resulted in a significant upregulation of endothelial PDGF-B message. This result is rather counter-intuitive considering that immediate EC replication occurred after 24 hours (Figs. 6-9, 6-10). The lack of early induction of endothelial PDGF-B after exposure to increased flow for 1 and 3 days suggests that perhaps the endothelium requires a prolonged time for sensing flow-associated stresses and may be specific for the arteries used in this experimental model.

Autocrine growth stimulation by PDGF has been characterized by several investigators (115, 154, 185). However, autocrine mitogenicity from PDGF-B does not seem to be involved in the current model, considering that differences were not detected between control and high flow vessels yet the high flow vessels experienced significant cellular hyperplasia and vessel wall hypertrophy. Only after 7 days of elevated flow does the endothelium exhibit significant PDGF-B expression (Fig. 10-2). According to Vlodavsky et al. (184), PDGF exerts its mitogenic action in a paracrine fashion affecting neighboring cells within the vessel wall. In the present study, elevated PDGF-A mRNA expression in the vessel media after 24 hours could reasonably act through a paracrine loop to induce subsequent endothelial transcription of PDGF-B chain after 7 days. Endothelial expression of PDGF-A chain was elevated after 3 and 7 days (Fig. 9-2), supporting evidence for this proposed feedback loop initially stimulated by medial PDGF-A mRNA.

A basal level of medial and endothelial PDGF-B expression was evident in this study, consistent with findings in cultured SMCs (125, 163) and ECs (64, 65, 66). Majesky et al. (106) suggested this constitutive expression of PDGF may allow normal vessels to synthesize and respond to both basal and increased levels of PDGF in order to maintain a normal cellular environment.

In conclusion, results from this chapter do not implicate medial or endothelial PDGF-B expression in regulating the flow-induced arterial remodeling observed in this study. Expression of endothelial PDGF-B message became significant only after exposure to flow for 7 days and was not involved in the earlier SMC or EC mitogenic events. Basal levels of both medial and endothelial PDGF-B mRNA were detected, providing support for its role in maintaining vascular homeostasis.

## CHAPTER XI

### NEITHER bFGF NOR TGF- $\beta$ 1 CONTRIBUTE TO VESSEL WALL

### REMODELING FROM INCREASED BLOOD FLOW

#### Introduction

As discussed in the previous chapters, PDGF is a vital growth factor capable of mediating vasoconstriction, chemotaxis, mitogenicity, and various other homeostatic and pathophysiologic functions in a variety of cell types. PDGF-A mRNA expression was found to be stimulated by flow-associated stresses possibly contributing to flow-induced vessel wall remodeling under *in vivo* conditions. Several other growth-regulating factors including bFGF and TGF- $\beta$ 1 have been implicated in the etiology of abnormal arterial growth and vascular remodeling. Basic FGF has important properties that readily influence migration and growth of vascular cells. Since bFGF has no obvious signal sequence (18), its secretion is thought to occur in combination with carrier proteins, through interaction with ECM proteins (22, 149, 158), or through disruption of the plasma membrane in cell lysis during vascular injuries (30). Mechanically-injured SMCs were found to release biologically active bFGF into the medium that was cytosolic in origin and not dependent on ECM-release (30). Significant release of bFGF was found in rat iliac veins exposed to elevated arterial flows from bypass grafting, suggesting a role for bFGF in stimulating myointimal hyperplasia after bypass surgery (161). Shear stress-induced alterations in bFGF transcription (107) and protein release (172) have also been characterized in cultured ECs and SMCs. The first goal of this present chapter is to

characterize the contribution of endothelial and smooth muscle bFGF expression in mediating flow-induced vessel wall remodeling under *in vivo* conditions.

Transforming growth factor- $\beta$ 1 exerts multiple effects on the vascular environment which depend on various parameters such as the presence of cytokines or other growth factors and on the stage of cellular differentiation. Owens et al. (135) observed TGF- $\beta$ 1 to inhibit SMC hyperplasia by increasing cell cycle time while concurrently inducing cellular hypertrophy by increasing accumulation of cells in the G<sub>2</sub> phase of the cell cycle. Gibbons and co-workers (53, 83) found AII stimulated conversion of the latent inactive form of TGF- $\beta$ 1 to a biologically active form which induced SMC hypertrophy. Presence of the latent inactive form of TGF- $\beta$ 1 resulted in SMC hyperplasia. TGF- $\beta$ 1 is also capable of autocrine stimulation of its own transcription in a positive feedback loop in normal and transformed cultured cells (182). TGF- $\beta$ 1 plays a role in stimulating synthesis of ECM components (71, 150). This growth factor has also been implicated in morphogenesis of fibroblasts, mitogenesis of osteoblasts and Schwann cells, and chemotaxis of fibroblasts and monocytes (reviewed in 161). Shear stress stimulated transcription and production of TGF- $\beta$ 1 has been characterized in cultured endothelium by Ohno et al. (128, 129, 131). The second goal of this chapter is to characterize the contribution of endothelial and smooth muscle TGF- $\beta$ 1 expression in mediating flow-induced vessel wall remodeling under *in vivo* conditions.

### Results

*In situ* hybridization data for medial wall and endothelial bFGF mRNA are graphically illustrated in Figures 11-1 and 11-2. No significant differences were detected between control and high flow vessels at any time in either the media or the endothelium.

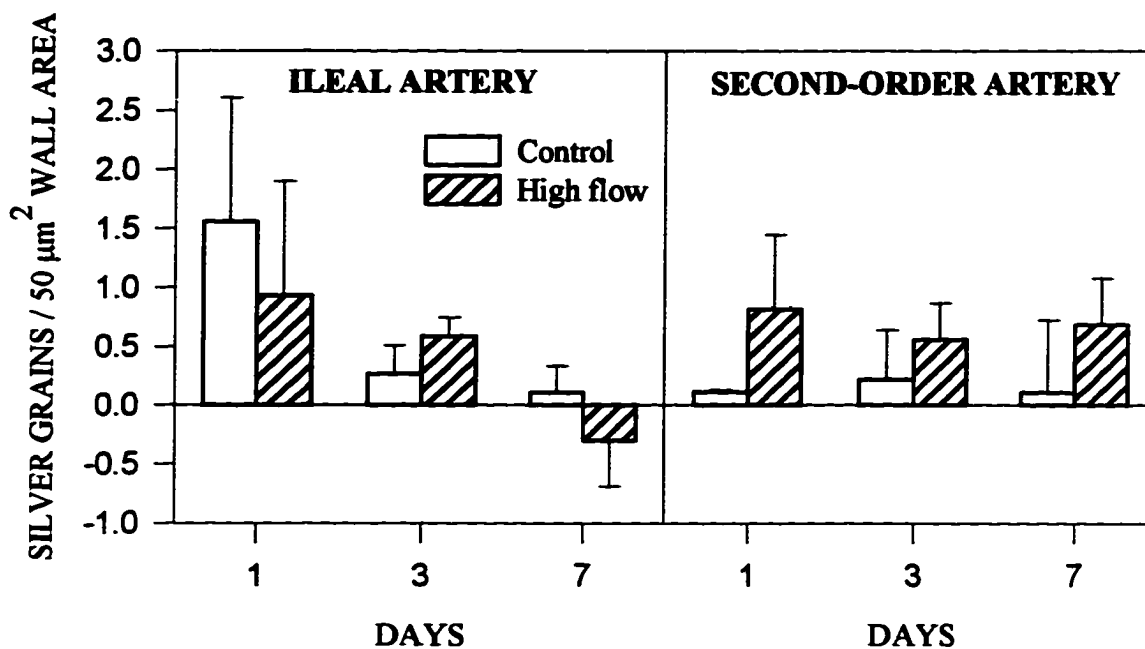


**Figure 11-1. Medial SMC bFGF mRNA Expression.** Medial wall SMC bFGF mRNA expression for control and high flow ileal and second-order branch vessels after *in situ* hybridization with  $^{35}\text{S}$ -CTP riboprobe and development of silver grain emulsion after 10 weeks. No significant differences were detected between control and high flow vessels at any time point. Medial SMC basal levels of expression were negligible for both ileal artery and second-order branch. Values represent mean  $\pm$  SEM, and  $n = 8$  for the ileal artery group and  $n = 6$  for the second-order artery group.

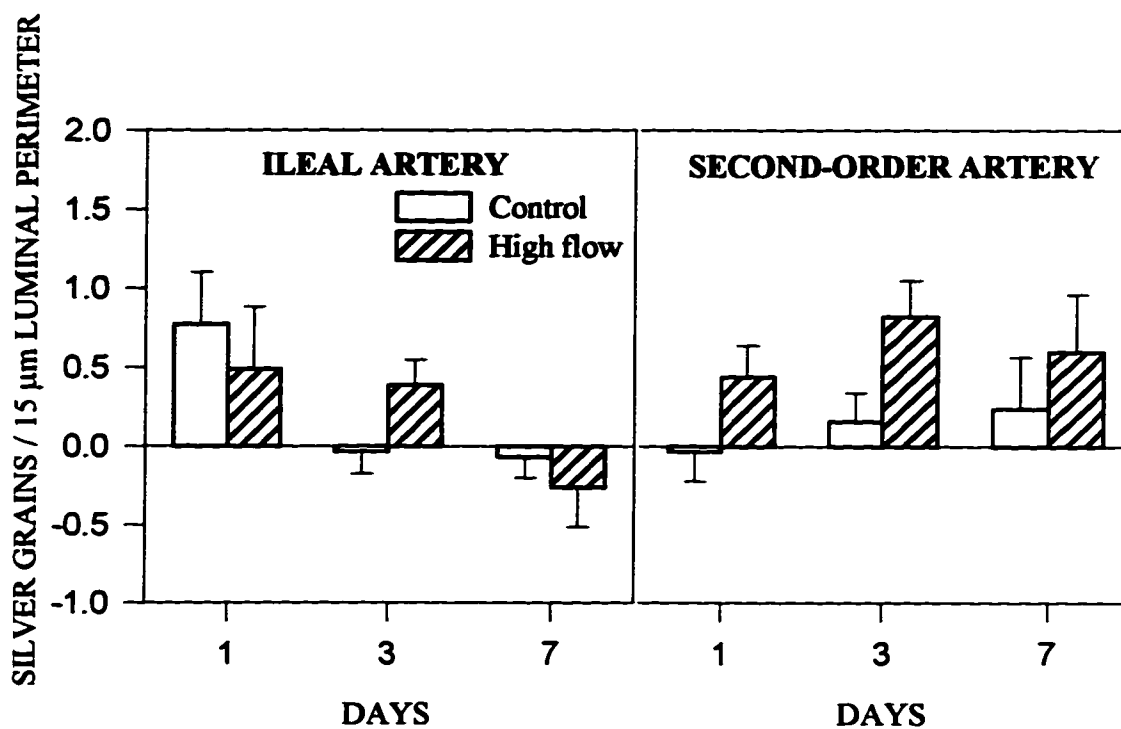


**Figure 11-2. Endothelial bFGF mRNA Expression.** Endothelial bFGF mRNA expression for control and high flow ileal and second-order branch vessels after *in situ* hybridization with  $^{35}\text{S}$ -CTP riboprobe and development of silver grain emulsion after 10 weeks. Endothelial bFGF expression was quite minimal, with no significant differences detected between control and high flow vessels. Values represent mean  $\pm$  SEM, and  $n = 8$  for the ileal artery group and  $n = 6$  for the second-order artery group.

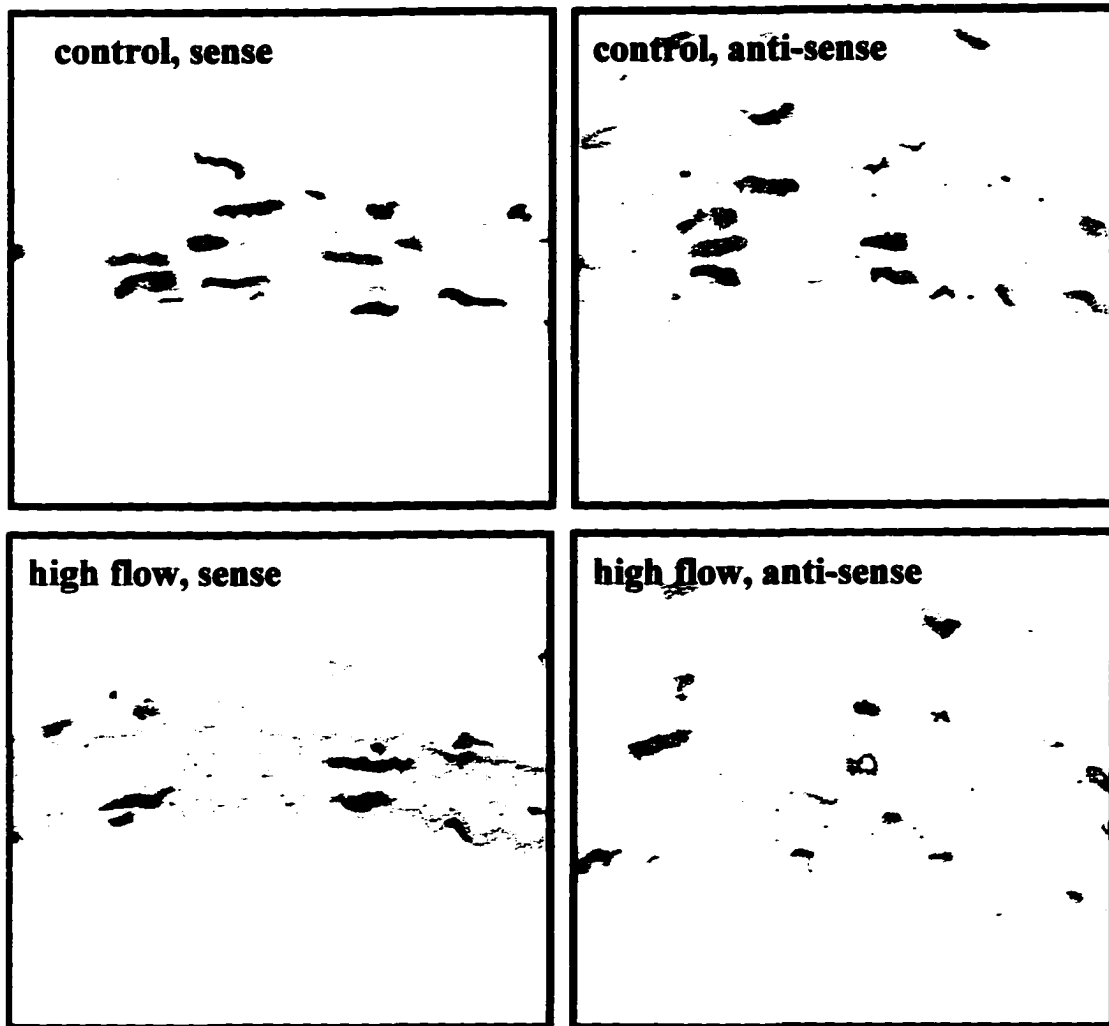


**Figure 11-3. Autoradiographs for bFGF mRNA Expression.**

Medial and endothelial expression of bFGF in the ileal artery and second-order branch were quite low. Figure 11-3 contains autoradiographs for bFGF mRNA expression for same animal sense and anti-sense control and high flow vessels. Figures 11-4 and 11-5 show medial and endothelial expression of TGF- $\beta$ 1, respectively. Similarly, most time points indicate low expression of TGF- $\beta$ 1 expression; however, ileal artery medial expression is significantly increased for high flow vessels compared to controls after 7 days (Fig. 11-4). An interesting but statistically insignificant upregulation of TGF- $\beta$ 1 is observed in both control and high flow second-order arteries after 24 hours in the media and endothelium. Figure 11-6 shows autoradiographs of TGF- $\beta$ 1 expression for same animal sense and anti-sense control and high flow vessels.

### Discussion

Results from *in situ* hybridization reveal low basal and flow-induced levels of expression of bFGF *in vivo* (Figs. 11-1, 11-2). Low levels of basal expression of bFGF have been documented elsewhere (18, 75); however, shear stress was found to upregulate bFGF mRNA and protein release in cultured BAECs (107, 172). Basic FGF peptides are predominantly associated with the ECM, and release can be stimulated by proteolytic enzymes (22). According to Baird and Ling (18), a major determinant of bFGF-induced neovascularization is not expression of the factor but the presence of these extracellular enzymes. In the current study as discussed in Chapter 7, flow-associated stresses stimulated increased extracellular connective tissue. Accordingly, flow could also stimulate increased production of extracellular enzymes, although no studies have focused on this to date. In the current study, bFGF expression was insignificant in mediating flow-induced remodeling in small arteries. In addition, cells generally increase transcription of

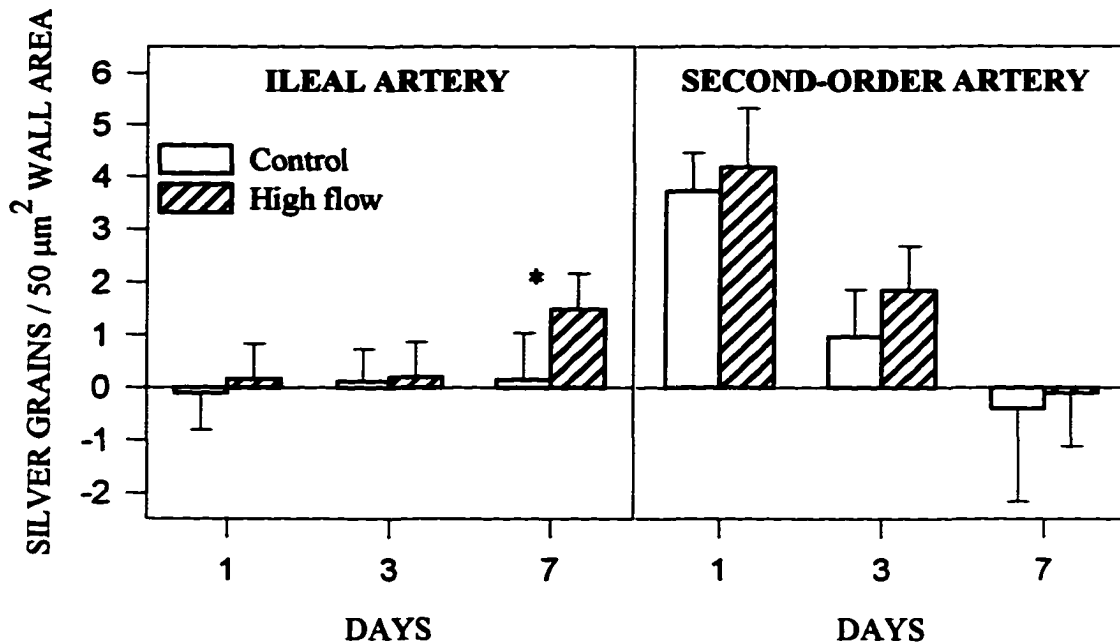


**Figure 11-4. Medial SMC TGF- $\beta$ 1 mRNA Expression.** Medial wall SMC TGF- $\beta$ 1 mRNA expression for control and high flow ileal and second-order branch vessels after *in situ* hybridization with <sup>35</sup>S-CTP riboprobe and development of silver grain emulsion after 10 weeks. Ileal artery basal expression was not observed, and a significant increase in high flow occurred after exposure to flow for 7 days. No other differences were detected between control and high flow vessels at any time. Interestingly, both control and high flow second-order arteries had elevated levels of TGF- $\beta$ 1 expression after 24 hours, and both decreased by 3 and 7 days. Values represent mean  $\pm$  SEM, and  $n = 7$  for the ileal artery group and  $n = 6$  for the second-order artery group.

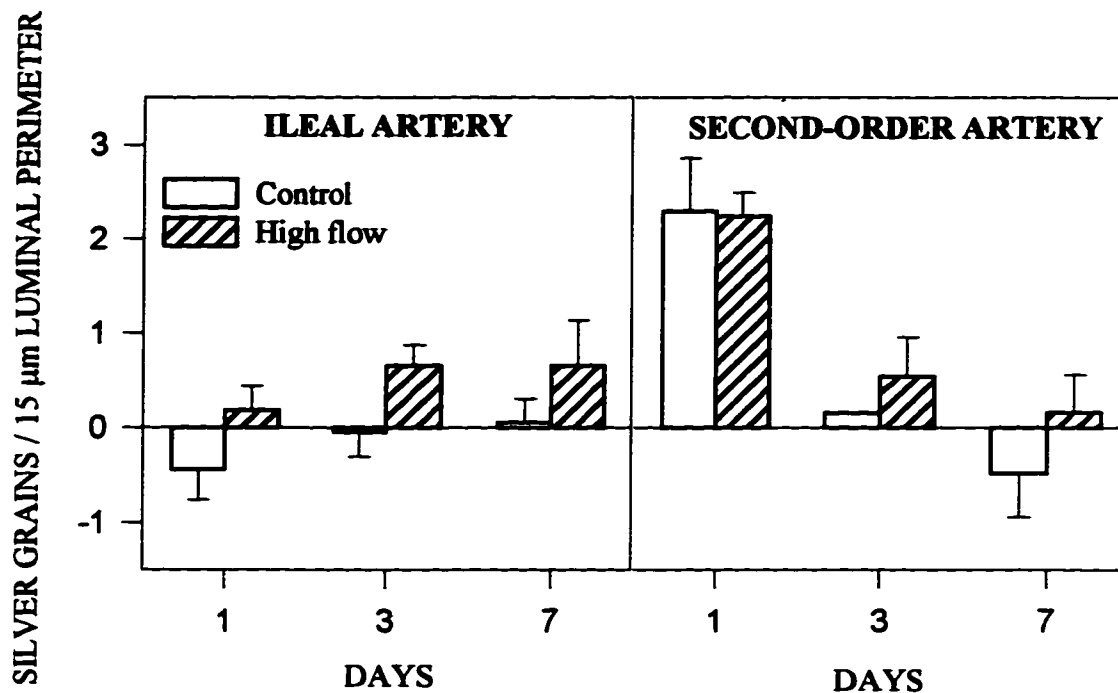


**Figure 11-5. Endothelial TGF- $\beta$ 1 mRNA Expression.** Endothelial TGF- $\beta$ 1 mRNA expression for control and high flow ileal and second-order branch vessels after *in situ* hybridization with  $^{35}\text{S}$ -CTP riboprobe and development of silver grain emulsion after 10 weeks. No significant differences were detected between control and high flow vessels at any time. Overall expression in the ileal artery was quite low. Both control and high flow second-order arteries experienced elevated levels of TGF- $\beta$ 1 expression after 24 hours, and both decreased by 3 and 7 days. Values represent mean  $\pm$  SEM, and  $n =$  for the ileal artery group and  $n =$  for the second-order artery group.

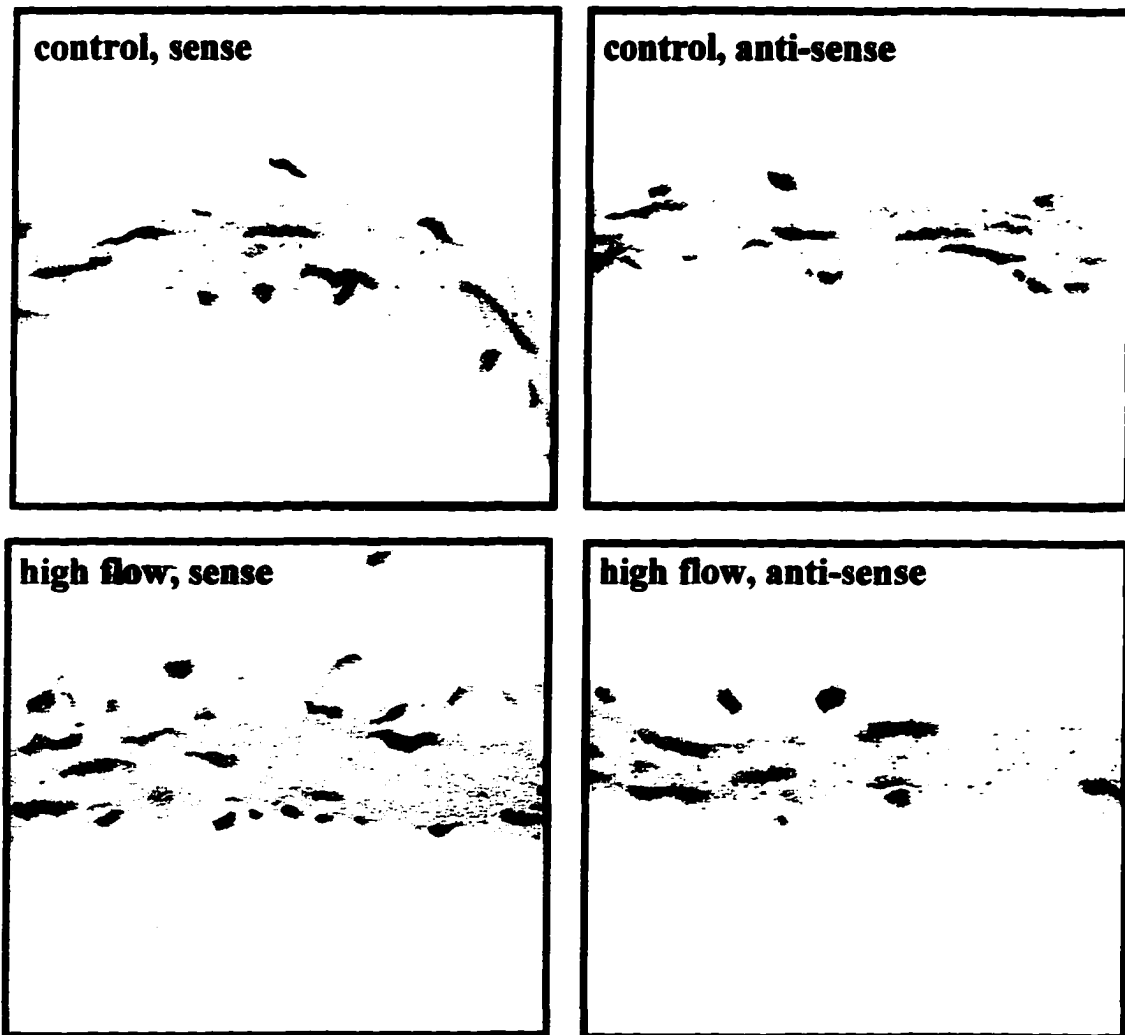


**Figure 11-6. Autoradiographs for TGF- $\beta$ 1 mRNA Expression.**

various growth factors when under culture conditions when compared to the *in vivo* state (18), so direct extrapolation of *in vitro* to *in vivo* results requires prudence.

The influence of TGF- $\beta$ 1 in mediating flow-induced vessel wall growth in the current model was negligible. Basal levels of TGF- $\beta$ 1 expression were low in both ileal and second-order arteries, although the smaller branch experienced increased expression after 24 hours in both control and high flow vessels. The ileal artery experiences a significant increase in medial TGF- $\beta$ 1 expression after exposure to flow for 7 days. Since TGF- $\beta$ 1 has been shown to be upregulated with shear stress (128, 129, 131), and considering that TGF- $\beta$ 1 can auto-stimulate its own message (182), perhaps after 7 days significant increases in self-stimulated expression are finally achieved (Fig. 11-4). The ileal artery at this time point is undergoing significant DNA replication and cellular hyperplasia (Figs. 6-6, 6-8, 6-9), which would correlate with the presence of a latent inactive form of TGF- $\beta$ 1 peptide. Also, TGF- $\beta$ 1 has been found to stimulate syntheses of extracellular fibronectin and collagen (71, 150), as well as their incorporation into the ECM (71). In the current model, however, TGF- $\beta$ 1 does not seem to be involved in increased synthesis of the extracellular connective tissue observed (Fig. 7-1). Generally speaking, the role of TGF- $\beta$ 1 in mediating flow-induced medial wall hypertrophy observed in this *in vivo* model is minimal.

In conclusion, results from this chapter imply that bFGF and TGF- $\beta$ 1 were not directly involved in the flow-mediated vessel wall remodeling observed under *in vivo* conditions. Elevated medial wall TGF- $\beta$ 1 expression after 7 days suggests the possibility of autocrine stimulation of TGF- $\beta$ 1 transcription in flow-exposed vessels.

## **CHAPTER XII**

### **CONCLUSIONS AND INFERENCES**

The investigation discussed in these chapters details a unique experimental model that allows molecular and histologic analyses of arterial wall remodeling in response to altered hemodynamic parameters under *in vivo* conditions. The primary stimulus in this model was flow-induced shear stress with possible contribution from stretch-induced wall stress in the ileal artery. Flow-induced luminal expansion and medial wall hypertrophy occurred in ileal and second-order branching arteries in a time-dependent fashion over a 7 day period. These structural adaptations involved early and dramatic EC hyperplasia after 24 hours with subsequent medial SMC DNA replication and hyperplasia after 3 days. These medial wall changes also involved a concomitant increase in extracellular connective tissue.

Nitric oxide is suggested as a possible signaling factor in these flow-mediated arterial alterations. Early medial and subsequent endothelial PDGF-A mRNA expression possibly contributes to SMC and EC replication and vessel wall remodeling. Expression of medial and endothelial PDGF-B, bFGF, and TGF- $\beta$ 1 was not significantly affected by flow-associated stresses in this model, and their roles in mediating the flow-induced alterations observed are believed to be minimal.

## LITERATURE CITED

1. **Abraham, J.A., A. Mergia, J.L. Whang, A. Tumolo, J. Friedman, K.A. Hjerrild, D. Gospodarowicz, and J.C. Fiddes.** Nucleotide sequence of a bovine clone encoding the angiogenic protein, basic fibroblast growth factor. *Science* 233: 545 - 548, 1986.
2. **Agrotis, A., P.J. Little, J. Saltis, and A. Bobik.** Dihydropyridine Ca<sup>2+</sup> channel antagonists inhibit the salvage pathway for DNA synthesis in human vascular smooth muscle cells. *Eur. J. Pharm.* 244: 269 - 275, 1993.
3. **Alshihabi, S., Y. Chang, Y.A. Frangos, and J.M. Tarbell.** Shear stress stimulates smooth muscle cells in vitro. *Ann. Biomed. Eng.* 22: 34 (Abstract), 1994.
4. **Alshihabi, S., Y. Chang, Z. Huang, D. Wang, J. Frangos, and J. Tarbell.** How does interstitial fluid flow affect smooth muscle cells in the arterial wall? *Adv. Bioeng.* 28: 327 - 328, 1994.
5. **Arndt, H., C.W. Smith, and D.N. Granger.** Leukocyte-endothelial cell adhesion in spontaneously hypertensive and normotensive rats. *Hypertension* 21: 667 - 673, 1993.
6. **Assoian, R., and M. Sporn.** Type  $\beta$  transforming growth factor in human platelets: release during platelet degranulation and action on vascular smooth muscle cells. *J. Cell Biol.* 102: 1217 - 1223, 1986.
7. **Assoian, R.K., G.R. Grotendorst, D.M. Miller, and M.B. Sporn.** Cellular transformation by coordinated action of three peptide growth factors from human platelets. *Nature* 309: 804 - 806, 1984.
8. **Assreuy, J., F.Q. Cunha, F.Y. Liew, and S. Moncada.** Feedback inhibition of nitric oxide synthase activity by nitric oxide. *Br. J. Pharm.* 108: 833 - 837, 1993.
9. **Awolesi, M.A., W.C. Sessa, and B.E. Sumpio.** Cyclic strain upregulates nitric oxide synthase in cultured bovine aortic endothelial cells. *J. Clin. Invest.* 96: 1449 - 1454, 1995.
10. **Awolesi, M.A., M.D. Widmann, W.C. Sessa, B.E. Sumpio.** Cyclic strain increases endothelial nitric oxide synthase activity. *Surgery* 116: 439 - 445, 1994.
11. **Baird, A., and N. Ling.** Fibroblast growth factors are present in the extracellular matrix produced by endothelial cells *in vitro*: implications for a role of heparinase-like enzymes in the neovascular response. *Biochem. Biophys. Res. Comm.* 142: 428 - 435, 1987.

12. **Barbee, K.A., P.F. Davies, and R. Lal.** Shear stress-induced reorganization of the surface topography of living endothelial cells imaged by atomic force microscopy. *Circ. Res.* 74: 163 - 171, 1994.
13. **Bardy, N., G.J. Karillon, R. Merval, J-L. Samuel, and A. Tedgui.** Differential effects of pressure and flow on DNA and protein synthesis and on fibronectin expression by arteries in a novel organ culture system. *Circ. Res.* 77: 684 - 694, 1995.
14. **Baroja, A., C. de la Hoz, A. Alvarez, A. Ispizua, J. Bilbao, and J.M. de Gandarias.** Genesis and evolution of high-ploidy tumour cells evaluated by means of the proliferation markers p34 (cdc2), cyclin B1, PCNA, and 3[H]-thymidine. *Cell Prolif.* 29: 89 - 100, 1996.
15. **Barrett, T.B., C.M. Gajdusek, S.M. Schwartz, J.K. McDougall, and E.P. Benditt.** Expression of the *sis* gene by endothelial cells in culture and *in vivo*. *Proc. Natl. Acad. Sci. USA* 81: 6772 - 6774, 1984.
16. **Beitz, J.G., I.S. Kim, P. Calabresi, and A.R. Frackleton, Jr.** Human microvascular endothelial cells express receptors for platelet-derived growth factor. *Proc. Natl. Acad. Sci. USA* 88: 2021 - 2025, 1991.
17. **Bilato, C., R.R. Pauly, G. Melillo, R. Monticone, D. Gorelick-Feldman, Y.A. Gluzband, S.J. Sollott, B. Ziman, E.G. Lakatta, and M.T. Crow.** Intracellular signaling pathways required for rat vascular smooth muscle cell migration. *J. Clin. Invest.* 96: 1905 - 1915, 1995.
18. **Bobik, A., and J.H. Campbell.** Vascular derived growth factors: cell biology, pathophysiology, and pharmacology. *Pharm. Rev.* 45: 1 - 42, 1993.
19. **Bonner, J.C., A. Badgett, P.M. Lindroos, and A.R. Osornio-Vargas.** Transforming growth factor beta 1 downregulates the platelet-derived growth factor alpha-receptor subtype on human lung fibroblasts in vitro. *Am. J. Respir. Cell Mol. Biol.* 13: 496 - 505, 1995.
20. **Bonthron, D.T., C.C. Morton, S.H. Orkin, and T. Collins.** Platelet-derived growth factor A chain: gene structure, chromosomal location, and basis for alternative mRNA splicing. *Proc. Natl. Acad. Sci.* 85: 1492 - 1496, 1988.
21. **Brindle, N.P.J.** Growth factor in endothelial regeneration. *Cardiovasc. Res.* 27: 1162 - 1172, 1993.
22. **Brunner, G., J. Gabilove, D.B. Rifkin, and E.L. Wilson.** Phospholipase C release of basic fibroblast growth factor from human bone marrow cultures as a biologically active complex with a phosphatidylinositol-anchored heparan sulfate proteoglycan. *J. Cell Biol.* 114: 1275 - 1283, 1991.

23. **Buga, G.M., M.E. Gold, J.M. Fukuto, and L.J. Ignarro.** Shear stress-induced release of nitric oxide from endothelial cells grown on beads. *Hypertension* 17: 187 - 193, 1991.
24. **Busse, R., and I. Fleming.** Regulation and functional consequences of endothelial nitric oxide formation. *Ann. Med.* 27: 331 - 340, 1995.
25. **Cahill, P.A., and A. Hassid.** Clearance receptor-binding atrial natriuretic peptides inhibit mitogenesis and proliferation of rat aortic smooth muscle cells. *Biochem. Biophys. Res. Comm.* 179: 1606 - 1613, 1991.
26. **Collins, T., J.S. Pober, M.A. Gimbrone, Jr., A. Hammacher, C. Betsholtz, B. Westermarck, and C.H. Heldin.** Cultured human endothelial cells express platelet-derived growth factor A chain. *Am. J. Pathol.* 126: 7 - 12, 1987.
27. **Cooke, J.P., E. Rossitch, Jr., N.A. Andon, J. Loscalzo, and V.J. Dzau.** Flow Activates an Endothelial Potassium Channel to Release an Endogenous Nitrovasodilator. *J. Clin. Invest.* 88: 1663 - 1671, 1991.
28. **Cooke, J.P., J. Stanler, N. Andon, P.F. Davies, G. McKinley, and J. Loscalzo.** Flow stimulates endothelial cells to release a nitrovasodilator that is potentiated by reduced thiol. *Am. J. Physiol.* 259 (*Heart Circ. Physiol.* 28): H804 - H812, 1990.
29. **Cromack, D.T., M.B. Sporn, A.B. Roberts, M.J. Merino, L.L. Dart, and J.A. Norton.** Transforming growth factor beta levels in rat wound chambers. *J. Surg. Res.* 42: 622 - 628, 1987.
30. **Crowley, S.T., C.J. Ray, D. Nawaz, R.A. Majack, and L.D. Horwitz.** Multiple growth factors are released from mechanically injured vascular smooth muscle cells. *Am. J. Physiol.* 269 (*Heart Circ. Physiol.* 38): H1641 - H1647, 1995.
31. **Cunningham, L.D., P. Brecher, and R.A. Cohen.** Platelet-derived growth factor receptors on macrovascular endothelial cells mediate relaxation via nitric oxide in rat aorta. *J. Clin. Invest.* 89: 878 - 882, 1992.
32. **Daemen, M.J.A.P., and J.G.R. De May.** Regional heterogeneity of arterial structural changes. *Hypertension* 25: 464 - 473, 1995.
33. **D'Angelo, G, and G.A. Meininger.** Transduction mechanisms involved in the regulation of myogenic activity. *Hypertension* 23: 1096 - 1105, 1994.
34. **Davies, P.F.** Endothelium as a signal transduction interface for flow forces: cell surface dynamics. *Thromb. Haemo.* 70: 124 - 128, 1993.

35. **Davies, P.F.** Flow-mediated endothelial mechanotransduction. *Physiol. Rev.* 75: 519 - 560, 1995.
36. **Davies, P.F.** How do vascular endothelial cells respond to flow? *News Physiol. Sci.* 4: 22 - 25, Feb., 1989.
37. **Davies, P.F. and K.A. Barbee.** Endothelial cell surface imaging: insights into hemodynamic force transduction. *News Physiol. Sci.* 9: 153 - 157, 1994.
38. **Davies, P.F., A. Robotewshyj, and M.L. Griem.** Quantitative studies of endothelial cell adhesion: directional remodelling of focal adhesion sites in response to flow. *J. Clin. Invest.* 93: 2031 - 2038, 1994.
39. **Davies, P.F. and S.C. Tripathi.** Mechanical stress mechanisms and the cell: an endothelial paradigm. *Circ. Res.* 72: 239 - 245, 1993.
40. **Diamond, S.L., S.G. Eskin, and L.V. McIntire.** Fluid flow stimulates tissue plasminogen activator secretion by cultured human endothelial cells. *Science* 243: 1483 - 1485, 1989.
41. **Field, S.L., L.M. Khachigian, M.J. Sleight, G. Yang, S.E. Vandermark, P.J. Hogg, and C.N. Chesterman.** Extracellular matrix is a source of mitogenically active platelet-derived growth factor. *J. Cell. Physiol.* 168: 322 - 332, 1996.
42. **Fiscus, R.R.** Molecular mechanisms of endothelium-mediated vasodilation. *Sem. Thromb. Hemo.* 14: 12 - 22, 1988.
43. **Fostermann, U., E.I. Closs, J.S. Pollock, M. Nakane, P. Schwarz, I. Gath, and H. Kleinhart.** Nitric oxide synthase isozymes: Characterization, purification, molecular cloning, and functions. *Hypertension* 23: 1121 - 1131, 1994.
44. **Fostermann, U., A. Mulsch, E. Bohme, and R. Busse.** Stimulation of soluble guanylate cyclase by an acetylcholine-induced endothelium-derived factor from rabbit and canine arteries. *Circ. Res.* 58: 531 - 538, 1986.
45. **Fostermann, U., J.S. Pollock, H.H. Schmidt, M. Heller, and F. Murad.** Calmodulin-dependent endothelium-derived relaxing factor/nitric oxide synthase activity is present in the particulate and cytosolic fractions of bovine aortic endothelial cells. *Proc. Natl. Acad. Sci.* 88: 1788 - 1792, 1991.
46. **Fung, Y.C.** *Biomechanics. Motion, Flow, Stress, and Growth.* 1990. Springer-Verlag, New York.

47. **Furchgott, R.F.** Studies on relaxation of rabbit aorta by sodium nitrite: The basis for the proposal that the acid-activable inhibitory factor from retractor penis is inorganic nitrite and the endothelium-derived relaxing factor is nitric oxide. In: *Vasodilatation: Vascular Smooth Muscle, Peptides, Autonomic Nerves and Endothelium* (ed. P.M. Vanhoutte), pp. 401 - 414. 1988. Raven, New York.
48. **Furchgott, R.F.** The role of the endothelium in the responses of vascular smooth muscle to drugs. *Annu. Rev. Pharmacol. Toxicol.* 24: 175 - 197, 1984.
49. **Furchgott, R.F., and J.V. Zawadzki.** The obligatory role of endothelial cells in the relaxation of arterial smooth muscle by acetylcholine. *Nature* 288: 373 - 376, 1980.
50. **Garcia-Cardena, G., P. Oh, J. Liu, J. Schnitzer, and W.C. Sessa.** Targeting of nitric oxide synthase to endothelial caveolae via palmitoylation. *FASEB J.*, Vol. 10, No. 3, p. A436, Abstract #2518, 1996.
51. **Garg, U.C., and A. Hassid.** Mechanisms of nitrosothiol-induced antimitogenesis in aortic smooth muscle cells. *Eur. J. Pharm.* 237: 243 - 249, 1993.
52. **Garg, U.C., and A. Hassid.** Nitric oxide-generating vasodilators and 8-bromo-cyclic guanosine monophosphate inhibit mitogenesis and proliferation of cultured rat vascular smooth muscle cells. *J. Clin. Invest.* 83: 1774 - 1777, 1989.
53. **Gibbons, G.H., R.E. Pratt, and V.J. Dzau.** Vascular smooth muscle cell hypertrophy vs. hyperplasia: autocrine transforming growth factor- $\beta$ 1 expression determines growth response to angiotensin II. *J. Clin. Invest.* 90: 456 - 461, 1992.
54. **Gordon, D., M.A. Reidy, E.P. Benditt, and S.M. Schwartz.** Cell proliferation in human coronary arteries. *Proc. Natl. Acad. Sci.* 87: 4600 - 4604, 1990.
55. **Grotendorst, G.R., T. Chang, H.E. Seppa, H.K. Kleinman, and G.R. Martin.** Platelet-derived growth factor is a chemoattractant for vascular smooth muscle cells. *J. Cell Physiol.* 113: 261 - 266, 1982.
56. **Gundersen, H.J.G., T.F. Bendtsen, L. Korbo, N. Marcussen, A. Moller, K. Nielsen, J.R. Nyengaard, B. Pakkenberg, F.B. Sorensen, A. Vesterby, and M.J. West.** Some new, simple and efficient stereological methods and their use in pathological research and diagnosis. *APMIS* 96: 379 - 394, 1988.
57. **Gupte, A., and J.A. Frangos.** Effects of flow on the synthesis and release of fibronectin by endothelial cells. *In Vitro Cell. Dev. Biol.* 26: 57 - 60, 1990.
58. **Guyton, J.R. and C.J. Hartley.** Flow restriction of one carotid artery in juvenile rats inhibits growth of arterial diameter. *Am. J. Physiol.* 248 (*Heart Circ. Physiol.* 17): H540 - H546, 1985.

59. **Hacking, W.J.G., E. VanBavel, and J.A.E. Spaan.** Shear stress is not sufficient to control growth of vascular networks: a model study. *Am. J. Physiol.* 270 (*Heart Circ. Physiol.* 39): H364 - H375, 1996.
60. **Halnon, N.J., T. Collins, M.A. Gimbrone, Jr., and N. Resnick.** Regulation of the endothelial PDGF-A gene by shear stress. *Circ.* 90: I-88 (0468A), 1994.
61. **Hassid, A., H. Arabshahi, T. Bourcier, G.S. Dhaunsi, and C. Matthews.** Nitric oxide selectively amplifies FGF-2-induced mitogenesis in primary rat aortic smooth muscle cells. *Am. J. Physiol.* 267 (*Heart Circ. Physiol.* 36): H1040 - H1048, 1994.
62. **Hecker, M., A. Mulsch, E. Bassenge, and R. Busse.** Vasoconstriction and increased flow: two principal mechanisms of shear stress-dependent endothelial autacoid release. *Am. J. Physiol.* 265 (*Heart Circ. Physiol.* 34): H828 - H833, 1993.
63. **Holman, E.** Problems in the dynamics of blood flow. I. Condition controlling collateral circulation in the presence of an arteriovenous fistula, following the ligation of an artery. *Surgey* 26: 889 - 917, 1949.
64. **Hsieh, H-J., N-Q. Li, and J.A. Frangos.** Pulsatile and steady flow induces c-fos expression in human endothelial cells. *J. Cell. Physiol.* 154: 143 - 151, 1993.
65. **Hsieh, H-J., N-Q. Li, and J.A. Frangos.** Shear-induced platelet-derived growth factor gene expression in human endothelial cells is mediated by protein kinase C. *J. Cell. Physiol.* 150: 552 - 558, 1992.
66. **Hsieh, H-J., N-Q. Li, and J.A. Frangos.** Shear stress increases endothelial platelet-derived growth factor mRNA levels. *Am. J. Physiol.* 260 (*Heart Circ. Physiol.* 29): H642 - H646, 1991.
67. **Hull, Jr., S.S., L. Kaiser, M.D. Jaffe, and H.V. Sparks, Jr.** Endothelium-dependent flow-induced dilation of canine femoral and saphenous arteries. *Blood Vessels* 23: 183 - 198, 1986.
68. **Ignarro, L.** Biological actions and properties of endothelium-derived nitric oxide formed and released from artery and vein. *Circ. Res.* 65: 1 - 21, 1989.
69. **Ignarro, L.J., R.E. Byrns, and K. Wood.** Biochemical and pharmacological properties of endothelium-derived relaxing factor and its similarity to nitric oxide radical. In: *Vasodilatation: Vascular Smooth Muscle, Peptides, Autonomic Nerves and Endothelium* (ed. P.M. Vanhoutte), pp. 427 - 436. 1988. Raven, New York.

70. **Ignarro, L.J., R.G. Harbison, K.S. Wood, and P.J. Kadowitz.** Activation of purified soluble guanylate cyclase by endothelium-derived relaxing factor from intrapulmonary artery and vein: stimulation by acetylcholine, bradykinin, and arachidonic acid. *J. Pharmacol. Exp. Ther.* 237: 893 - 900, 1986.
71. **Ignatz, R., and J. Massague.** Transforming growth factor- $\beta$  stimulates the expression of fibronectin and collagen and their incorporation into the extracellular matrix. *J. Biol. Chem.* 261: 4337 - 4345, 1986.
72. **Ito, M., K. Yamada, J. Masuda, A. Kinoshita, H. Otsuki, and T. Hayakawa.** Expression of PDGF in relation to cell division in atherosclerotic intima of human carotid arteries. *Neurol. Res.* 17: 345 - 348, 1995.
73. **Iwata, F., T. Joh, T. Kawai, and M. Itoh.** Role of EDRF in splanchnic blood flow of normal and chronic portal hypertensive rats. *Am. J. Physiol.* 263 (*Gastrointest. Liver Physiol.* 26): G149 - G154, 1992.
74. **Jawien, A., D.F. Bowen-Pope, V. Lindner, S.M. Schwartz, and A.W. Clowes.** Platelet-derived growth factor promotes smooth muscle migration and intimal thickening in a rat model of balloon angioplasty. *J. Clin. Invest.* 89: 507 - 511, 1988.
75. **Jaye, M., R. Howk, W. Burgess, G.A. Ricca, I.-M. Chin, M.W. Ravera, S.J. O'Brien, W.S. Modi, T. Maciag, and W.N. Drohan.** Human endothelial cell growth factor: cloning, nucleotide sequence and chromosome localization. *Science* 233: 541 - 545, 1986.
76. **Kaiser, L. and H.V. Sparks, Jr.** Mediation of flow-dependent dilation by endothelial cells. *Circulatory Shock* 18: 109 - 114, 1986.
77. **Kamiya, A., and T. Togowa.** Adaptive regulation of wall shear stress to flow change in the canine carotid artery. *Am. J. Physiol.* 239 (*Heart Circ. Physiol.* 8): H14 - H21, 1980.
78. **Kanai, A.J., H.C. Strauss, G.A. Truskey, A.L. Crews, S. Grunfeld, and T. Malinski.** Shear stress induces ATP-independent transient nitric oxide release from vascular endothelial cells, measured directly with a porphyrinic microsensor. *Circ. Res.* 77: 284 - 293, 1995.
79. **Kariya, K.I., Y. Kawahara, S.I. Araki, H. Fukuzaki, and Y. Takai.** Antiproliferative action of cGMP-elevating vasodilators in cultured rabbit aortic smooth muscle cells. *Atherosclerosis* 80: 143 - 147, 1989.
80. **Kelly, J.L., A. Sanchez, G.S. Brown, C.N. Chesterman, and M.J. Sleight.** Accumulation of PDGF-B and cell-binding forms of PDGF-A in the extracellular matrix. *J. Cell. Biol.* 121: 1153 - 1163, 1993.

81. **Khachigian, L.M., V. Lindner, A.J. Williams, and T. Collins.** Egr-1-induced endothelial gene expression: a common theme in vascular injury. *Science* 271: 1427 - 1431, 1996.
82. **Kodama, T., L.M. Marmon, R. Vargas, M. Farhat, G.R. Hoy, and P.W. Ramwell.** The interaction between endothelium-derived relaxing factor (EDRF) and eicosanoids in the regulation of the mesenteric microcirculation. *J. Surg. Res.* 58: 227 - 232, 1995.
83. **Koibuchi, Y., W.S. Lee, G.H. Gibbons, and R.E. Pratt.** Role of transforming growth factor- $\beta$ 1 in the cellular growth response to angiotensin II. *Hypertension* 21: 1046 - 1050, 1993.
84. **Koller, A. and G. Kaley.** Endothelial regulation of wall shear stress and blood flow in skeletal muscle microcirculation. *Am. J. Physiol.* 260 (*Heart Circ. Physiol.* 29): H862 - H868, 1991.
85. **Kraiss, L.W., R.L. Geary, E.J.R. Mattsson, S. Vergel, Y.P. Tina Au, and A.W. Clowes.** Acute reductions in blood flow and shear stress induce platelet-derived growth factor-A expression in baboon prosthetic grafts. *Circ. Res.* 79: 45 - 53, 1996.
86. **Kraiss, L.W., T.R. Kirkman, T.R. Kohler, B. Zierler, and A.W. Clowes.** Shear stress regulates smooth muscle proliferation and neointimal thickening in porous polytetrafluoroethylene grafts. *Arterio. Thromb.* 11: 1844 - 1852, 1991.
87. **Kuchan, M.J. and J.A. Frangos.** Role of calcium and calmodulin in flow-induced nitric oxide production in endothelial cells. *Am. J. Physiol.* 266 (*Heart Circ. Physiol.* 35): C628 - C636, 1994.
88. **Kuchan, M.J., H. Jo, and J.A. Frangos.** Role of G proteins in shear stress-mediated nitric oxide production by endothelial cells. *Am. J. Physiol.* 267 (*Heart Circ. Physiol.* 36): C753 - C758, 1994.
89. **Labat-Robert, J., M. Bihari-Varga, and L. Robert.** Extracellular matrix. *FEBS Letters* 268: 386 - 393, 1990.
90. **Landgren, E., A. Eriksson, S. Wennstrom, S. Kanda, and L. Claesson-Welsh.** Induction of fibroblast growth factor receptor-1 mRNA and protein by platelet-derived growth factor BB. *Exp. Cell Res.* 223: 405 - 411, 1996.
91. **Langille, B.L., M.P. Bendeck, and F.W. Keeley.** Adaptations of carotid arteries of young and mature rabbits to reduced carotid blood flow. *Am. J. Physiol.* 256 (*Heart Circ. Physiol.* 25): H931 - H939, 1989.

92. **Langille, B.L. and F. O'Donnell.** Reductions in arterial diameter produced by chronic decreases in blood flow are endothelium-dependent. *Science* Wash. DC 231: 405 - 407, 1986.
93. **Lansman, J.B., T.J. Hallam, and T.J. Rink.** Single stretch-activated ion channels in vascular endothelial cells as mechanotransducers? *Nature* 325: 811 - 813, 1987.
94. **Lawrence, D., R. Pircher, and P. Jullien.** Conversion of a high molecular weight latent beta-TGF from chicken embryo fibroblasts into a low molecular weight active beta-TGF under acidic conditions. *Biochem. Biophys. Res. Comm.* 133: 1026 - 1034, 1985.
95. **Lee, R.M.K.W., J.B. Forrest, R.E. Garfield, and E.E. Daniel.** Comparison of blood vessel wall dimensions in normotensive and hypertensive rats by histometric and morphometric methods. *Blood Vessels* 20: 245 - 254, 1983.
96. **Lehman, R.M., G.K. Owens, N.F. Kassell, K. Hongo.** Mechanism of enlargement of major cerebral collateral arteries in rabbits. *Stroke* 22: 499 - 504, 1991.
97. **Leibovich, S.J., P.J. Polverini, T.W. Fong, L.A. Harlow, and A.E. Koch.** Production of angiogenic activity by human monocytes requires an L-arginine/nitric oxide-synthase-dependent effector mechanism. *Proc. Natl. Acad. Sci.* 91: 4190 - 4194, 1994.
98. **Lepidi, S., A.V. Sterpetti, A. Cucina, A. Di Carlo, A.L. Patrizi, R. Palumbo, P. Bernucci, L. Santoro-D'Angelo, and A. Cavallaro.** bFGF release is dependent on flow conditions in experimental vein grafts. *Eur. J. Vasc. Endovasc. Surg.* 10: 450 - 458, 1995.
99. **Levesque, M.J., R.M. Nerem, and E.A. Sprague.** Vascular endothelial cell proliferation in culture and the influence of flow. *Biomaterials* 11: 702 - 707, 1990.
100. **Liebow, A.A.** Situations which lead to changes in vascular patterns. In: *Handbook of Physiology. Circulation.* Washington, DC: Am. Physiol. Soc., 1963, sect. 2, vol. 2, chapt. 37, pp. 1251 - 1276.
101. **Lindner, V., D.A. Lappi, A. Baird, R.A. Majack, and M.A. Reidy.** Role of basic fibroblast growth factor in vascular lesion formation. *Circ. Res.* 68: 106 - 113, 1991.
102. **Lindner, V., and M.A. Reidy.** Proliferation of smooth muscle cells after vascular injury is inhibited by an antibody against basic fibroblast growth factor. *Proc. Natl. Acad. Sci.* 88: 3739 - 3743, 1991.

103. **Losano, G., P. Pagliaro, D. Gatullo, and N.A. Marsh.** Control of coronary blood flow by endothelial release of nitric oxide. *Clin. Exp. Pharm. Physiol.* 21: 783 - 789, 1994.
104. **Majesky, M.W., E.P. Benditt, and S.M. Schwartz.** Expression and developmental control of platelet-derived growth factor A-chain and B-chain / *Sis* genes in rat aortic smooth muscle cells. *Proc. Natl. Acad. Sci. USA* 85: 1524 - 1528, 1988.
105. **Majesky, M.W., V. Lindner, D.R. Twardzik, S.M. Schwartz, and M.A. Reidy.** Production of transforming growth factor  $\beta 1$  during repair of arterial injury. *J. Clin. Invest.* 88: 904 - 910, 1991.
106. **Majesky, M.W., M.A. Reidy, D.F. Bowen-Pope, C.E. Hart, J.N. Wilcox, and S.M. Schwartz.** PDGF ligand and receptor gene expression during repair of arterial injury. *J. Cell Biol.* 111: 2149 - 2158, 1990.
107. **Malek, A.M., G.H. Gibbons, V.J. Dzau, and S. Izumo.** Fluid shear stress differentially modulates expression of genes encoding basic fibroblast growth factor and platelet-derived growth factor B chain in vascular endothelium. *J. Clin. Invest.* 92: 2013 - 2021, 1993.
108. **Malek, A.M., A.L. Greene, and S. Izumo.** Regulation of endothelin 1 gene by fluid shear stress is transcriptionally mediated and independent of protein kinase C and cAMP. *Proc. Natl. Acad. Sci.* 90: 5999 - 6003, 1993.
109. **Malek, A.M. and S. Izumo.** Molecular aspects of signal transduction of shear stress in the endothelial cell. *J. Hypertens.* 12: 989 - 999, 1994.
110. **Marsden, P.A., H.H.Q. Heng, S.W. Scherer, R.J. Stewart, A.V. Hall, X-M. Shi, L-C. Tsui, and K.T. Schappert.** Structure and chromosomal localization of the human constitutive endothelial nitric oxide synthase gene. *J. Biol. Chem.* 268: 17478 - 17488, 1993.
111. **Masuda, H., K. Kawamura, K. Tohda, T. Shozawa, M. Sageshima, and A. Kamiya.** Increase in endothelial cell density before artery enlargement in flow-loaded canine carotid artery. *Arteriosclerosis* 9: 812 - 823, 1989.
112. **Mathews, M.B., R.M. Bernstein, B.R. Franza, Jr., and J.I. Garrels.** Identity of the proliferating cell nuclear antigen and cyclin. *Nature* 309: 374 - 376, 1984.
113. **Matsui, T., M. Heidaran, T. Miki, N. Popescu, W. La Rochelle, M. Kraus, J. Pierce, and S. Aaronson.** Isolation of a novel receptor cDNA establishes the existence of two PDGF receptor genes. *Science (Wash. DC)* 243: 800 - 804.

114. **Melkumyants, A.M., S.A. Balashaov, E.S. Veselova, and V.M. Khayutin.** Continuous control of the lumen of feline conduit arteries by blood flow rate. *Cardiovasc. Res.* 21: 863 - 870, 1987.
115. **Miano, J.M., N. Vlastic, R.R. Tota, and M.B. Stemerman.** Smooth muscle cell immediate-early gene and growth factor activation follows vascular injury. *Arterio. Thromb.* 13: 211 - 219, 1993.
116. **Michel, T., G.K. Li, and L. Busconi.** Phosphorylation and subcellular translocation of endothelial nitric oxide synthase. *Proc. Natl. Acad. Sci.* 90: 6252 - 6256, 1993.
117. **Mignatti, P., T. Morimoto, and D.B. Rifkin.** Basic fibroblast growth factor released by single, isolated cells stimulates their migration in an autocrine manner. *Proc. Natl. Acad. Sci.* 88: 11007 - 11011, 1991
118. **Mitsumata, M., R.S. Fishel, R.M. Nerem, R.W. Alexander, and B.C. Berk.** Fluid shear stress stimulates platelet-derived growth factor expression in endothelial cells. *Am. J. Physiol.* 265 (*Heart Circ. Physiol.* 34): H3 - H8, 1993.
119. **Mitsumata, M., R.M. Nerem, R.W. Alexander, and B. Berk.** Shear stress inhibits endothelial cell proliferation by growth arrest in the G<sub>0</sub>/G<sub>1</sub> phase of the cell cycle. *FASEB J.* 5: A527, 1991.
120. **Morbidelli, L., C-H. Chang, J.C. Douglas, H.J. Granger, F. Ledda, and M. Ziche.** Nitric oxide mediates mitogenic effect of VEGF on coronary venular endothelium. *Am. J. Physiol.* 270 (*Heart Circ. Physiol.* 39): H411 - H415, 1996.
121. **Mow, V.C., F. Guliak, R. Tran-Son-Tay, and R.M. Hochmuth.** *Cell mechanics and cellular engineering.* 1994. Springer-Verlag, New York.
122. **Nakaki, T., M. Nakayama, and R. Kato.** Inhibition by nitric oxide and nitric oxide-producing vasodilators of DNA synthesis in vascular smooth muscle cells. *Eur. J. Pharmacol.* 189: 347 - 353, 1990.
123. **Negoro, N., Y. Kanayama, M. Haraguchi, N. Umetani, M. Nishimura, Y. Konishi, J. Iwai, M. Okamura, T. Inoue, and T. Takeda.** Blood pressure regulates platelet-derived growth factor A-chain gene expression in vascular smooth muscle cells in vivo. *J. Clin. Invest.* 95: 1140 - 1150, 1995.
124. **Newby, A.C., and S.J. George.** Proposed roles for growth factors in mediating smooth muscle proliferation in vascular pathologies. *Cardiovasc. Res.* 27: 1173 - 1183, 1993.

125. Nilsson, J., M. Sjolund, L. Palmberg, J. Thyberg, and C.-H. Heldin. Arterial smooth muscle cells in primary culture produce a platelet-derived growth factor-like protein. *Proc. Natl. Acad. Sci.* 82: 4418 - 4422, 1985.
126. Nishida, K., D.G. Harrison, J.P. Navas, A.A. Fisher, S.P. Dockery, M. Uematsu, R.M. Nerem, R.W. Alexander, and T.J. Murphy. Molecular cloning and characterization of the constitutive bovine endothelial cell nitric oxide synthase. *J. Clin. Invest.* 90: 2092 - 2096, 1992.
127. Noris, M., M. Morigi, R. Donadelli, S. Aiello, M. Foppolo, M. Todeschini, S. Orisio, G. Remuzzi, and A. Remuzzi. Nitric oxide synthesis by cultured endothelial cells is modulated by flow conditions. *Circ. Res.* 76: 536 - 543, 1995.
128. Ohno, M., J.P. Cooke, V.J. Dzau, and G.H. Gibbons. Fluid shear stress induces endothelial transforming growth factor beta-1 transcription and production: modulation by potassium channel blockade. *J. Clin. Invest.* 95: 1363 - 1369, 1995.
129. Ohno, M., J.P. Cooke, and G.H. Gibbons. Shear-stress induced TGF $\beta$ 1 gene transcription via a flow-activated potassium channel. *Circulation* 88: I183 (0975A), 1993.
130. Ohno, M., G.H. Gibbons, V.J. Dzau, and J.P. Cooke. Shear stress elevates endothelial cGMP: role of a potassium channel and G protein coupling. *Circ.* 88: 193 - 197, 1993.
131. Ohno, M., G.H. Gibbons, F. Lopez, J.P. Cooke, and V.J. Dzau. Shear stress induces transforming growth factor beta 1 (TGF- $\beta$ 1) expression via a flow-activated potassium channel. *Clin. Res.* 40: 294A, 1992.
132. Ono, O., J. Ando, A. Kamiya, Y. Kuboki, and H. Yasuda. Flow effects on cultured vascular endothelial and smooth muscle cell functions. *Cell. Struct. Funct.* 16: 365 - 374, 1991.
133. Ookawa, K., M. Sato, and N. Ohshima. Morphological changes of endothelial cells after exposure to fluid-imposed shear stress: differential responses induced by extracellular matrices. *Biorheology* 30: 131 - 140, 1993.
134. Owens, G. Control of hypertrophic versus hyperplastic growth of vascular smooth muscle cells. *Am. J. Physiol.* 257 (Heart Circ. Physiol. 26): H1755 - H1765, 1989.
135. Owens, K.K., A.A.T. Geisterfer, Y.W.-H. Yang, and A. Komoriya. Transforming growth factor- $\beta$ -induced growth inhibition and cellular hypertrophy in cultured vascular smooth muscle cells. *J. Cell Biol.* 107: 771 - 780, 1988.

136. **Perry, P.B., and W.C. O'Neill.** Flow stimulates nitric oxide synthesis in endothelial cells through a calcium-independent mechanism. *Circulation* 88: I-134, A-0712, 1993.
137. **Pohl, U., J. Holtz, R. Busse, and E. Bassenge.** Crucial role of endothelium in the vasodilator response to increased flow *in vivo*. *Hypertension* 8: 37 - 44, 1986.
138. **Qian, S.W., P. Kondaiah, A.B. Roberts, and M.B. Sporn.** cDNA cloning by PCR of rat transforming growth factor  $\beta$ -1. *Nucleic Acids Res.* 18: 3059, 1990.
139. **Qui, H.Y., D. Henrion, and B.L. Levy.** Alterations in flow-dependent vasomotor tone in spontaneously hypertensive rats. *Hypertension* 24: 474 - 479, 1994.
140. **Radomski, M.W., R.M. Palmer, and S. Moncada.** The role of nitric oxide and cGMP in platelet adhesion to the vascular endothelium. *Biochem. Biophys. Res. Comm.* 148: 1482 - 1489, 1987.
141. **Radomski, M.W., R.M. Palmer, and S. Moncada.** The anti-aggregating properties of vascular endothelium: interactions between prostacyclin and nitric oxide. *Br. J. Pharmacol.* 92: 639 - 646, 1987.
142. **Ranjan, V., Z. Xiao, and S.L. Diamond.** Constitutive NOS expression in cultured endothelial cells is elevated by fluid shear stress. *Am. J. Physiol.* 269 (*Heart Circ. Physiol.* 38): H550 - H555, 1995.
143. **Rao, C.D., H. Igarashi, I-M. Chiu, K.C. Robbins, and S.A. Aaronson.** Structure and sequence of the human *c-sis*/platelet-derived growth factor 2 (*SIS/PDGF2*) transcriptional unit. *Proc. Natl. Acad. Sci.* 83: 2392 - 2396, 1986.
144. **Reid, M.R.** Abnormal arteriovenous communications; acquired and congenital. III. The effect of abnormal arteriovenous communications on the heart, blood vessels, and other structures. *Arch. Surg.* 11: 25 - 42, 1925.
145. **Reinhart, W.H.** Shear-dependence of endothelial functions. *Experientia* 50: 87 - 93, 1994.
146. **Rembold, C.M.** Regulation of contraction and relaxation in arterial smooth muscle. *Hypertension* 20: 129 - 137, 1992.
147. **Resnick, N., T. Collins, W. Atkinson, D.T. Bonthron, C.F. Dewey, Jr., and M.A. Gimbrone, Jr.** Platelet-derived growth factor B chain promoter contains a cis-acting fluid shear-stress-responsive element. *Proc. Natl. Acad. Sci.* 90: 4591 - 4595, 1993.

148. **Resnick, N. and M.A. Gimbrone, Jr.** Hemodynamic forces are complex regulators of endothelial gene expression. *FASEB J.* 9: 874 - 882, 1995.
149. **Rifkin, D.B., and D. Moscatelli.** Recent developments in the cell biology of basic fibroblast growth factor. *J. Cell Biol.* 109: 1 - 6, 1989.
150. **Roberts, A.B., M.B. Sporn, R.K. Assoian, J.M. Smith, N.S. Roche, L.M. Wakefield, U.I. Heine, L.A. Liotta, V. Falanga, J.H. Kehrl, and A.S. Fauci.** Transforming growth factor type  $\beta$ : rapid induction of fibrosis and angiogenesis *in vivo* and stimulation of collagen formation *in vitro*. *Proc. Natl. Acad. Sci.* 83: 4167 - 4171, 1986.
151. **Robinson, L.J., L. Busconi, and T. Michel.** Agonist-modulated palmitoylation of endothelial nitric oxide synthase. *J. Biol. Chem.* 270: 995 - 998, 1995.
152. **Rodbard, S.** Vascular caliber. *Cardiology* 60: 649 - 651, 1975.
153. **Ross, R.** The pathogenesis of atherosclerosis: a perspective for the 1990s. *Nature* 362: 801 - 809, 1993.
154. **Ross, R.** The pathogenesis of atherosclerosis. In: *Heart Disease: A Textbook of Cardiovascular Medicine*. Braunwald, E. (ed.). W.B. Saunders Company, Philadelphia. pp. 1106 - 1124, 1992.
155. **Ross, R., J. Masuda, and E.W. Raines.** Cellular interactions, growth factors, and smooth muscle proliferation in atherogenesis. *Ann. NY Acad. Sci.* 598: 102 - 112, 1990.
156. **Sakaguchi, M., T. Kajio, K. Kawahara, and K. Kato.** Antibodies against basic fibroblast growth factor inhibit the autocrine growth of pulmonary artery endothelial cells. *FEBS Lett.* 233: 163 - 166, 1988.
157. **Saksela, O., and D.B. Rifkin.** Release of basic fibroblast growth factor-heparan sulfate complexes from endothelial cells by plasminogen activator-mediated proteolytic activity. *J. Cell Biol.* 110: 767 - 775, 1990.
158. **Saksela, O., D. Moscatelli, A. Sommer, and D.B. Rifkin.** Endothelial cell-derived heparan sulfate binds basic fibroblast growth factor and protects it from proteolytic degradation. *J. Cell Biol.* 107: 743 - 751, 1988.
159. **Sankar, S., N. Mahooti-Brooks, L. Bensen, T.L. McCarthy, M. Centrella, and J.A. Madri.** Modulation of transforming growth factor  $\beta$  receptor levels on microvascular endothelial cells during *in vitro* angiogenesis. *J. Clin. Invest.* 97: 1436 - 1446, 1996.

160. **Schaper, W., and W.D. Ito.** Molecular mechanisms of coronary collateral vessel growth. *Circ. Res.* 79: 911 - 919, 1996.
161. **Schott, R.J., and L.A. Morrow.** Growth factors and angiogenesis. *Cardiovasc. Res.* 27: 1155 - 1161, 1993.
162. **Schweigerer, L., G. Neufeld, J. Friedman, J.A. Abraham, J.C. Fiddes, and D. Gospodarowicz.** Capillary endothelial cells express basic fibroblast growth factor, a mitogen that promotes their own growth. *Nature* 325: 257 - 259, 1987.
163. **Seifert, R.A., S.M. Schwartz, and D.F. Bowen-Pope.** Developmentally regulated production of platelet-derived growth factor-like molecules. *Nature* 311: 669 - 671, 1984.
164. **Sessa, W.C., G. Garcia-Cardena, J. Liu, A. Keh, J.S. Pollock, J. Bradley, S. Thiru, I.M. Braverman, and K.M. Desai.** The golgi association of endothelial nitric oxide synthase is necessary for the efficient synthesis of nitric oxide. *J. Biol. Chem.* 270: 17641 - 17644, 1995.
165. **Skalak, T.C., and R.J. Price.** The role of mechanical stresses in microvascular remodeling. *Microcirc.* 3: 143 - 165, 1996.
166. **Smieško, V. and P.C. Johnson.** The arterial lumen is controlled by flow-related shear stress. *News Physiol. Sci.* 8: 34 - 38, 1993.
167. **Smieško, V., J. Kozík, and S. Dolezel.** Role of endothelium in the control of arterial diameter by blood flow. *Blood Vessels* 22: 247 - 251, 1985.
168. **Smieško, V., D.J. Lang, and P.C. Johnson.** Dilator response of rat mesenteric arcading arterioles to increased blood flow velocity. *Am. J. Physiol.* 257 (*Heart Circ. Physiol.* 26): H1958 - H1965, 1989.
169. **Snow, H.M., S.J.G. McAuliffe, J.A. Moors, and R. Brownlie.** The relationship between blood flow and diameter in the iliac artery of the anaesthetized dog: the role of endothelium-derived relaxing factor and shear stress. *Exp. Physiol.* 79: 635 - 645, 1994.
170. **Stavri, G.T., Y. Hong, I.C. Zachary, G. Breier, P.A. Baskerville, S. Yla-Herttuala, W. Risau, J.F. Martin, and J.D. Erusalimsky.** Hypoxia and platelet-derived growth factor-BB synergistically upregulate the expression of vascular endothelial growth factor in vascular smooth muscle cells. *FEBS Letters* 358: 311 - 315, 1995.
171. **Sterpetti, A.V., A. Cucina, L.S. D'Angelo, B. Cardillo, and A. Cavallaro.** Shear stress modulates the proliferation rate, protein synthesis, and mitogenic activity of arterial smooth muscle cells. *Surgery* 113: 691 - 699, 1993.

172. **Sterpetti, A.V., A. Cucina, A. Fragale, S. Lepidi, A. Cavallaro, and L. Santoro-D'Angelo.** Shear stress influences the release of platelet derived growth factor and basic fibroblast growth factor by arterial smooth muscle cells. *Eur. J. Vasc. Surg.* 8: 138 - 142, 1994.
173. **Sumpio, B.E., A.J. Banes, G.W. Link, and T. Iba.** Modulation of endothelial cell phenotype by cyclic stretch: inhibition of collagen synthesis. *J. Surg. Res.* 48: 415 - 420, 1990.
174. **Thommes, K.B., J. Hoppe, H. Vetter, and A. Sachinidis.** The synergistic effect of PDGF-AA and IGF-1 on VSMC proliferation might be explained by the differential activation of their intracellular signaling pathways. *Exp. Cell Res.* 226: 59 - 66, 1996.
175. **Thoumine, O., R.M. Nerem, and P.R. Girard.** Changes in organization and composition of the extracellular matrix underlying cultured endothelial cells exposed to laminar steady shear stress. *Lab. Invest.* 73: 565 - 576, 1995.
176. **Thoumine, O., R.M. Nerem, and P.R. Girard.** Oscillatory shear stress and hydrostatic pressure modulate cell-matrix attachment proteins in cultured endothelial cells. *In Vitro Cell. Dev. Biol. Anim.* 31: 45 - 54, 1995.
177. **Uematsu, M., Y. Ohara, J.P. Navas, K. Nishida, T.J. Murphy, R.W. Alexander, R.M. Nerem, and D.G. Harrison.** Regulation of endothelial cell nitric oxide synthase mRNA expression by shear stress. *Am. J. Physiol.* 269 (*Cell Physiol.* 38): C1371 - C1378, 1995.
178. **Umans, J.G., and R. Levi.** Nitric oxide in the regulation of blood flow and arterial pressure. *Ann. Rev. Physiol.* 57: 771 - 790, 1995.
179. **Unthank, J.L., S.W. Fath, H.M. Burkhart, S.C. Miller, and M.C. Dalsing.** Wall remodeling during luminal expansion of mesenteric arterial collaterals in the rat. *Circ. Res.* 79: 1015 - 1023, 1996.
180. **Unthank, J.L., J.M. Lash, and H.G. Bohlen.** Maturation of the rat intestinal microvasculature from juvenile to early adult life. *Am. J. Physiol.* 259 (*Gastrointest. Liver Physiol.* 22): G282 - G289, 1990.
181. **Unthank, J.L., J.C. Nixon, H.M. Burkhart, S.W. Fath, and M.C. Dalsing.** Early collateral and microvascular adaptations to intestinal artery occlusion in the rat. *Am. J. Physiol.* 271 (*Heart Circ. Physiol.* 40): H914 - H923, 1996.
182. **Van Obberghen-Schilling, E., N.S. Roche, K.C. Flanders, M.B. Sporn, and A.B. Roberts.** Transforming growth factor  $\beta$ 1 positively regulates its own expression in normal and transformed cells. *J. Biol. Chem.* 263: 7741 - 7746, 1988.

183. **Venema, R.C., H.S. Sayegh, J-F. Arnal, and D.G. Harrison.** Role of the enzyme calmodulin-binding domain in membrane association and phospholipid inhibition of endothelial nitric oxide synthase. *J. Biol. Chem.* 270: 14705 - 14711, 1995.
184. **Vlodavsky, I, R. Fridman, R. Sullivan, J. Sasse, and M. Klagsbrun.** Aortic endothelial cells synthesize basic fibroblast growth factor which remains cell associated and platelet-derived growth factor-like protein which is secreted. *J. Cell. Physiol.* 131: 402 - 408, 1987.
185. **Walker, L.N., D.F. Bowen-Pope, R. Ross, and M.A. Reidy.** Production of platelet-derived growth factor-like molecules by cultured arterial smooth muscle cells accompanies proliferation after arterial injury. *Proc. Natl. Acad. Sci.* 83: 7311 - 7315, 1986.
186. **Walpole, P.L., A.I. Gotlieb, and B.L. Langille.** Monocyte adhesion and changes in endothelial cell number, morphology, and F-actin distribution elicited by low shear stress *in vivo*. *Am. J. Pathol.* 142: 1392 - 1400, 1993.
187. **Wang, D.H. and R.L. Prewitt.** Microvascular development during normal growth and reduced blood flow: introduction of a new model. *Am. J. Physiol.* 260 (*Heart Circ. Physiol.* 29): H1966 - H1972, 1991.
188. **Wang, D.M., and J.M. Tarbell.** Modeling interstitial flow in an artery wall allows estimation of wall shear stress on smooth muscle cells. *J. Biomech. Eng.* 117: 358 - 363, 1995.
189. **Wechezak, A.R., R.F. Viggers, and L.R. Sauvage.** Fibronectin and F-actin redistribution in cultured endothelial cells exposed to shear stress. *Lab. Invest.* 53: 639 - 647, 1985.
190. **Weibel, E.** Early stages in the development of collateral circulation to the lung in the rat. *Circ. Res.* 8: 353 - 376, 1960.
191. **Wilcox, J.** Fundamental principles of in situ hybridization. *J. Histochem. Cytochem.* 41: 1725 - 1733, 1993.
192. **Wilcox, J.N., K.M. Smith, L.T. Williams, S.M. Schwartz, and D. Gordon.** Platelet-derived growth factor mRNA detection in human atherosclerotic plaques by in situ hybridization. *J. Clin. Invest.* 82: 1134 - 1143, 1988.
193. **Wilson, E., Q. Mai, K. Sudhir, R.H. Weiss, and H.E. Ives.** Mechanical strain induces growth of vascular smooth muscle cells via autocrine action of PDGF. *J. Cell Biol.* 123: 741 - 747, 1993.

194. **Wilson, E., K. Sudhir, and H.E. Ives.** Mechanical strain of rat vascular smooth muscle cells is sensed by specific extracellular matrix/integrin interactions. *J. Clin. Invest.* 96: 2364 - 2372, 1995.
195. **Xue, C., S.J. Botkin, and R.A. Johns.** Localization of endothelial NOS at the basal microtubule membrane in ciliated epithelium of rat lung. *J. Histochem. Cytochem.* 44: 463 - 471, 1996.
196. **Yu, Z.-X., S. Biro, Y.-M. Fu, J. Sanchez, G. Smale, J. Sasse, V.J. Ferrans, and W. Casscells.** Localization of basic fibroblast growth factor in bovine endothelial cells: immunohistochemical and biochemical studies. *Exp. Cell Res.* 204: 247 - 259, 1993.
197. **Zarins, C.K., M.A. Zatina, D.P. Giddens, D.N. Ku, and S. Glagov.** Shear stress regulation of artery lumen diameter in experimental atherogenesis. *J. Vasc. Surg.* 5: 413 - 420, 1987.
198. **Ziche, M., L. Morbidelli, E. Masini, H. Granger, P. Geppetti, and F. Ledda.** Nitric oxide promotes DNA synthesis and cyclic GMP formation in endothelial cells from postcapillary venules. *Biochem. Biophys. Res. Comm.* 192: 1198 - 1203, 1993.
199. **Ziche, M., L. Morbidelli, E. Masini, S. Amerini, H.J. Granger, C.A. Maggi, P. Geppetti, and F. Ledda.** Nitric oxide mediates angiogenesis in vivo and endothelial cell growth and migration in vitro promoted by substance P. *J. Clin. Invest.* 94: 2036 - 2044, 1994.
200. **Ziegler, T., and R.M. Nerem.** Effect of flow on the process of endothelial cell division. *Arteriosclerosis Thromb.* 14: 636 - 643, 1994.

**VITA**  
David Anthony Tulis

**Address:**

Department of Physiology  
Eastern Virginia Medical School  
Norfolk, Virginia 23501-1980  
(757) 446-5607 (office)  
(757) 624-2269 (fax)  
TULIS@WESLEY.EVMS.EDU (e-mail)

**Personal:**

Date of Birth: 11-03-64  
Place of Birth: Frederick, MD  
Citizenship: USA  
Social Security No.: 246-21-0530  
Marital Status: Single

**Education:**

Doctor of Philosophy, Cardiovascular Science, Biomedical Sciences Ph.D. Program, Old Dominion University and Eastern Virginia Medical School, Norfolk, VA, 1997

Master of Science, Toxicology (major) and Genetics (minor), North Carolina State University, Raleigh, NC, 1990

Bachelor of Science, Biology, University of North Carolina at Chapel Hill, 1987

**Publications:**

Tulis, D.A., S.D. Schriver, J.L. Unthank, and R.L. Prewitt. In vivo alterations in arterial growth and endothelial nitric oxide synthase (eNOS) in response to increased shear stress. *J. Vasc. Res.* 33: A400, 1996.

Tulis, D.A., S.D. Schriver, J.L. Unthank, and R.L. Prewitt. Shear stress-mediated vascular growth. *FASEB J.* 10: A54, 1996.

Tulis, D.A., J.L. Unthank, and R.L. Prewitt. Flow-induced arterial remodeling in rat mesenteric vasculature. *J. Vasc. Res.* 34: A143, 1997.

**Professional Memberships:**

1997 - present	Phi Kappa Phi
1996 - present	American Physiological Society
1996 - present	North American Vascular Biology Organization

**Competitive Awards:**

North American Vascular Biology Organization Student Scholarship, IX International Vascular Biology Meeting, Seattle, WA (1996)

Proctor and Gamble Professional Opportunity Award, 1996 Experimental Biology Meeting, Washington, D.C. (1996)

Servier Young Investigator Award, 7<sup>th</sup> International Symposium on Mechanisms of Vasodilatation, Maastricht, The Netherlands (1997)